

CHAPTER 2

RECOMMENDED CITATION

Jackson, M., Azam, M.F., Baral, P., Benestad, R., Brun, F., Muhammad, S., Pradhananga, S., Shrestha, F., Steiner, J.F., & Thapa, A. (2023). Consequences of climate change for the cryosphere in the Hindu Kush Himalaya. In ICIMOD (P. Wester, S. Chaudhary, N. Chettri, M. Jackson, A. Maharjan, S. Nepal & J. F. Steiner [Eds.]), *Water, ice, society, and ecosystems in the Hindu Kush Himalaya: An outlook* (pp. 17–71). ICIMOD. <https://doi.org/10.53055/ICIMOD.1030>

Consequences of climate change for the cryosphere in the Hindu Kush Himalaya

CHAPTER LEAD AUTHOR

Miriam Jackson

International Centre for Integrated Mountain Development (ICIMOD), Lalitpur, Nepal

AUTHORS

Mohd Farooq Azam

Indian Institute of Technology Indore, India

Prashant Baral

International Centre for Integrated Mountain Development (ICIMOD), Lalitpur, Nepal

Rasmus Benestad

Norwegian Meteorological Institute, Oslo, Norway

Fanny Brun

Institute of Environmental Geosciences (IGE), Univ. Grenoble Alpes, France

Sher Muhammad

International Centre for Integrated Mountain Development (ICIMOD), Lalitpur, Nepal

Saurav Pradhananga

International Centre for Integrated Mountain Development (ICIMOD), Lalitpur, Nepal

Finu Shrestha

International Centre for Integrated Mountain Development (ICIMOD), Lalitpur, Nepal

Jakob F Steiner

Institute of Geography and Regional Science, University of Graz, Austria

International Centre for Integrated Mountain Development (ICIMOD), Lalitpur, Nepal

Amrit Thapa

Department of Geosciences, University of Alaska Fairbanks, Alaska, USA

International Centre for Integrated Mountain Development (ICIMOD), Lalitpur, Nepal

Chapter overview

KEY FINDINGS

Major advances in HKH glacier monitoring and analysis made in recent years show a significant acceleration of glacier mass loss by 65% in the HKH (*high confidence*) and reversal from mass gain/steady state to mass loss in the Karakoram (*medium confidence*). Glacier mass changes between the 1970s and 2019 in most areas of the HKH have now been quantified with increased accuracy. The rate of mass loss increased by 65% through the study period with an average of -0.17 metres water equivalent (m w.e.) per year for the period 2000–2009 to -0.28 m w.e. per year for 2010–2019 (*high confidence*). The most negative mass balances are observed in the eastern part of the HKH. The Karakoram region, previously known for stable regional mass balances, showed slight wastage of -0.09 ± 0.04 m w.e. per year during 2010–2019, indicating the end of the Karakoram Anomaly (*medium confidence*).

Snow cover extent has shown a clearly negative trend in the HKH region since the early twenty-first century with a few exceptions including the Karakoram (*high confidence*). There has been a significant decrease in the seasonal snow cover during the summer and winter

months, as well as a decline from mid-spring through mid-fall, indicating a seasonal shift (*high confidence*). Snow cover days generally declined at an average rate of five snow cover days per decade with most of the changes at lower elevation (*high confidence*). Snow cover is likely to experience an accelerated loss under different global warming levels in the HKH (*medium confidence*).

Still very little is known about permafrost, but what is known points to a decrease in permafrost occurrence (*medium confidence*). There are few field observations of permafrost in the HKH, but existing measurements show changes in permafrost, and remote sensing confirms a decrease in permafrost cover in studied regions (*medium confidence*). Modelled results calculate a loss of about 8,340 km² in permafrost area in the western Himalaya between 2002–2004 and 2018–2020; and a loss of about 965 km² in the Uttarakhand Himalaya between 1970–2000 and 2001–2017. On the Tibetan Plateau, the area of permafrost degradation will increase, with most (about two-thirds) of the permafrost being degraded by 2071–2099 under high emissions scenarios.

POLICY MESSAGES

The evidence of the impact of a changing climate on glaciers is clear. Policy makers need to evaluate the effects these changes are having and will have in the future as glaciers continue to shrink. It will be crucial to identify the expected changes as well as associated opportunities and risks that glacier changes will have on ecosystems and livelihoods in order to develop appropriate adaptation strategies.

There is strong evidence that snowmelt plays the most important role for river run-off in the HKH among all cryosphere components but that its absolute volume will decrease in future and peak flow will shift, with large variability between basins. Snowfall is projected

to become less frequent but more intense and increasing temperatures will affect the volume of the snowpack negatively. Governments should be aware of the expected changes and align their planning for infrastructure and agriculture accordingly.

Permafrost is the cryosphere component for which there is the least knowledge. Potential consequences of changing permafrost include elevated risks for livelihoods and infrastructure. Hence, governments should emphasise ground monitoring, especially where there are substantial infrastructure or communities that could be affected. Communication of the potential consequences should be included in strategies related to the cryosphere.

CHAPTER SUMMARY

The mean temperature is significantly increasing in all the regions of the HKH (*high confidence*) with an average observed trend of +0.28°C per decade (range +0.15°C per decade to +0.34°C per decade for individual basins) for the period 1951–2020. The highest trends are observed for the Tibetan Plateau, Amu Darya, and Brahmaputra basins and headwaters of the Mekong and Yangtze basins (up to +0.66°C per decade in parts of these river basins). The trend in precipitation is mostly insignificant except in the high elevated areas of the Tarim Basin and some parts of the Ganges Basin and shows a significant decrease in parts of the Yellow, Brahmaputra, and Irrawaddy basins (*medium confidence*). It ranges between –3% to +3% per decade in the 12 river basins of the HKH.

Increased warming rates at higher elevations are observed in nine of the 12 basins with the strongest amplification with elevation in the Brahmaputra Basin (*medium confidence*). A similar effect is observed in the Ganges, Yangtze, and Indus basins. However, the Amu Darya, Irrawaddy, and Upper Helmand basins show a warming trend that is higher in low-elevation areas than in high-elevation ones.

In recent years, there have been major advances in glacier monitoring, and in quantifying with higher precision the magnitude and extent of changes in glacier area

and volume. The release of previously classified high-resolution satellite imagery and the ever-improving spatio-temporal resolutions of contemporary satellite imagery mean that glacier mass changes (from the 1970s to 2019) of glaciers in the HKH have now been quantified with an unprecedented accuracy (*high confidence*). The measurement of meteorological variables in different regions has increased. As the number of glacier mass balance (and energy balance) series of more than a few years, as well as the length of these series, increases, there are growing opportunities to better understand the sensitivity of glacier surface mass balance to climate. Satellite-derived glacier surface velocities are now more readily available, with annual surface velocities available for 1985–2020 for almost all of the glaciers in the HKH (with voids in many of the glacier accumulation areas).

Glacier mass balance has become increasingly negative, with rates increasing from –0.17 m w.e. per year from 2000–2009 to –0.28 m w.e. per year from 2010–2019, suggesting an acceleration in mass loss. The most negative mass balances are observed in the eastern part of the HKH within the Southeast Tibet and Nyainqentanglha regions showing -0.78 ± 0.10 m w.e. per year for 2010–2019, while the West Kunlun region shows a near-balanced mass budget of -0.01 ± 0.04 m w.e. per year. The Karakoram region, known previously for balanced regional mass

balances, showed a slight wastage of -0.09 ± 0.04 m w.e. per year for 2010–2019. These results indicate moderate mass loss of the Karakoram glaciers, especially post-2013 and suggest that the Karakoram Anomaly – anomalous behaviour of glaciers in the Karakoram, showing stability or even growth – has probably come to an end.

The number of available future glacier projections under different climate projections has increased in recent years. For a global warming level between 1.5°C to 2°C, the HKH glaciers are expected to lose 30%–50% of their volume by 2100 (*very high confidence*). The corresponding remaining glacier-covered areas range from 50% to 70%. The mass losses will be continuous through the twenty-first century. The specific mass balance rate will remain negative, even though it will become less negative by the end of the century as glaciers retreat to higher elevations. For higher global warming levels, the remaining glacier volume will range from 20% to 45%, with the specific mass balance rates more and more negative throughout the twenty-first century. For a global warming level of +4°C, the heavily glacier-covered regions of West Kunlun and Karakoram will have their remaining glacier area reduced to about 50% of their 2020 area; in all other regions, glacier-covered area will be reduced to less than 30% of the 2020 area.

Globally, glacial lakes have increased and expanded as a result of glacier recession. The total area and number of glacial lakes have increased significantly since the 1990s (*very high confidence*). More proglacial lakes will develop over the next decades due to continued glacier retreat (*high confidence*). Lake expansion is expected to create new hotspots of potentially dangerous glacial lakes, with implications for glacial lake outburst flood (GLOF) hazards and risk (*high confidence*). GLOF risk is expected to increase in the future, also increasing the potential for transboundary events with cross-border impacts, e.g. a glacial lake may lie within the borders of one country, but the main impact of a GLOF event may be across the border in another country.

Snow cover has shown a decreasing trend since the middle of the twentieth century, probably due to an earlier onset of snowmelt (*very high confidence*). Snow cover trends have been clearly negative in most of the HKH since the early twenty-first century with only a

few exceptions. There has been a significant decrease in seasonal snow cover during the summer and winter months. Snow cover days have generally declined at an average rate of five snow cover days per decade with most of the changes at lower elevations. Snowline elevation at the end of the melting season over the HKH shows a statistically significant upward shift in over a quarter of the area and a statistically significant downward trend in less than 1% of the area. Although there are few projections of future snowpack in the region, snow cover is likely to have an accelerated loss under different global warming levels over the HKH, including the Tibetan Plateau (*medium confidence*). The snow cover extent will reduce by between 1% and 26% for an average temperature rise between 1.1°C and 4°C. Heavy snowfall has increased in recent years with frequent snowstorms observed over the Tibetan Plateau and the Himalaya (*high confidence*). These events are predicted to continue to become more frequent and intense in the future. The contribution of snowmelt to streamflow is expected to decrease under all climate scenarios. The onset of snow melting is expected to occur earlier in the future but its influence on the seasonality of river run-off in larger rivers may be dampened by increased rainfall.

Field observations show changes in Himalayan permafrost, and remote sensing estimates confirm decrease in permafrost cover in the Indian Himalayan region. Modelled results show a loss of about 8,340 km² in permafrost area for the western Himalaya between 2002–2004 and 2018–2020 and that the probable areal extent of permafrost decreased from 7,897 km² to 6,932 km² in the Uttarakhand Himalaya between 1970–2000 and 2001–2017. On the Tibetan Plateau, the area of permafrost degradation could range from 0.22×10^6 km² (13% area) in 2011–2040 to 1.07×10^6 km² in 2071–2099 (64.3% area). Changes in permafrost account for about 30% of road damage in the Qinghai–Tibet Plateau. Many mass wasting events are associated with permafrost degradation and are projected to increase in future (*medium confidence*). Change in the active layer thickness ranges from 5–30 cm in 2011–2040 for different warming levels. The active layer thickness is projected to further increase in 2041–2070 and exceed 30 cm in 2071–2099 for warming of 3.1°C or higher above the 1981–2010 baseline.

KEY KNOWLEDGE GAPS

There are very few direct measurements of ice and debris thickness on debris-covered glaciers. Estimates at a global scale show significant variations. More field measurements of these variables as well as ice temperature and annual/seasonal glacier surface mass balances are highly recommended to get a better understanding of how glaciers will react to future climate change and their subsequent effect on basin hydrology.

There are few in situ measurements of snow depth and snow water equivalent resulting in a limited understanding of spatial variability of snowpack changes. In many parts of the HKH, snowmelt is much more important to run-off than glacier melt. These measurements and related measurements (such as high altitude hydrometeorological measurements) urgently need to be increased and expanded.

There are very few in situ measurements of ground temperature and borehole measurements to obtain both the present ground temperature as well as historical changes. There is also a lack of knowledge of the existence of permafrost and its importance to both the water cycle and natural hazards. More measurements are needed, especially in regions where road construction projects are being planned or undertaken and where people live in the vicinity of permafrost and are hence more vulnerable to landslides caused by permafrost degradation.

There are very few studies in the HKH on the effects of changes in all elements of the cryosphere on ecosystems and livelihoods. This also includes the relationship between changes in the cryosphere and natural hazards related to these changes. A greater emphasis should be placed on holistic studies.

Contents

| | | |
|------------|---|-----------|
| 2.1 | Introduction | 23 |
| 2.2 | The climate of the HKH region | 26 |
| 2.2.1 | The observed climate in the HKH | 26 |
| 2.2.2 | Trends in temperature and precipitation | 29 |
| 2.2.3 | Elevation-dependent warming | 30 |
| 2.2.4 | The complexity of extreme events | 32 |
| 2.3 | Glaciers | 34 |
| 2.3.1 | Observed glacier area, surface velocity, thickness, and debris cover in the HKH | 35 |
| 2.3.2 | Observed changes in glacier mass | 36 |
| 2.3.3 | Projected changes in glacier mass | 39 |
| 2.3.4 | Towards a better understanding of glacier response to climate change | 40 |
| 2.4 | Glacial lakes | 42 |
| 2.5 | Snow | 45 |
| 2.5.1 | Observed and projected changes in snow cover and snow line elevations | 45 |
| 2.5.2 | Measurements and changes in snow depth and snow water equivalent | 48 |
| 2.5.3 | Observed and projected changes in the snow season and extreme snow events | 49 |
| 2.5.4 | Relationship between elevation-dependent warming and snow | 49 |
| 2.6 | Permafrost | 50 |
| 2.6.1 | Observed changes in permafrost | 50 |
| 2.6.2 | Consequences of changes in permafrost | 50 |
| 2.6.3 | Projections for permafrost | 52 |
| 2.7 | Major knowledge gaps | 53 |
| 2.7.1 | Glaciers | 53 |
| 2.7.2 | Glacial lakes | 53 |
| 2.7.3 | Snow | 54 |
| 2.7.4 | Permafrost | 55 |
| 2.7.5 | Conclusions and policy recommendations | 55 |
| | References | 52 |
| | Appendix | 68 |

2.1. Introduction

The most important components of the cryosphere in the Hindu Kush Himalaya (HKH) are glaciers, snow, and permafrost. Glaciers and snow are highly visible features of the mountains in the HKH. In situ measurements of glaciers and snow are limited in extent and, where they exist, are generally sparse and lack continuity. However, recent advances in spatial and temporal resolution in satellite imagery have meant that our knowledge of snow and glacier extent and changes they have undergone has increased rapidly in just the last few years. More coordinated efforts by the glaciological community, such as in glacier projections under different climate scenarios, have meant that this field has also expanded rapidly.

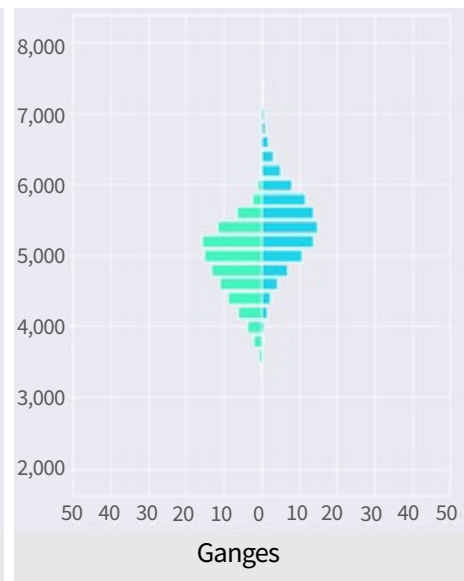
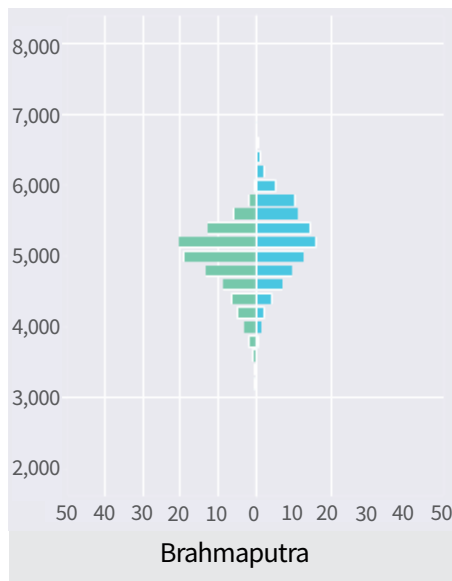
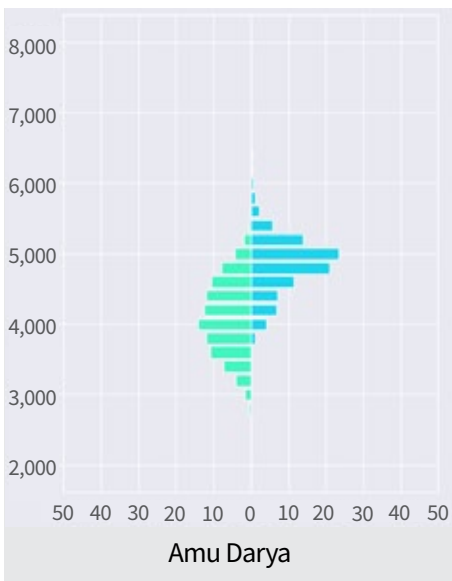
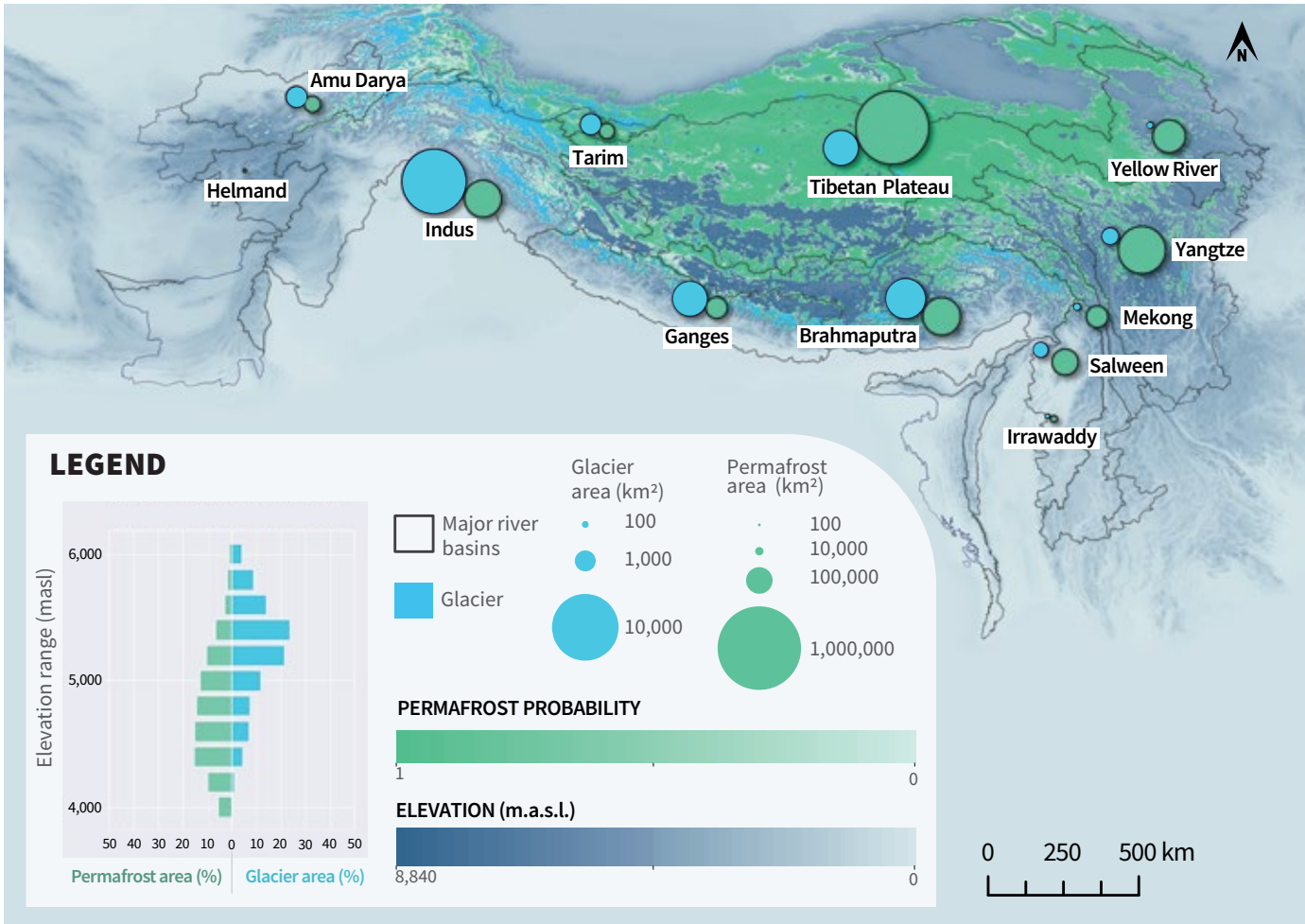
Permafrost is defined as ground that remains at or below 0 degrees Celsius (°C) for at least two consecutive years. By its nature, it is not visible in the same way that glaciers and snow cover are, but it covers a considerable area of the HKH (Figure 2.1). Hence, it is not possible to measure its extent from satellite imagery, although ground features related to

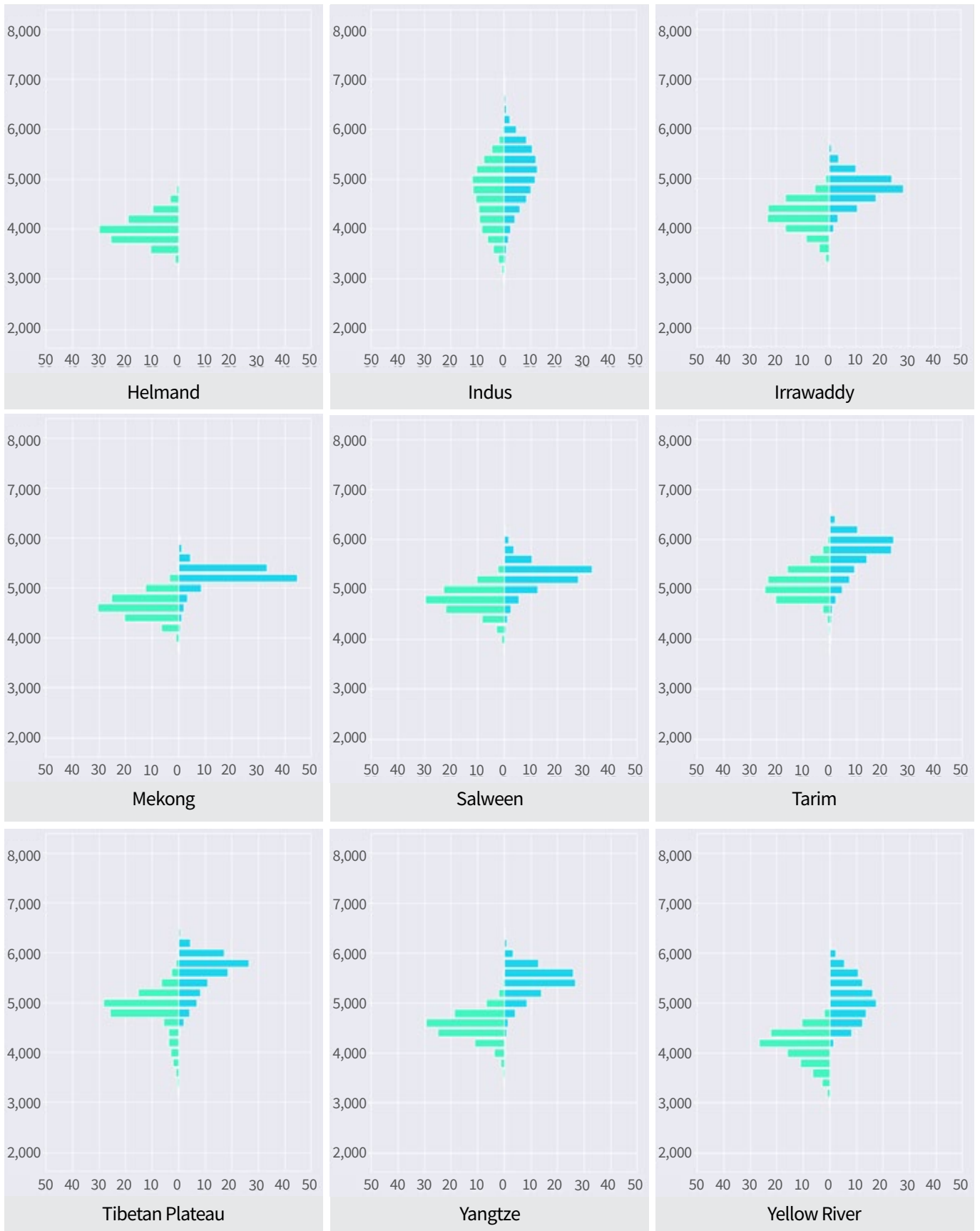
permafrost can be detected and used to train models to generate probability maps for the existence of permafrost. There have been several of these studies in recent years, but there are still very few ground-based measurements.

This chapter examines the effects that climate change will have on different components of the cryosphere in the HKH in the near future and the drivers of those changes. Advances in scientific understanding since the publication of *The Hindu Kush Himalaya assessment* report (Wester et al., 2019) are included as well as new knowledge on the status of the cryosphere since its publication. The chapter concludes by summarising the main current knowledge gaps concerning glaciers, glacial lakes, snow, and permafrost, and makes recommendations to address these gaps. The impacts of changes in the cryosphere on downstream hydrology and water resources, and natural hazards related to a changing cryosphere are covered in Chapter 3 of this report. The consequent impacts on ecosystems and livelihoods are covered in chapters 4 and 5 respectively.

FIGURE 2.1

DISTRIBUTION OF PERMAFROST (IN GREEN) AND GLACIERS (IN BLUE) AND SUMMARY STATISTICS FOR GLACIERS AND PERMAFROST IN THE MAJOR RIVER BASINS OF THE HKH





Notes: Boundaries of the portions of the river basins falling in the HKH outlined in dark grey. Blue circles represent glacier area (Randolph Glacier Inventory 6.0) and green circles represent permafrost area (Obu et al., 2019) in each river basin. Bar plots for each river basin indicate permafrost and glacier area in 200-metre elevation bins as a percentage of total permafrost and glacier area in the river basin falling in the boundary of the HKH, respectively.

2.2. The climate of the HKH region

2.2.1. The observed climate in the HKH

Tropical/subtropical climatic conditions dominate in the foothills of the HKH, transitioning to an alpine climate at higher elevations with permanently snow- and ice-covered peaks. The HKH region's meteorology is a unique example of the direct interplay of high-altitude mountains with complicated terrains, locally originating atmospheric weather patterns, and large-scale migratory weather systems. Because orography, the topographic relief of mountains, has an impact on large-scale air flows, mountain systems produce weather patterns that are highly changeable and relatively less predictable. Dynamic alterations brought on by orographic barriers and surface boundary forcings, such as changes in local temperature or humidity, created in difficult terrains further complicate this effect. In general, mountains have frictional effects on surface winds, block the passage of wind and weather systems, and cause vertical ascents and gliding flows across valleys. Mountains have the capacity to significantly alter the properties of weather systems through their interactions with them at various temporal and spatial scales (Pant et al. 2018).

The mountain ranges of the HKH are situated in a region of subtropical high pressure where seasonal pressure and the movement of wind systems from north to south typically affect seasonal weather. The amount of annual rainfall increases from west to east along the southern front of the range (Sabin et al., 2020). Most monsoon precipitation falls in the Lower Siwalik and Pir Panjal mountains of the Himalaya, whereas the high Himalaya, trans-Himalaya, and Karakoram ranges receive less precipitation (Bookhagen & Burbank, 2006). Over the western Himalaya, Hindu Kush, and Karakoram regions, these winter circulations and disturbances bring chilly winds and precipitation in the form of snow, largely connected with the troughs and low-pressure systems buried in these circulations known as western disturbances, which are mid-latitude weather systems that originate in the Mediterranean region (Madhura et al., 2015). There are different climatic sub-zones due to the large elevational range within the HKH, ranging

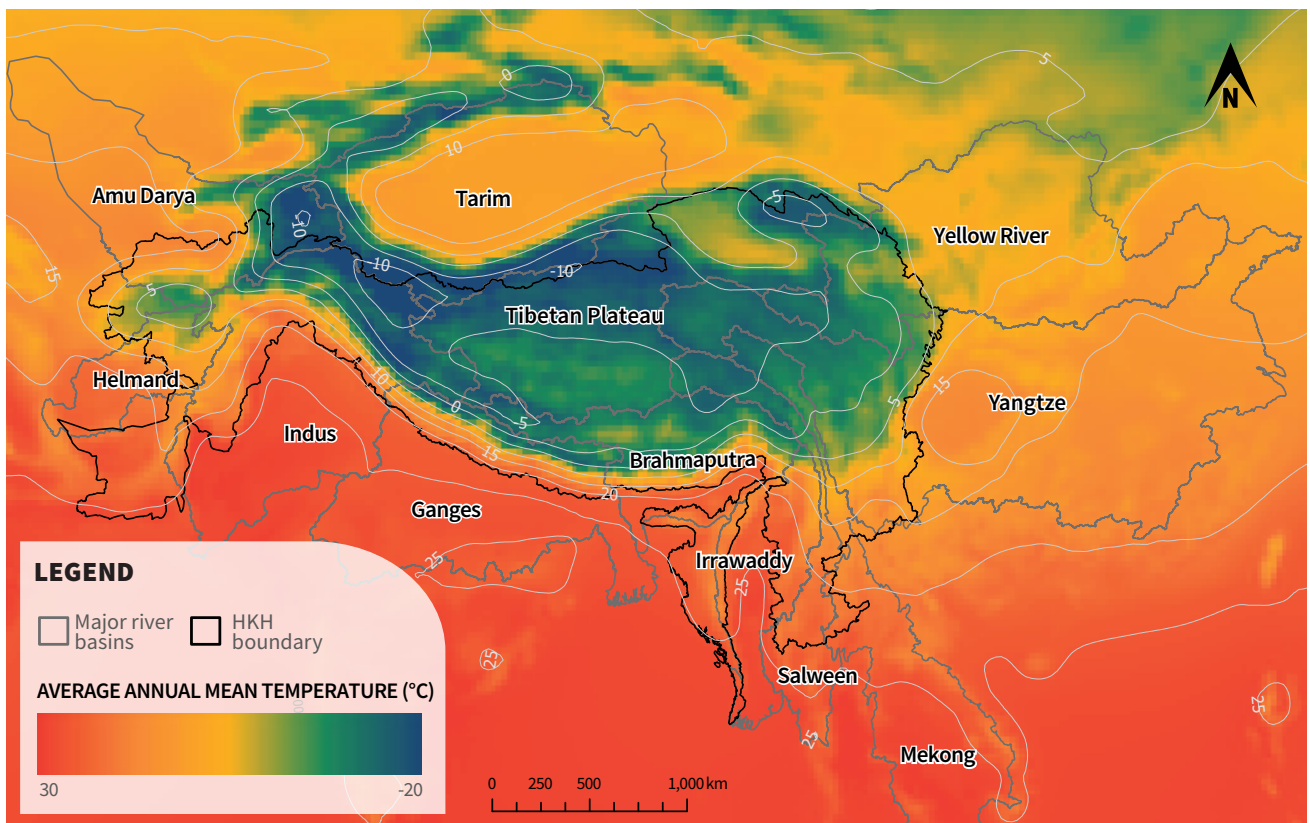
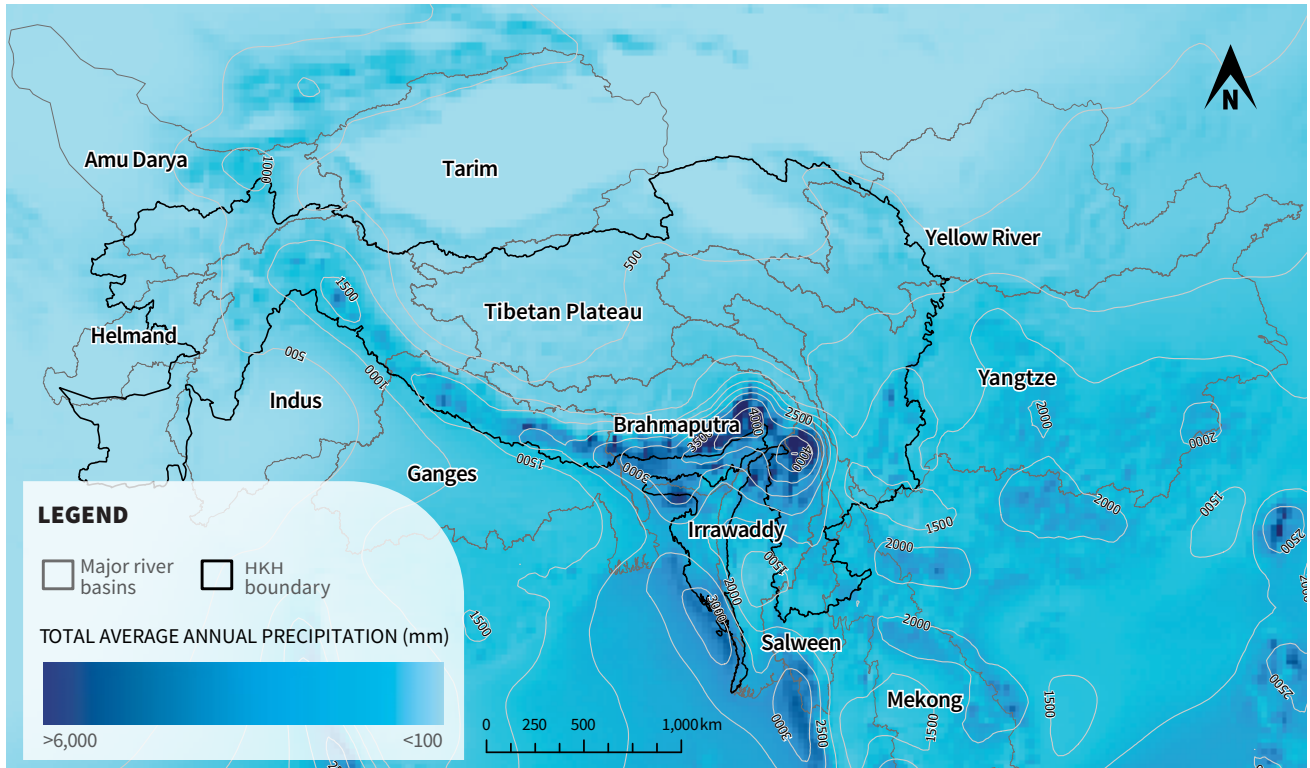
from the tropical zone below 1,000 metres above sea level (m a.s.l.) to the trans-Himalayan zone above 5,000 m a.s.l. The annual cycle of temperature and precipitation differs substantially in these different zones. Seasonal variations in the mean climate of the HKH are closely tied to the seasonal cycle of the regional atmospheric processes (Sabin et al., 2020). The observed weather and mean climate conditions over the HKH are summarised in Chapter 3 (see subsection 3.2) of *The Hindu Kush Himalaya assessment* report (Krishnan et al., 2019).

In this chapter, trends in precipitation and temperature have been presented from reanalysis data provided by ECMWF (European Centre for Medium-Range Weather Forecasts) using the ERA5 (ECMWF Reanalysis v5) version (Muñoz Sabater, 2021), which is the latest comprehensive ECMWF reanalysis climate data. ERA5 provides hourly estimates of the global atmosphere, land surface, and ocean waves from 1950, is updated daily with a latency of 5 days (Hersbach et al., 2020), and has a horizontal resolution of 31 kilometres (km). Seasonal distinctions may vary between and across basins, depending on the climatic variables considered for a given season. However, for the sake of consistency in making the comparison, we have chosen the following definitions for the four seasons across the basins: pre-monsoon (March–May), monsoon (June–September), post-monsoon (October–November), and winter (December–February).

The mean precipitation ranges from <100 millimetres (mm) to over 6,000 mm per year within the HKH (Figure 2.2, top). The precipitation hotspots lie in the Brahmaputra (~2,200 mm per year) and Irrawaddy river basins (~2,400 mm per year) whereas the lowest precipitation is observed on the Tibetan Plateau (~380 mm per year), Helmand (~380 mm per year), and Tarim (~210 mm per year) basins (Table 2.1). The western basins generally receive more precipitation during the winter months (mainly as snow), whereas more than 70% of the annual precipitation in the central and eastern basins of the Himalaya falls during the summer monsoon season. Most of the monsoon precipitation falls as rain. However, snowfall

FIGURE 2.2

TOTAL AVERAGE ANNUAL PRECIPITATION (TOP) AND AVERAGE ANNUAL MEAN TEMPERATURE (BOTTOM) FOR THE 12 MAJOR RIVER BASINS OF THE HKH FOR THE PERIOD 1951–2020



Data source: ERA5 (Muñoz Sabater, 2021)

is prevalent in the high-elevation areas of the basins. The annual and seasonal precipitation for 12 major river basins of the HKH are presented in Table 2.1.

The average annual mean temperature within the HKH ranges from -20°C to 30°C . The plains experience higher temperatures than the middle and high mountain regions throughout the year. The lowest basin average annual mean temperature is about -4°C , on the Tibetan Plateau, while the highest basin average (22°C) is observed in the Irrawaddy River Basin. The seasonal mean temperature is the lowest during the winter season and highest during the monsoon season in all the river basins. The mean temperature during the pre-monsoon and post-monsoon seasons is above zero for all the basins except the Tibetan Plateau. The seasonal mean

temperature decreases drastically after the monsoon, by at least 6°C , barring in the Irrawaddy and Mekong basins. In these two basins, the mean temperature stays relatively similar during the pre-monsoon, monsoon, and post-monsoon seasons. The average annual and seasonal mean temperatures for 12 major river basins of the HKH are presented in Table 2.1.

However, there are some studies which suggest that ERA5 data have a cold bias over the mountains (A. Khadka et al., 2022; Orsolini et al., 2019). This results in a considerable overestimation of snow depth, by a factor of up to 10, over the Tibetan Plateau (Orsolini et al., 2019) as well as of precipitation in the Himalaya above 4,000 m, by a factor of up to 3 (A. Khadka et al., 2022).

| TABLE 2.1 AVERAGE SEASONAL AND ANNUAL PRECIPITATION AND MEAN TEMPERATURE FOR THE 12 MAJOR RIVER BASINS OF THE HKH FOR THE PERIOD 1951–2020 | | | | | | | | | | |
|---|--------------------|-------------|---------|--------------|--------|------------------------------------|-------------|---------|--------------|--------|
| River basin | Precipitation (mm) | | | | | Temperature ($^{\circ}\text{C}$) | | | | |
| | Winter | Pre-monsoon | Monsoon | Post-monsoon | Annual | Winter | Pre-monsoon | Monsoon | Post-monsoon | Annual |
| Amu Darya | 121.2 | 164.1 | 56.6 | 50.2 | 392 | -3.8 | 9.5 | 20.4 | 5.0 | 9.1 |
| Helmand | 118.8 | 88.6 | 11.1 | 14.7 | 233 | 3.4 | 16.6 | 26.6 | 13.2 | 14.9 |
| Indus | 114.8 | 141.2 | 314.8 | 37.9 | 609 | 4.4 | 16.1 | 23.3 | 12.8 | 15.0 |
| Tarim | 16.4 | 52.4 | 127.5 | 15.8 | 212 | -9.4 | 7.5 | 17.2 | 0.7 | 5.4 |
| Ganges | 72 | 116.6 | 1,050.6 | 68.7 | 1,308 | 13.3 | 24.2 | 25.8 | 19.5 | 21.2 |
| Tibetan Plateau | 18.4 | 62.7 | 282.8 | 19.5 | 383 | -15.0 | -4.3 | 6.0 | -7.8 | -4.1 |
| Brahmaputra | 152.8 | 513.6 | 1,383.2 | 170.9 | 2,221 | -1.9 | 6.2 | 13.5 | 4.9 | 6.4 |
| Irrawaddy | 84.5 | 386.4 | 1,698.6 | 273.8 | 2,443 | 17.5 | 24.5 | 24.8 | 21.6 | 22.4 |
| Salween | 62.1 | 274.5 | 1,190.9 | 179.8 | 1,707 | 8.0 | 15.3 | 18.5 | 12.6 | 14.1 |
| Mekong | 61.6 | 343.8 | 1,090.0 | 214.9 | 1,710 | 17.5 | 22.7 | 23.5 | 20.1 | 21.2 |
| Yangtze | 127.5 | 365.9 | 739.7 | 142.4 | 1,376 | 0.8 | 11.4 | 20.4 | 9.4 | 11.4 |
| Yellow River | 26.6 | 109.8 | 408.3 | 59.7 | 604 | -6.8 | 7.8 | 17.7 | 3.2 | 6.7 |

Data source: ERA5 (Muñoz Sabater, 2021)

Note: Under 'Tibetan Plateau', endorheic basins of the plateau are summarised.

2.2.2. Trends in temperature and precipitation

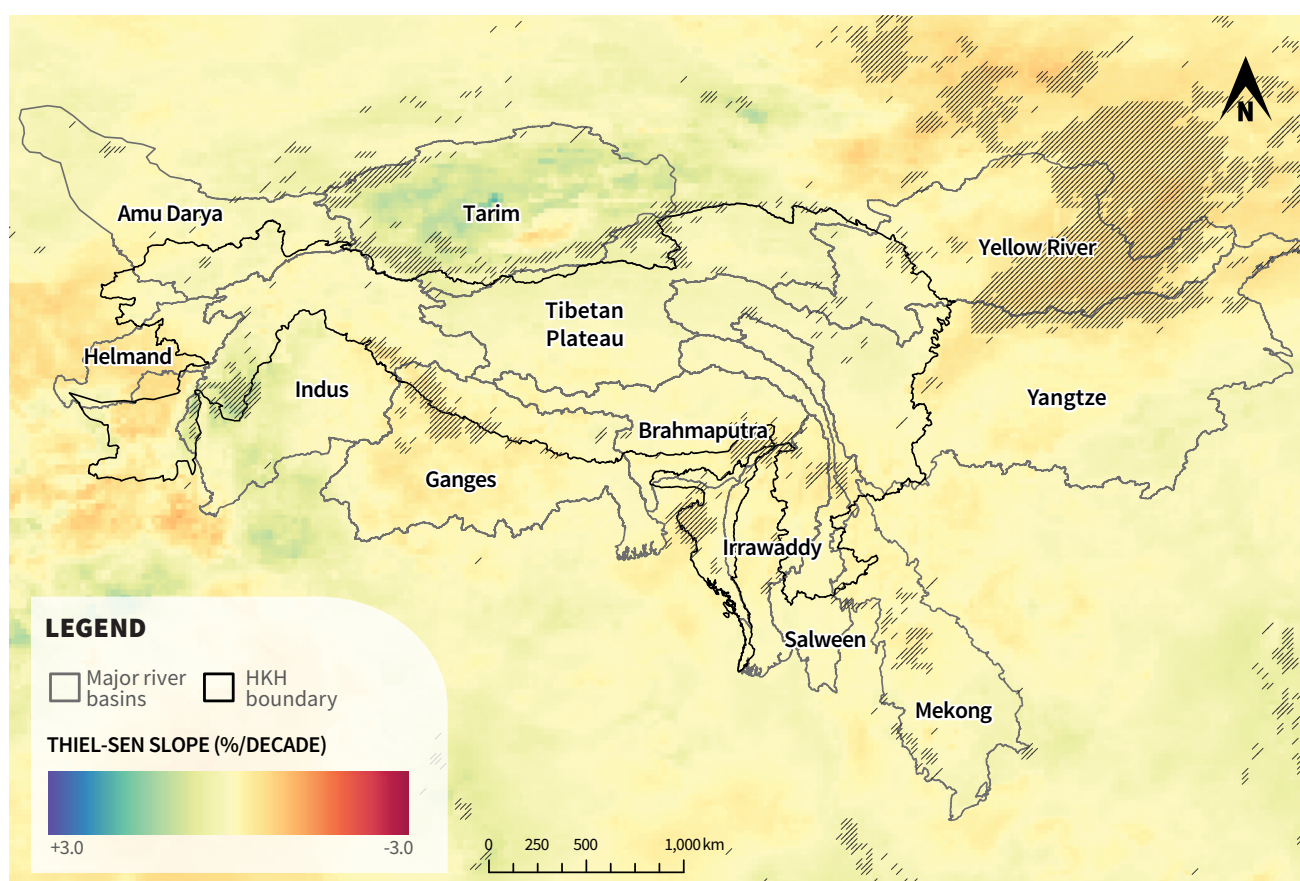
The decadal trends in precipitation and mean temperature have been calculated using the ERA5 reanalysis dataset for the 12 major river basins of the HKH for the period 1951–2020. It is important to note that reanalyses such as ERA5 may have limited accuracy due to inhomogeneities connected to changing inputs from observations over time, such as data from new and improved instruments on satellites becoming available. Nevertheless, the accuracy of ERA5 may be assessed to some extent through comparison with local, in situ observations. The significance and magnitude of the trends are determined using the non-parametric Mann–Kendall test and Thiel-Sen slope, respectively. The trend in precipitation ranges between -3% and $+3\%$ per decade in the 12 river basins (Figure 2.3, top).

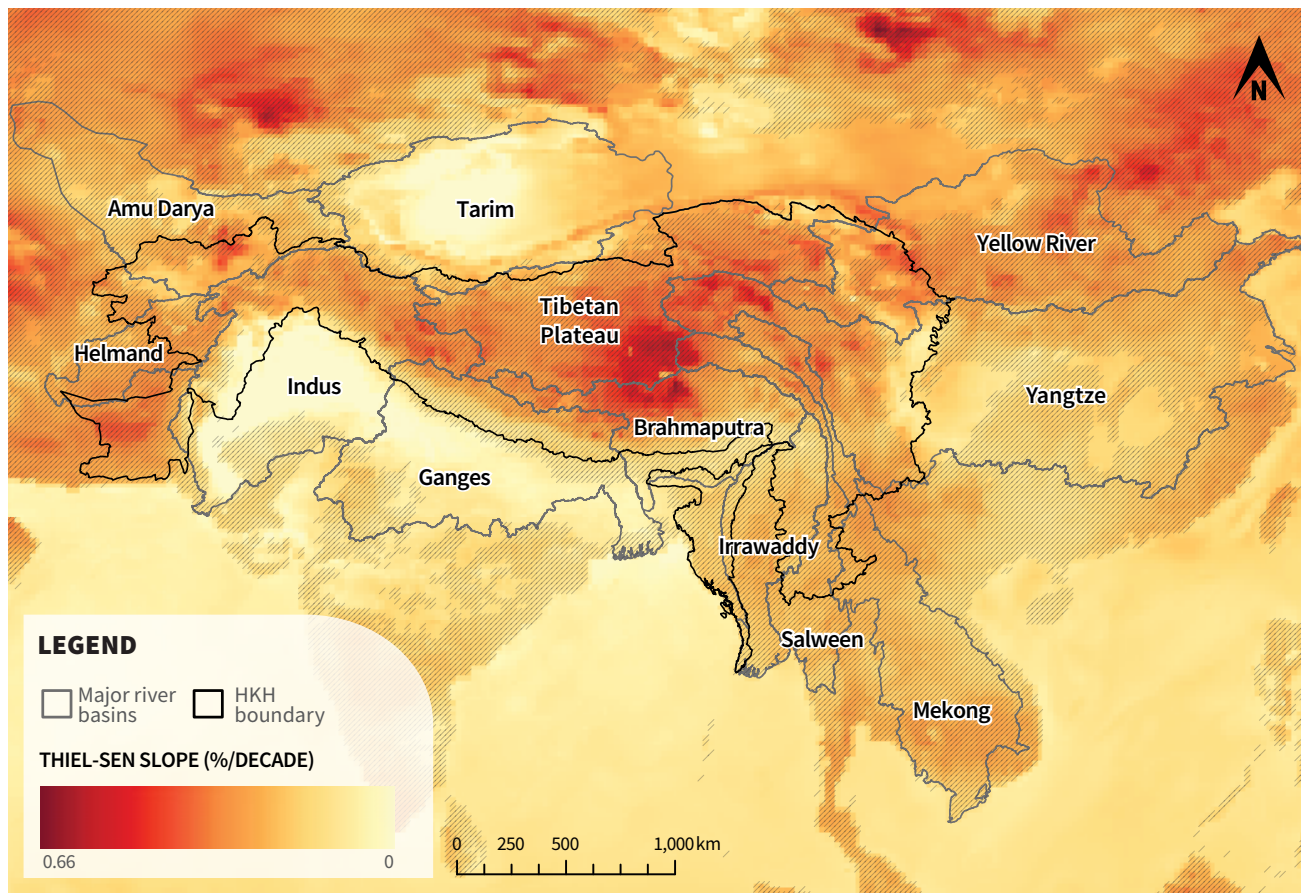
However, the trend is mostly non-significant in all areas except for the high-elevation areas of the Tarim Basin, some parts of the Ganges River Basin, and parts of the Yellow, Brahmaputra, and Irrawaddy river basins, where a significant decrease is noted. Similar results have also been observed over the HKH by Ren et al. (2017) using the China Meteorological Administration’s CMA Global Precipitation dataset V1.0 (CGP1.0). Kraaijenbrink et al. (2021) also found a similar range ($\pm 4\%$ per year) for the trend in annual precipitation using the ERA5 dataset over the HKH region for the period 1979–2019. The *Hindu Kush Himalaya assessment* report also concluded that, with the present data, precipitation did not show clear trends in the past six decades (Krishnan et al., 2019).

Conversely, the mean temperature is increasing significantly in all regions of the HKH with an average observed increase of $+0.28^{\circ}\text{C}$ per decade for the period

FIGURE 2.3

DECADAL TRENDS IN TOTAL ANNUAL PRECIPITATION (TOP) AND AVERAGE ANNUAL MEAN TEMPERATURE (BOTTOM) FOR THE 12 MAJOR RIVER BASINS OF THE HKH FOR THE PERIOD 1951–2020





Note: The diagonal lines indicate the regions where the trend is significant at a 0.01 level.
Data source: ERA5 (Muñoz Sabater, 2021)

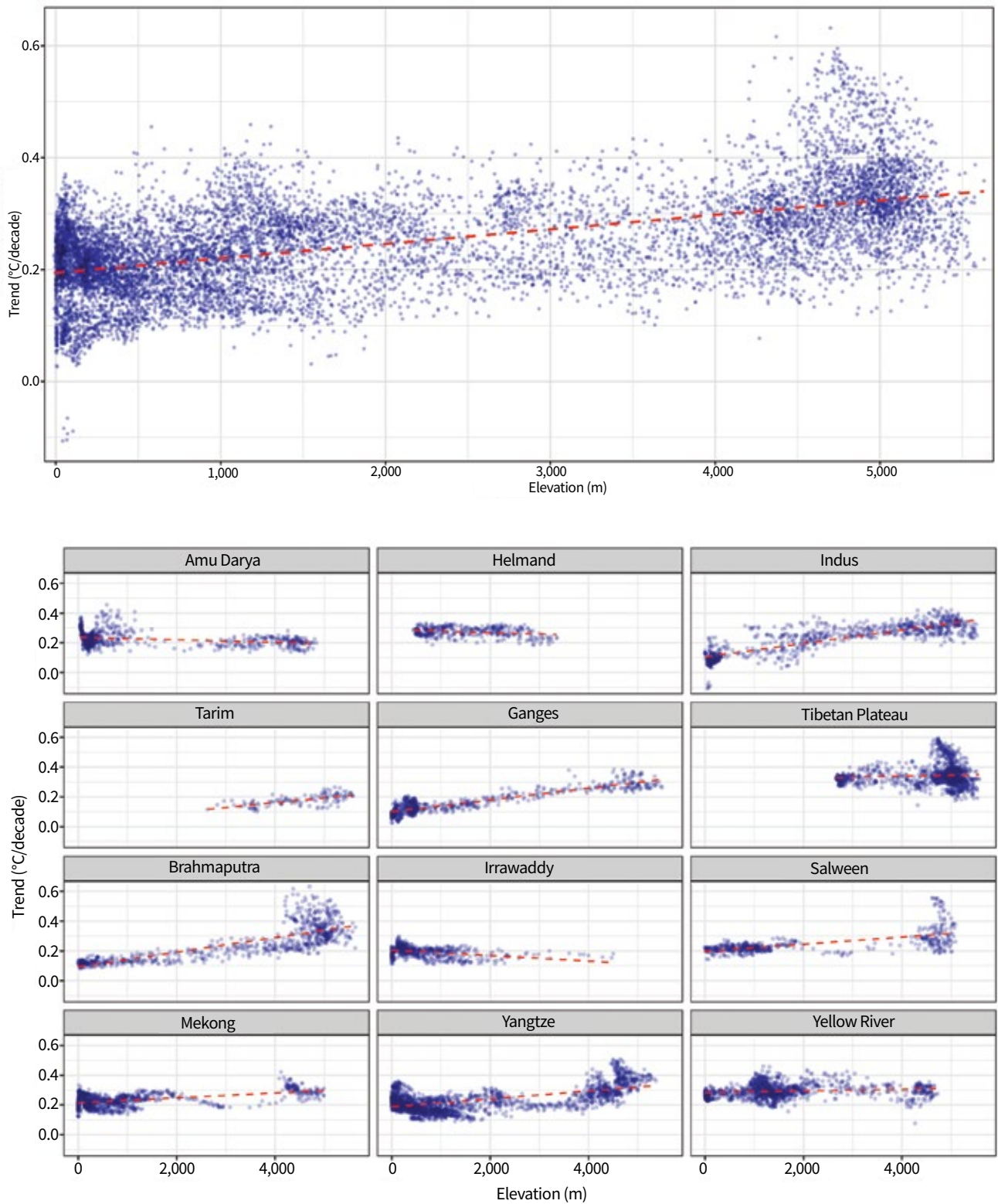
1951–2020. The range in the observed trends for the 12 river basins varies from +0.15°C per decade to +0.34°C per decade for the same period. The observed trend was up to +0.66°C per decade in parts of the Tibetan Plateau, Brahmaputra, Amu Darya, and the headwaters of the Mekong and Yangtze basins (Figure 2.2, bottom). This agrees with the analyses of observed changes and reanalysis products for the few areas of the HKH where data are available (Chhetri et al., 2020; Ren et al., 2017; Q.-L. You et al., 2017). Kraaijenbrink et al. (2021) also found similar trends (0°C–0.6°C per decade) in the mean temperature using the ERA5 dataset over the HKH region for the period 1979–2019. The mean temperature trend is non-significant in some regions of the Indus, Ganges, and Tarim basins. The strongest trends are observed for the Tibetan Plateau, Amu Darya, and Brahmaputra basins, and the headwaters of the Mekong and Yangtze basins. The results also show temperatures to be decreasing over northern India, but those trends are influenced by air pollution (aerosols) and land-use change (for example, irrigation) (Jia, et al., 2019).

2.2.3. Elevation-dependent warming

The ERA5 dataset for the period 1951–2020, including the trends in average temperatures at higher elevations, shows that the rate of warming is amplified with elevation (Figure 2.4). Here, grids where the values are significant at a 0.01 level (considered highly significant) have been used for the analysis. Areas of higher elevation (>4,000 m) show a greater decadal warming trend (~0.34°C per decade) than areas of lower elevation (<2,000 m) (~0.20°C per decade) for the whole of the HKH (Figure 2.4, top). Figure 2.4 (bottom) shows the decadal trends for the 12 major river basins of the HKH. The *Hindu Kush Himalaya assessment* report also documented the elevation dependence of the climate warming signal. A greater increase in winter mean temperature was seen, up to 0.6°C in high-elevation areas (>2,000 m) of the Tibetan Plateau, in comparison to low-elevation areas (<2,000 m) (Krishnan et al., 2019). Elevation-dependent warming (EDW) is observed in 9 out of 12 major river basins in the HKH with the strongest amplification

FIGURE 2.4

SCATTER PLOTS OF SIGNIFICANT DECADAL TEMPERATURE TRENDS WITH ELEVATION FOR THE PERIOD 1951–2020 FOR THE HKH (TOP) AND ITS 12 MAJOR RIVER BASINS (BOTTOM)



with elevation in the Brahmaputra Basin. Similar EDW is observed for the Ganges, Yangtze, and Indus basins. The Mekong, Tibetan Plateau, Salween, Yellow River, and Tarim basins also show EDW but to a lesser extent. However, in the Amu Darya, Irrawaddy, and Helmand basins, the warming trends are higher in low-elevation areas than at higher altitudes.

2.2.4. The complexity of extreme events

Extreme events can have severe consequences for nature and society, according to the contribution of Working Group I (WGI) to the *Sixth assessment report (AR6)* of the Intergovernmental Panel on Climate Change (IPCC) (IPCC, 2021). The term 'extreme events' generally refers to a wide class of phenomena that historically have taken place only infrequently but with 'great force'. In the context of climate, an extreme weather event is defined in the AR6's WGII glossary (IPCC, 2022b) as 'an event that is rare at a particular place and time of year. Definitions of "rare" vary, but an extreme weather event would normally be as rare as or rarer than the 10th or 90th percentile of a probability density function estimated from observations. The characteristics of what is called extreme weather may vary from place to place in an absolute sense.'

Many phenomena that are considered extreme weather events are difficult to study due to a lack of reliable observations. For the climate in the HKH region, relevant extreme events include heatwaves, extreme precipitation, extreme snowfall, and typhoons, hence extreme precipitation and temperature events. However, they may also include 'compound events' in which several factors coincide and can lead to cascading risks. An example of such a compound event is high temperature that causes rapid snowmelt simultaneously with high rainfall. A recent example of a compound event combining a heatwave and high precipitation is the 2022 summer floods in Pakistan that had devastating consequences downstream.

The risk of heavy rainfall that may lead to flooding and mudslides (Fowler et al., 2021) is influenced both by the mean rainfall intensity (wet-day mean precipitation) as well as how often it rains (wet-day frequency). A recent analysis suggests that the probability of receiving more than 50 mm of rainfall

in a day has increased over Europe and the USA, where daily rain gauge data are readily available, and the increased risk is mainly attributable to higher mean rainfall intensities (Benestad et al., 2019). In the HKH region too, extreme precipitation is expected as the result of either more intense precipitation events, more days with precipitation, or a combination of both higher intensity rainfall and more rainy days.

An analysis of global rainfall patterns suggests that they have undergone dynamic changes over the period 1950–2020, leading to more concentrated and intense events, and that these changes seem to match the evolution in global mean temperature (Benestad et al., 2022; Bove et al., 2022; Fowler et al., 2021). This suggests that the rainfall amounts increase and become more extreme as (i) higher temperatures near the surface favour higher rates of evaporation and a faster turnaround of the global hydrological cycle, and (ii) because the rainfall is becoming more unevenly distributed and concentrated in localised wet spots.

According to Hock et al. (2019), even a low emissions climate projection suggests future increases in annual precipitation in the HKH of 5%–20% over the twenty-first century. Changes in the frequency and intensity of extreme precipitation events vary according to season and region. For example, the frequency and intensity of extreme rainfall events are projected to increase throughout the twenty-first century across the Himalayan–Tibetan Plateau mountains, particularly during the summer monsoon (Panday et al., 2015; Sanjay et al., 2017). This suggests a transition toward more episodic and intense monsoonal precipitation, especially in the easternmost part of the Himalayan range (Palazzi et al., 2013). At higher elevations, where local warming is insufficient to affect rain–snow partitioning, increases in total winter precipitation can lead to more snowfall; the *IPCC special report on the ocean and cryosphere in a changing climate* (Hock et al., 2019) has attributed 'medium confidence' to this finding.

Changing rainfall patterns and more frequent extreme events call for adaptation to a changed future climate in order for societies to cope (IPCC, 2022a). Climate change adaptation requires local or regional climate information. However, global climate models used for providing future outlooks (projections) are designed only to reproduce large-scale aspects of the Earth's climate system. Most extreme events occur at more

regional or local spatial scales. Having said that, the local climate is nevertheless dependent on the large-scale atmospheric circulation in addition to local geographical conditions. Information about these dependencies can be added to information we can draw from the global climate models themselves. The introduction of additional information concerning scale dependencies in climate research is called 'downscaling' (Benestad, 2016), but neither the global model nor downscaling (especially one single downscaling method) provides perfect information. Thus, it is important to use more than one strategy for downscaling (both dynamic and empirical–statistical) and to evaluate all steps of the process, from the global climate models to the downscaling methods. It is also important to take into account the presence of pronounced, natural regional climate variations that are chaotic, unpredictable, yet well-captured by global climate models (Deser et al., 2012), and to downscale a large selection of independent global climate model simulations in order to get robust results.

IPCC (2022a) also states, with medium confidence, that there have been increases in climate- and weather-related disasters in mountain regions over the last three decades, and that the frequency of such disasters has shown an increasing trend in the HKH. It is expected that changes in ice and snowmelt, seasonal increases in extreme rainfall, and the thawing of permafrost, all of which are projected for

the future with high confidence, will favour chain reactions and cascading processes that can have devastating effects downstream, well beyond the site of the original event (Beniston et al., 2018; Cui & Jia, 2015; Shugar et al., 2021; Terzi et al., 2019; Vaidya et al., 2019). Such effects involve both extreme events and their consequences for the cryosphere, as extreme temperatures affect conditions for thawing and freezing. Cascading hazards are discussed in Chapter 3, subsection 3.2.2.

The incidence of disasters is expected to worsen in the future due to some hazards becoming more pervasive, and also because the exposure of people and infrastructure is expected to increase with future environmental and socio-economic changes, both of which will deepen the disaster risks. For instance, in the Technical Summary of AR6's WGI report, Arias et al. (2021) observe, with medium confidence, that extreme precipitation is expected to increase in major mountain regions, with consequences such as increased floods and landslides. Rain-on-snow events intensify floods and result in widespread consequences for societies, and their recurrence is expected to increase (Hock et al., 2019). There is also high confidence that glacier retreat, slope instabilities, and heavy precipitation will affect the occurrence of landslides and floods, although there is considerable uncertainty in the direction of change regarding landslides (IPCC, 2021).

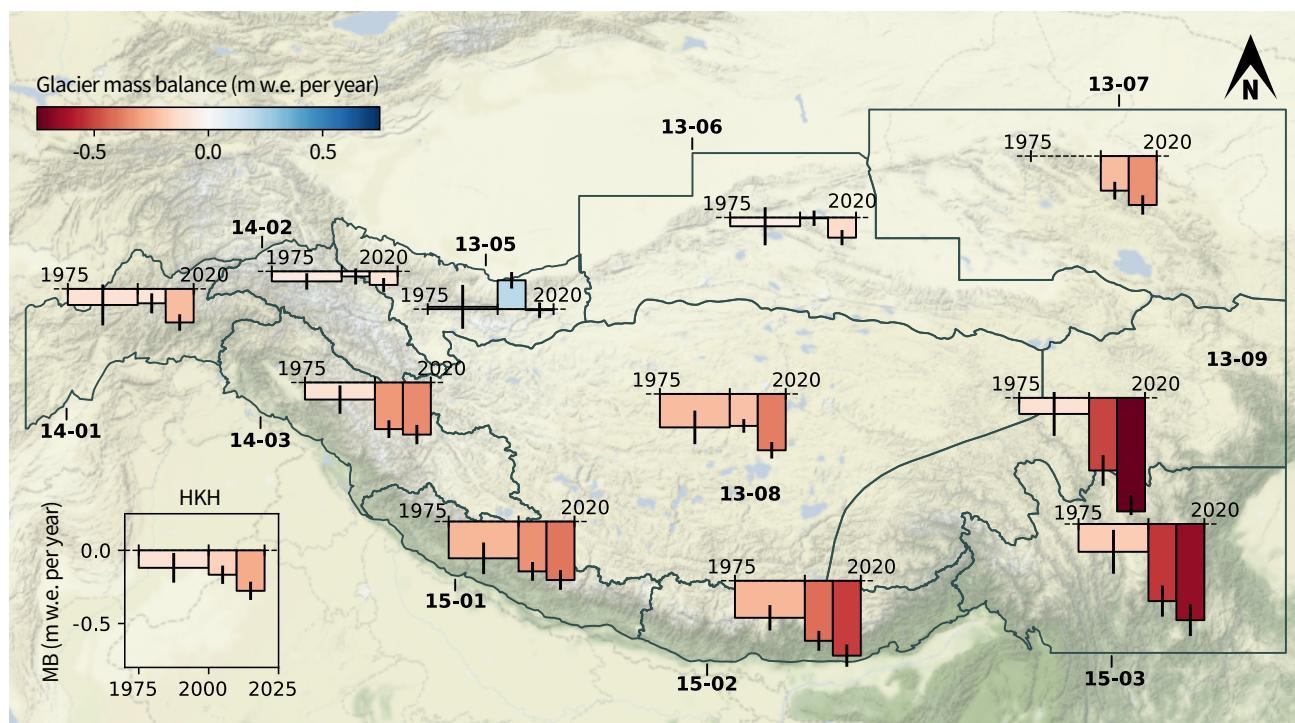
2.3. Glaciers

Glaciers are recognised as identifiers of climate change (Hock et al., 2019), with changes in mass clearly indicative of their response to changes in temperature especially, as well as to snowfall and other meteorological variables. Their contribution to streamflow varies in the extended HKH, from being relatively high in its western parts (Indus, Amu Darya) to a more limited contribution in the eastern parts (Ganges, Brahmaputra) (Lutz et al., 2014). Glaciers play an important role during droughts in maintaining streamflow (Pritchard, 2019). Since the publication of the *HKH assessment report* (Bolch et al., 2019), major advances in the monitoring and understanding of

glaciers in the HKH have been achieved. For example, mass changes between the 1970s and 2020 of large glacier-covered areas of the HKH have been quantified with unprecedented accuracy (King et al., 2019; Maurer et al., 2019; Zhou et al., 2018). Additionally, the sensitivity of glacier mass balance to meteorological variables has been assessed in different regions of the HKH (Sakai & Fujita, 2017; R. Wang et al., 2019). Nevertheless, knowledge gaps remain, and this report enables them to be refined and identifies which scientific questions ought to be prioritised in future (section 2.7).

FIGURE 2.5

GEODETIC MASS BALANCE OF GLACIERS IN EACH REGION OF THE HKH AND FOR THE WHOLE REGION (INSET) FOR 1975–1999, 2000–2009, AND 2010–2019



Notes and sources: The size of the bars and their colour depend on changes in the average mass balance, expressed in metres water equivalent per year (m w.e. per year). The vertical black lines show the uncertainty. The bold numbers beside each basin give the glacier region in the Randolph Glacier Inventory. For 1975–1999, we rely on a compilation of data from the literature; for the other periods, we rely solely on Hugonnet et al. (2021). Note that the spatial coverage for 1975–1999 is generally much lower than for the following two periods, during which the spatial coverage is always higher than 92% of the total glacier-covered regional area (see Table 2.2 for the spatial coverage for each region). The source data used to compile the region-wide mean mass balances for 1975–1999 are listed in Appendix 1.

TABLE 2.2

REGION-WIDE GLACIER MASS BALANCES FROM DIFFERENT REGIONS IN THE HKH OVER THE PERIODS 1975–1999, 2000–2009, AND 2010–2019

| Region | Glacier area (km ²) | 1975–1999 (m w.e. per year) | 2000–2009 (m w.e. per year) | 2010–2019 (m w.e. per year) |
|--|---------------------------------|-----------------------------|-----------------------------|-----------------------------|
| 13-05 (West Kunlun) | 8,141 | 0.02 ± 0.14 (2,356) | 0.20 ± 0.05 | -0.01 ± 0.04 |
| 13-06 (East Kunlun) | 3,254 | -0.06 ± 0.12 (642) | -0.01 ± 0.04 | -0.14 ± 0.04 |
| 13-07 (Qilian Shan) | 1,640 | N. A. (0) | -0.24 ± 0.05 | -0.33 ± 0.06 |
| 13-08 (Inner Tibet) | 7,923 | -0.23 ± 0.10 (1,947) | -0.22 ± 0.04 | -0.39 ± 0.05 |
| 13-09 (South-east Tibet and Nyainqentanglha) | 3,876 | -0.11 ± 0.14 (1,055) | -0.50 ± 0.09 | -0.78 ± 0.10 |
| 14-01 (Hindu Kush) | 2,941 | -0.11 ± 0.13 (841) | -0.10 ± 0.06 | -0.23 ± 0.05 |
| 14-02 (Karakoram) | 22,881 | -0.07 ± 0.05 (10,694) | -0.03 ± 0.05 | -0.09 ± 0.04 |
| 14-03 (Spiti Lahaul – West Himalaya) | 7,776 | -0.12 ± 0.09 (2,155) | -0.32 ± 0.05 | -0.36 ± 0.06 |
| 15-01 (Central Himalaya) | 5,450 | -0.25 ± 0.10 (4,812) | -0.34 ± 0.05 | -0.40 ± 0.06 |
| 15-02 (Eastern Himalaya) | 4,904 | -0.25 ± 0.08 (5,129) | -0.41 ± 0.06 | -0.51 ± 0.07 |
| 15-03 (West Nyainqentanglha) | 4,386 | -0.19 ± 0.14 (615) | -0.53 ± 0.10 | -0.66 ± 0.10 |
| HKH | 73,173 | -0.12 ± 0.18 (30,246) | -0.17 ± 0.05 | -0.28 ± 0.05 |

Notes: Region numbers follow the Randolph Glacier Inventory (RGI) numbering. For 1975–1999, the area covered by the different studies is indicated in brackets (in km²). Note that the spatial coverage for 1975–1999 is generally much lower than for the following periods, during which the spatial coverage is always higher than 92% of the total glacier-covered area. Some areas have been counted twice for the 1975–1999 period, leading to a total surveyed area larger than the glacier-covered area in the region 15-02. The term m w.e. per year refers to metres water equivalent per year.

Source data: See Appendix 1.

2.3.1. Observed glacier area, surface velocity, thickness, and debris cover in the HKH

Local and global observations of glacier mass balance and other glacier variables have been steadily increasing since the publication of *The Hindu Kush Himalaya assessment* (Bolch et al., 2019), benefiting both from long-term institutional support for field-based measurements, and from global-scale observations.

Glaciers occupy an area of approximately 73,173 ± 7,000 square kilometres (km²) in the HKH (Sakai, 2019) (Figure 2.1). The revised GAMDAM (Glacial Area Mapping for Discharge from the Asian Mountains) glacier inventory, GAMDAM V2 (Sakai, 2019), is now the consensus inventory from which almost all outlines of RGI 7.0 (Randolph Glacier Inventory Version 7) originate. Regionally homogeneous inventories, such as GAMDAM V2, are used extensively for geodetic and modelling studies at regional to global scales. However, local, and often more detailed, inventories contribute to supplementing and improving the regional

inventories and are thus highly valuable (Mölg et al., 2018; Racoviteanu et al., 2015), especially if multi-temporal and time stamped. Most of the available glacier outlines are accessible through the Glacier Land Ice Measurements from Space database (GLIMS & NSIDC, 2005, updated in 2018), which increases their visibility and availability.

Data regarding glacier surface velocities have become more readily available in recent years. First, NASA's ITS_LIVE (Inter-Mission Time Series of Land Ice Velocity and Elevation) project (Gardner et al., 2022) provides glacier surface velocity data as annual fields for all the glaciers of High Mountain Asia (HMA) at a 120-metre (m) resolution. The velocity fields are derived from the correlation of pairs of Landsat images and span the period 1985–2020. Similarly, Dehecq et al. (2019) derived annual surface velocities for the period 2000–2017 by applying feature tracking to over 900,000 pairs of Landsat-7 images, at a 240-m resolution, for 94% of all glaciers of HMA. However, the annual velocity fields have large voids in the glacier accumulation areas prior to 2013, due to the lack of contrast in textureless areas (Dehecq et al., 2019). Second, Millan et al. (2022) produced a high-

resolution (50-m) map of glacier velocity for the period 2017–2018, based on multi-sensor displacement measurements. The increased resolution is especially helpful for measuring the velocity of small glaciers; however, the velocity is available only for a given time stamp, which does not allow for the exploration of temporal changes in velocity (Dehecq et al., 2019). Using repeat-pass synthetic aperture radar (SAR) data acquired by the Sentinel-1 satellite constellation, Freidl et al. (2021) derived glacier surface velocity fields at a global scale, including all glaciers in the HKH, at up to a 6-day temporal resolution and at a 200-m spatial resolution, independent of weather conditions, daylight, and season.

Ice thickness is a critical parameter to model the future evolution of a glacier. Ice thickness is generally measured using radar sounding (Welty et al., 2020), which is a demanding and costly method. Consequently, very few measurements are publicly available for the region, through the GlaThiDa database (Glacier Thickness Database) for the HKH, only twelve glaciers have had their ice thickness measured and this number rises to 88 for the whole HMA, due to more numerous measurements in central Asia (Welty et al., 2020). Field measurements are complemented by model output estimates, which are based on glacier geometry, the regional field measurements, and incidentally ice surface velocity (Farinotti et al., 2019; Millan et al., 2022). Due to the scarcity of field measurements in HMA, the discrepancy between the two most up-to-date studies is the largest in this region, with the estimate from Millan et al. (2022) being 44% larger than the estimate from Farinotti et al. (2019). Uncertainties are large in both studies, and it is not possible to assess which study provides the best estimates of thickness for glaciers in the HKH, as there are no additional in situ measurements available to validate the two datasets. Both studies are based on an inverse modelling of surface velocities and are probably more accurate than estimates from the GlabTop (Glacier bed Topography) model (Frey et al., 2014). Airborne radar systems are a promising tool to map ice thickness over larger areas of HMA (Pritchard et al., 2020).

Many glaciers in the HKH have debris-covered tongues, whose debris thickness ranges from a few centimetres to more than one metre (Herreid & Pellicciotti, 2020). Depending on the RGI region and inventory considered, debris occupies 6%–19% of

the glacier area in HMA, with the highest coverage in the central Himalaya (Herreid & Pellicciotti, 2020; Scherler et al., 2018). Debris thickness and its properties are important factors in glacier surface mass balance, as thin debris tends to enhance ice melt whereas thick debris reduces ice melt (Nicholson & Benn, 2006). At a global scale, debris is found to reduce sub-debris ice melt by 37%. However, in some regions, similar rates of elevation change on debris-covered and clean-ice glacier tongues have also been observed, partially due to differences in glacier dynamics (Rounce et al., 2021). Field mapping of debris thickness is based primarily on manual excavation, which is extremely time-consuming and demanding. Alternatively, radar sounding allows the measurement of debris thickness, but is still a demanding task. As a consequence, available measurements of debris thickness in the HKH are very scarce (Giese et al., 2021; McCarthy et al., 2017; Nicholson & Mertes, 2017). The extent of debris cover can be mapped from optical and thermal imagery, with some inherent challenges (McCarthy et al., 2022; Rounce & McKinney, 2014).

2.3.2. Observed changes in glacier mass

While changes in glacier length and area show a delayed signal, glacier mass balance responds directly to climate and weather; thus, an assessment of glacier mass balance is essential to understanding climate change (Oerlemans, 2001; Zemp et al., 2019). The mass balance of glaciers has been measured using different methods, including conventional field methods (Østrem & Stanley, 1969), remote sensing methods (Bamber & Rivera, 2007; Brun et al., 2017; Shean et al., 2020), integration of remote sensing and field observations (Muhammad et al., 2019), and a variety of modelling approaches (Azam et al., 2018; Bolch et al., 2019; Shea et al., 2015).

OBSERVED GLACIER CHANGES FROM FIELD MEASUREMENTS

Long-term, continuous, and high-quality series of annual and seasonal mass balance measurements are needed to understand the variability in glacier mass balance under a changing climate (Zemp et al., 2019). Glacier mass balances have been measured using the conventional glaciological method (Østrem &

Stanley, 1969). The huge manual efforts on the ground needed, the high elevations, and harsh weather conditions in the HKH make it difficult to conduct long-term glaciological measurements; hence, the existing in situ studies are mostly of easily accessible, small-sized, and less debris-covered glaciers (Azam et al., 2018; Vishwakarma et al., 2022). Glacier mass balance observations have been conducted on 28 glaciers in the Himalayan Range (Table 2.3), 9 glaciers in the Pamir Range, and 11 glaciers on the Tibetan Plateau (Miles et al., 2021, supplementary Table 1; Yao et al., 2022). Unfortunately, no glacier has been observed for mass balance in the Karakoram. Some of the observations in the HKH are for a year only while some series are intermittent. Chhota Shigri Glacier provides the longest continuous mass balance series – since 2002 – and has had a mean mass wastage of -0.46 ± 0.40 metres water equivalent per year (m w.e. per year) (Mandal et al., 2020). The Mera, West

Changri Nup, Chorabari, Pokalde, Rikha Samba, Trakarding–Trambau, and Yala glaciers comprise the other continuous/ongoing observation series in the Himalaya (Table 2.3). Some of the observed glaciers, for example, Hamtah and Satopanth glaciers, are highly debris-covered and with steep headwalls, where accumulation often occurs through sporadic avalanches and regular accumulation measurements cannot be carried out (Azam et al., 2018). Due to the presence of inaccessible areas and debris cover, and avalanche feeding, the observed mass balance series are often biased, and hence need to be corrected using geodetic mass balance measurements over the same period (Zemp et al., 2015). The mass balance series for Chhota Shigri, Mera, and West Changri Nup glaciers have been systematically checked and corrected (Azam et al., 2016; Sherpa et al., 2017; Wagnon et al., 2020).

TABLE 2.3 FIELD GLACIOLOGICAL MASS BALANCE OBSERVATIONS IN THE HIMALAYA

| Glacier name and location | Area (km ²) | Debris cover area (%) | Period studied | Mass balance (m w.e. per year) | Reference |
|---|-------------------------|-----------------------|-----------------------|--------------------------------|--|
| Eastern Himalaya | | | | | |
| 1. Changmexhangpu, Sikkim, India | 5.6 | 50 | 1979–1986 | -0.26 | GSI (2001) |
| 2. Gangju La, Pho Chhu, Bhutan | 0.3 | Clean | 2003–2004; 2012–2014 | -1.38 ± 0.18 | Tshering & Fujita (2016) |
| Central Himalaya | | | | | |
| 3. AX010, Shorang Himat, Nepal | 0.6 | Clean | 1978–1979; 1995–1999 | -0.69 ± 0.08 | Fujita et al. (2001) |
| 4. Chorabari, Garhwal Himalaya, India | 6.7 | 53 | 2003–2010; 2015–2016 | -0.72 | Dobhal et al. (2013); Dobhal et al. (2021) |
| 5. Dokriani, Garhwal Himalaya, India | 7.0 | 6 | 1992–1995; 1997–2000; | -0.32 | Dobhal et al. (2008) |
| 6. Dunagiri, Garhwal Himalaya, India | 2.6 | ~80 | 1984–1990 | -1.04 | GSI (1991) |
| 7. Kangwure, Xixiabangma, China | 1.9 | Clean | 1991–1993; 2008–2010 | -0.57 | S. Liu et al. (1996); Yao et al. (2012) |
| 8. Mera, Dudh Koshi Basin, Nepal* | 5.1 | Clean | 2007–2019 | -0.41 ± 0.20 | Wagnon et al. (2020) |
| 9. Naimona'nyi, Naimona'nyi region, China | 7.8 | Clean | 2005–2010 | -0.56 | Yao et al. (2012) |
| 10. Pokalde, Dudh Koshi Basin, Nepal | 0.1 | Clean | 2009–2015 | -0.69 ± 0.28 | Wagnon et al. (2013); Sherpa et al. (2017) |
| 11. Rikha Samba, Hidden Valley, Nepal | 4.6 | Clean | 2011–2017 | -0.39 ± 0.32 | Stumm et al. (2021) |

| | | | | | |
|---|------|-------|-----------|--------------|---|
| 12. Satopanth, Alaknanda Basin, India | 19.0 | 58 | 2014–2015 | –2 | Laha et al. (2017) |
| 13. Tipra Bank, Garhwal Himalaya, India | 7.0 | 15 | 1981–1988 | –0.14 | Gautam and Mukherjee (1992) |
| 14. Trakarding–Trambau Rolwaling Region, Nepal | 31.7 | 14 | 2016–2018 | –0.74 | Sunako et al. (2019) |
| 15. West Changri Nup, Dudh Koshi Basin, Nepal* | 0.9 | Clean | 2010–2015 | –1.24 ± 0.27 | Wagnon et al. (2013); Sherpa et al. (2017) |
| 16. Yala, Langtang Valley, Nepal | 1.6 | Clean | 2011–2012 | –0.80 ± 0.28 | Stumm et al. (2021) |

Western Himalaya

| | | | | | |
|---|------|-------|-------------------------|--------------|--|
| 17. Chhota Shigri, Lahaul–Spiti Valley, India* | 15.5 | 3.4 | 2002–2014 | –0.46 ± 0.40 | Azam et al. (2016); Mandal et al. (2020) |
| 18. Hamtah, Lahaul–Spiti Valley, India | 3.2 | ~70 | 2000–2009; 2010–2012 | –1.43 | GSI (2011); Mishra et al. (2014) |
| 19. Gara, Baspa Basin, India | 5.2 | 17 | 1974–1983 | –0.27 | Raina (1977); Sangewar and Siddiqui (2007) |
| 20. Gor Garang, Baspa Basin, India | 2.0 | ~60 | 1976–1985 | –0.38 | Sangewar and Siddiqui (2007) |
| 21. Kolahoi, Jhelum Basin, India | 11.9 | Clean | 1983–1984 | –0.27 | Kaul (1986) |
| 22. Naradu, Baspa Basin, India | 4.6 | ~60 | 2000–2003; 2011–2015 | –0.72 | Koul and Ganjoo (2010) |
| 23. Neh Nar, Jhelum Basin, India | 1.3 | Clean | 1975–1984 | –0.43 | GSI (2001) |
| 24. Patsio, Lahaul–Spiti Valley, India | 2.25 | 10 | 2010–2017 | –0.34 | Angchuk et al. (2021) |
| 25. Rulung, Zaskar Range, India | 1.1 | Clean | 1979–1981 | –0.11 | Srivastava (2001); Sangewar and Siddiqui (2007) |
| 26. Shaune Garang, Baspa Basin, India | 4.9 | 24 | 1981–1991 | –0.42 | GSI (1992); Sangewar and Siddiqui (2007) |
| 27. Shishram, Jhelum Basin, India | 9.9 | Clean | 1983–1984 | –0.29 | Kaul (1986) |
| 28. Stok, Ladakh, India | 0.74 | 5 | 2014–2019 | –0.39 | Soheb et al. (2020) |

Notes: Mass balance uncertainty is included when given in the original source. The asterisk refers to glaciers for which the glaciological and the geodetic mass balances have been compared.

OBSERVED GLACIER CHANGES FROM GEODETIC MEASUREMENTS

Despite a wide range of spaceborne sensors, such as GRACE (Gravity Recovery and Climate Experiment), GRACE-FO (GRACE Follow-On), ICESat (Ice, Cloud, and Land Elevation Satellite), and ICESat-2, measuring changes in mass or elevational changes (X. Wang et al., 2020), most of the recent knowledge about glacier

mass change at the scale of the HKH originates via geodetic measurements from satellite optical photogrammetry. Geodetic measurements consist of measuring changes in glacier volume from observed changes in elevation (Bolch et al., 2011). Elevation data originate from digital elevation models (DEMs), derived either from SAR or optical methods. In the HKH, the most successful methods relied on spy imagery from the 1960s and 1970s (from the satellites

Corona KH-4 and Hexagon KH-9) (for example, Bhattacharya et al., 2021; Bolch et al., 2011; Maurer et al., 2019), and on ASTER (Advanced Spaceborne Thermal Emission and Reflection Radiometer), Worldview, and Pléiades images for the period 2000–present (for example, Bhattacharya et al., 2021; Hugonnet et al., 2021; Shean et al., 2020).

Despite progress made in the automation of processing Kh-9 Hexagon images from the 1970s and 1980s (Dehecq et al., 2020; Maurer et al., 2016), there are still many uncovered areas, in particular on the Tibetan Plateau. The most comprehensive studies focused on the central Himalaya (King et al., 2019; Maurer et al., 2019), the Karakoram (Bolch et al., 2017; Zhou et al., 2017), the eastern Himalaya (Maurer et al., 2016), and the Tibetan Plateau and its surroundings (Zhou et al., 2018). In this assessment, we do not aim to be exhaustive, but consider selected studies with a large spatial coverage. These studies found moderate losses in glacier mass, with an average HKH-wide mass balance of -0.12 ± 0.18 m w.e. per year for the period 1975–2000. Over the same period, the most negative mass balance values are observed in the central and eastern Himalayan regions, of -0.25 m w.e. per year, while some regions are close to balance (Figure 2.5; Table 2.2).

For the period 2000–2019, the most comprehensive results were obtained from time series of the ASTER, Worldview, and Pléiades DEMs, which provided almost complete coverage of all glaciers in the HKH (Brun et al., 2017; Hugonnet et al., 2021; Shean et al., 2020). The three studies are based on different methodologies, that consist of extracting trends of elevation time series. They cover different periods, 2000–2016, 2000–2018, and 2000–2019 for Brun et al. (2017), Shean et al. (2020), and Hugonnet et al. (2021), respectively. Even though the periods covered differ slightly, the results for region-wide mass balances are in good agreement between the three studies. We present the most up-to-date results from Hugonnet et al. (2021) only, which has the advantage of splitting the results into sub-periods of 5/10 years. The rate of mass losses in the HKH accelerated through the study period. The mass balance is -0.17 m w.e. per year for the period 2000–2009 and -0.28 m w.e. per year for 2010–2019. The most negative mass balances are observed in the eastern HKH with the South-east Tibet and Nyainqentanglha regions reaching -0.78 ± 0.10 m w.e. per year for the period 2010–2019, while

the West Kunlun region shows a near-balanced mass budget of -0.01 ± 0.04 m w.e. per year over the same period (Figure 2.5). The Karakoram region, known for its balanced regional mass budget, showed slight wastage of -0.09 ± 0.04 m w.e. per year for 2010–2019. Bhattacharya et al. (2021) also suggested a phase of mass loss of the Karakoram glaciers, especially post-2013. These recent negative mass balance estimates suggest that the ‘Karakoram anomaly’ is probably over.

2.3.3. Projected changes in glacier mass

At the time of publication of the *Hindu Kush Himalaya assessment* report, only a few model runs were available to quantify the future evolution of glaciers in the HKH (Bolch et al., 2019). Coordinated efforts by the glacier community’s Glacier Model Intercomparison Project (known as glacierMIP) to model future glacier changes have led to a significant increase in the number of available projections under different shared socio-economic pathways (SSPs), with nine models now contributing to simulations (Edwards et al., 2021; Marzeion et al., 2020), versus only six models being included in the *Hindu Kush Himalaya assessment* report (Bolch et al., 2019)

PROJECTED CHANGES AT GLOBAL WARMING LEVELS UNDER THE PARIS AGREEMENT

At a global warming level (GWL) between 1.5°C and 2°C mentioned in the Paris Agreement, the glaciers of the HKH are expected to lose 30%–50 % of their volume by 2100 relative to 2015 (Edwards et al., 2021; Kraaijenbrink et al., 2017; Marzeion et al., 2020; Rounce et al., 2020). The corresponding, remaining glacier-covered areas range from 50% to 70%. At this GWL, the losses in glacier mass will be continuous through the twenty-first century. The specific mass balance rate (that is, the annual amount of mass loss and gain) will remain negative, even though it will become less negative by the end of the century, as glaciers retreat to higher elevations.

The regional differences between projected mass losses depend on the present-day mass balance, projected changes in air temperature and precipitation, and various glacier attributes, such as ice thickness (Shea et al., 2015), hypsometry (Miles et al., 2021), debris cover (Kraaijenbrink et al., 2017),

and whether they are lake- or land-terminating glaciers (King et al., 2019), etc. It is difficult to untangle each contribution, but the largest losses in mass and area will happen in areas with the lowest glacier cover. Regions with limited ice coverage (such as the northeastern Tibetan Plateau) will lose up to 70% of their glacier-covered area by 2100 (Kraaijenbrink et al., 2017).

PROJECTED CHANGES AT OTHER GLOBAL WARMING LEVELS

For higher GWLs of +3°C or +4°C, the remaining glacier volume by 2100 will range from 25% to 45% and from 20% to 30%, respectively, relative to 2015 (Edwards et al., 2021; Marzeion et al., 2020). For these GWLs, the specific mass balance rates are more and more negative throughout the twenty-first century, meaning that, on average, the annual mass losses each year are more than the losses of the year before. For a GWL of +4°C, only the heavily glacierised regions of West Kunlun and the Karakoram have a remaining glacier area of about 50% of their area in 2020. All other regions have a glacierised area that is less than 30% of their area in 2020 (Kraaijenbrink et al., 2017).

2.3.4. Towards a better understanding of glacier response to climate change

DRIVERS OF REGIONAL GLACIER MASS CHANGES

There is a growing body of literature that discusses the drivers of the observed glacier mass changes, in particular the contrasting pattern of recent glacier mass balance at the scale of the HKH. Depending on the climatology, glaciers are defined as maritime glaciers if they receive a large amount of precipitation, or as continental glaciers if they are in drier and colder environments. Maritime glaciers are more sensitive to climate change than their continental counterparts. In the HKH, the maritime glaciers of the eastern Himalaya and Nyainqentanglha regions are losing the most mass, while the continental glaciers of West Kunlun are stable (Sakai & Fujita, 2017; R. Wang et al., 2019).

However, the differential sensitivity hypothesis fails to fully explain the gains in glacier mass in the Karakoram and West Kunlun regions, which is referred to as the ‘Karakoram anomaly’ (Farinotti

et al., 2020; Gardelle et al., 2012). The precise physical drivers of the anomaly can be established with only moderate confidence, but some notable drivers are the summer cooling (Forsythe et al., 2017), increased winter snowfall (Norris et al., 2019), higher sensitivity to snowfall (Kumar et al., 2019), and increased irrigation which results in more evapotranspiration, and hence greater snowfall, which has reduced the net energy balance (de Kok et al., 2020). Two main explanations, probably both true and complementary, have been proposed to explain the Karakoram anomaly. A change in the large-scale atmospheric circulation may have contributed to intensified westerlies over this region, leading to more precipitation (Forsythe et al., 2017). And at a regional scale, an intensification of irrigation in the Tarim Basin over the last few decades has enhanced the local/regional convection and thus precipitation over the mountains. However, the persistence of the anomaly in the coming years is uncertain, and the most recent geodetic mass balance measurements hint at the apparent end of the anomaly due to strong increases in summer temperatures (Bhattacharya et al., 2021; Hugonnet et al., 2021).

DEBRIS COVER

As debris cover is an important control of glacier surface mass balance, there is a need to assess whether accounting for debris would modify glacier projections. Several major advances have been made recently in the understanding of the influence of debris and surface features (such as ice cliffs and supraglacial ponds) on the surface mass balance and dynamics of glaciers in the HKH. Maps of debris cover and debris thickness are now available for every glacier in the HKH (Herreid & Pellicciotti, 2020; Rounce et al., 2021; Scherler et al., 2018). A comprehensive mapping of surface features is not yet available, due to the challenges in mapping these small-scale features. The increasing availability of high-resolution multispectral images is a promising development (Kneib et al., 2021). Approaches combining modelling, field measurements, and remote sensing techniques have demonstrated the quantitative importance of ice cliffs and supraglacial ponds, which enhance melt by a factor of between 3 and 13 for ice cliffs (Buri et al., 2021) and between 9 and 17 for supraglacial ponds (Miles et al., 2018) relative to the melting of ice beneath debris.

All these process-based studies feed model parameterisations. Englacial debris transport is now modelled explicitly for individual glaciers (Scherler & Egholm, 2020; Wirbel et al., 2018), or can be parameterised for all the glaciers of the HKH (Compagno et al., 2022; Rowan et al., 2015). Distributed melt model parameterisation has also improved, and such models can now be applied at glacier to regional scales (Kraaijenbrink et al., 2017; Steiner et al., 2021). There are only two studies accounting explicitly for the effect of debris on future glacier evolution in the HKH (Compagno et al., 2022; Kraaijenbrink et al., 2017). Both found that including debris has only a small effect on the regional-scale evolution of glacier volume and area, as long-term, the thinning of debris-covered and debris-free glaciers under a changing climate is similar (Banerjee, 2017). However, for individual glaciers, the models show that the inclusion of debris has a strong influence on the dynamics and timing of glacier retreat.

HIGH-ELEVATION PROCESSES

Other elements of the surface mass and energy balance of glaciers have been investigated in selected places. These studies investigate surface mass balance processes in different regions (Fugger et al., 2022; Mandal et al., 2022). Some of the major uncertainties in surface mass balance are related to the role of turbulent fluxes, and in particular, sublimation (Steiner et al., 2018; Stigter et al., 2018). Wind erosion

(Litt et al., 2019) and refreezing (Saloranta et al., 2019; Stigter et al., 2021; Veldhuijsen et al., 2021) are likely major contributors to the surface mass and energy balance of glaciers and snow, especially at high elevations. However, the lack of automatic weather stations (AWSs) and mass balance measurements limits the applicability of these models to other climate settings. Recent campaigns aimed at installing and maintaining these AWSs might be fruitful, even though they are limited to specific and limited locations (A. Khadka et al., 2022; Matthews, Perry, Koch et al., 2020).

OTHER FACTORS RESPONSIBLE FOR GLACIER MASS CHANGES

Some specific features may also influence the response of glaciers to climate change. Lake-terminating glaciers are known to systematically lose more mass on average than neighbouring land-terminating glaciers (Brun et al., 2019, King et al., 2019; Pronk et al., 2021; Tsutaki et al., 2019). Moreover, the mass budgets of surge type glaciers and non-surge type glaciers are similar overall, showing that such instabilities in flows do not affect the glacier-wide mass balance of glaciers (Gardelle et al., 2013). Nevertheless, when glaciers are in a surging state, mass balance is impacted, negatively or positively, depending on the surge stage (Guillet et al., 2022, King et al., 2021; Sevestre & Benn, 2015).

2.4. Glacial lakes

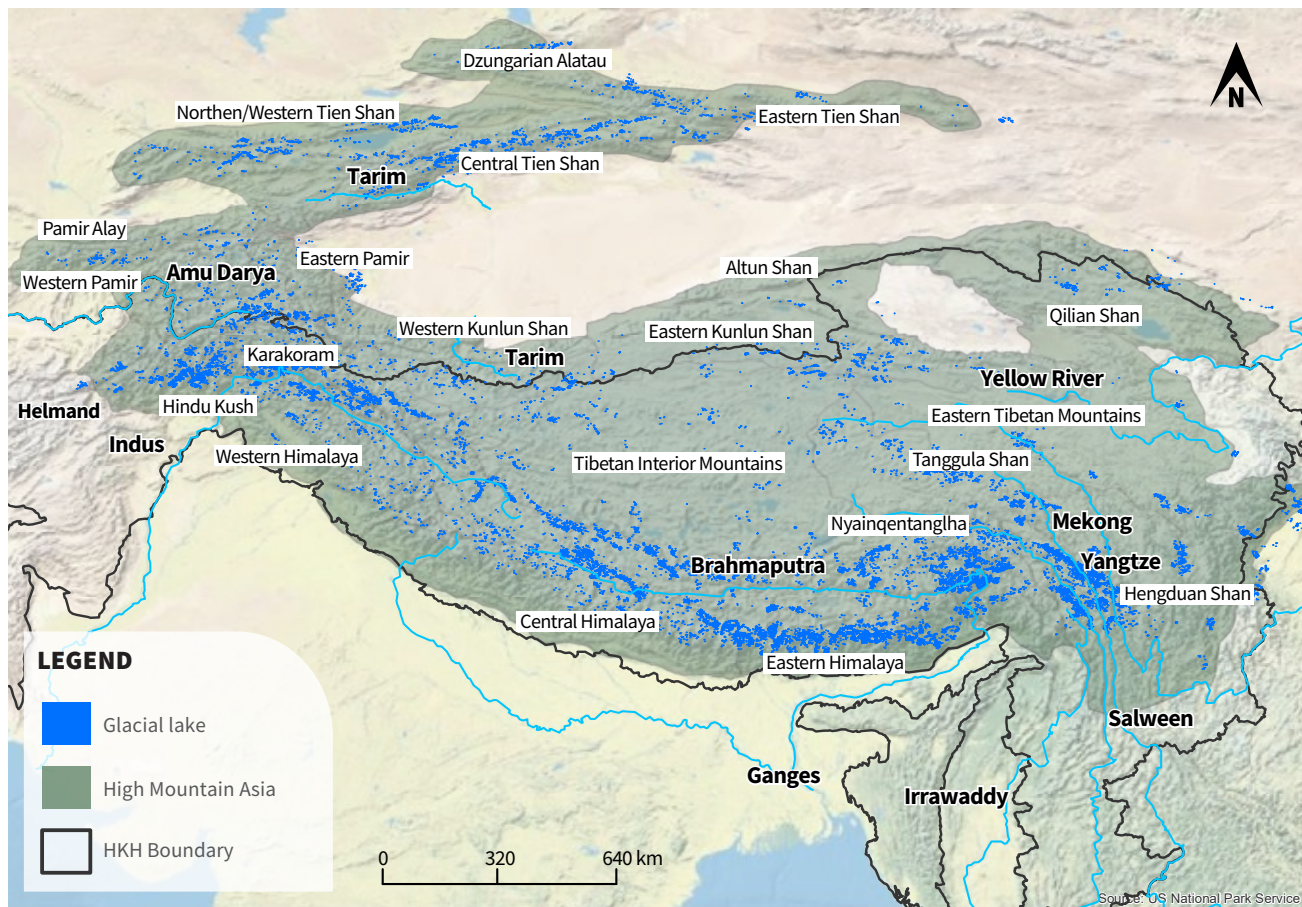
Glacial lakes form from glacial depressions, eroding the soil and sediment around them as they move. Glacial lakes form on the surface of glaciers (generally, debris-covered glaciers) as supraglacial lakes (Miles et al., 2017), behind moraines as proglacial lakes (Carrivick & Tweed, 2013), and beneath glaciers as subglacial lakes or englacial lakes (Livingstone et al., 2022). Some lakes formed during previous glacial recessions since the Little Ice Age from the early 14th to the mid-19th century but are now completely disconnected from the glacial source (Cook & Quincey, 2015). Glacier recession in response to climate change has resulted in an increase in, and expansion of glacial lakes globally (Shugar et al., 2020), in HMA (Cook & Quincey, 2015; Zheng et al., 2021), and in the HKH (Ahmed et al., 2021; W. Li et al., 2022).

Between 1990 and 2018, the number of known glacial lakes globally had increased to 14,394 (a 53% increase), with a total area of $8.95 \times 10^3 \text{ km}^2$ (a 51% increase) and an estimated volume of 156.5 km^3 (a 48% increase) (Shugar et al., 2020). W. Li et al. (2022) identified 9,673 glacial lakes in the HKH in 2020, with an increase in their number by 5,974 and in their area by 409 km^2 in the 30 years since 1990. Across HMA as a whole, 30,121 glacial lakes were mapped in 2018 with an area of $2080.12 \pm 2.28 \text{ km}^2$ (X. Wang et al., 2020) (see Figure 2.6).

Numerous studies have been conducted to map glacial lakes and changes in them over time in HMA and the HKH (Chen et al., 2021; W. Li et al., 2022; Maharjan et al., 2018; X. Wang et al., 2020; Zheng

FIGURE 2.6

DISTRIBUTION OF GLACIAL LAKES IN THE HKH AND THE REST OF HIGH MOUNTAIN ASIA IN 2018.



Source: Glacial lakes data X. Wang et al. (2020), HMA boundary Bolch et al. (2019)

et al., 2021). However, there are still discrepancies in their number and area (see Table 2.4) due to differences in the methodology applied, extent of lake inventory, the threshold size chosen, and delineation techniques used. Recently, an advanced technology based on SAR data and machine learning approaches has been used to identify and map glacial lakes in the HKH and HMA regions (Ortiz et al., 2022; Wangchuk & Bolch, 2020). Unmanned aerial vehicle (UAV) surveys, DEM differencing, time series of SAR data, and Google Earth Engine have been used to monitor and evaluate glacier flow velocity, moraine dam stability, ice-core moraine degradation, and slope stability of the headwalls surrounding glacial lakes (Nuth & Kaab, 2011; Wangchuk et al., 2022). This advanced technology and computing resources enable the development of an integrated approach for monitoring the susceptibility of glacial lakes to glacial lake outburst floods (GLOFs).

Numerous studies have suggested that the total area and number of glacial lakes have increased significantly since the 1990s (Nie et al., 2017; Shugar et al., 2020; G. Zhang et al., 2015; Zheng et al., 2021). The expansion of proglacial lakes as glaciers recede (Zheng et al., 2021), as well as the break-up of glacial snouts (Thompson et al., 2012) drive the increase in

the total area covered by glacial lakes. However, it is not the same for glacial lakes that are separated from glaciers. The development of distant glacial lakes is primarily influenced by regional precipitation, temperature, evapotranspiration, and human factors (C. Guo, 2017). Increased precipitation is most likely the primary driver of lake growth on the Tibetan Plateau (Brun et al., 2020). Based on approaches to modelling the development of future glacial lakes in HMA, a total of 25,285 overdeepenings with a total volume of $99.1 \pm 29.5 \text{ km}^3$ covering $2,683 \pm 812 \text{ km}^2$ was computed (Furian et al., 2021). The number and area of proglacial lakes are anticipated to increase substantially in the future, and lakes become increasingly vulnerable to mass movement (Furian et al., 2021).

Ice-adjacent lakes – as compared to disconnected lakes – can drain rapidly, resulting in the release of a significant volume of water, causing a GLOF that can damage downstream settlements and infrastructure. Many proglacial as well as ice-dammed lakes are expected to develop over the next decade due to continued glacier retreat (Furian et al., 2021; Zheng et al., 2021) with the emergence of new GLOF hotspots (Linsbauer et al., 2016; Zheng et al., 2021). A global database of recorded GLOFs (Lützow and

TABLE 2.4

NUMBER AND AREA OF GLACIAL LAKES IN SPECIFIED REGIONS FOR INDIVIDUAL YEARS, AND CHANGES IN NUMBER AND AREAS OF GLACIAL LAKES FOR DEFINED PERIODS.

| Region | Year/Period | Number | Area (km ²) | Methodology | Reference |
|--|-------------|--------|-------------------------|----------------|------------------------|
| Central Himalaya | 2010 | 1,314 | 197.22 | Semi-automatic | Nie et al. (2013) |
| Eastern, central, and western Himalaya | 2015 | 4,950 | 455.3 | Semi-automatic | Nie et al. (2017) |
| HKH | 2005 | 25,614 | 1,444 | Semi-automatic | Maharjan et al. (2018) |
| HKH | 1990–2020 | 5,974 | 408.93 | Automatic | W. Li et al. (2022) |
| HMA | 2010 | 5,701 | 682.4 | Manual | G. Zhang et al. (2015) |
| HMA | 2015 | 26,633 | 1,968.8 | Semi-automatic | Zheng et al. (2021) |
| HMA | 2016 | 21,249 | 1,577.38 | Automatic | M. Zhang et al. (2021) |
| HMA | 2017 | 15,348 | 1,395.24 | Semi-automatic | Chen et al., (2021) |
| HMA | 2018 | 30,121 | 2,080.12 | Semi-automatic | X. Wang et al. (2020) |
| HMA | 1990–2015 | 1,481 | 125.8 | Semi-automatic | Zheng et al. (2021) |
| HMA | 1990–2018 | 2,916 | 273.65 | Semi-automatic | X. Wang et al. (2020) |
| HMA | 2009–2017 | 3,342 | 220.64 | Semi-automatic | Chen et al. (2021) |

Note: The number and area for a period (such as 1990 – 2020) refers to an increase in these parameters over that time.

Veh, 2022) reports a total of 350 events for the HKH with 325 events occurring in the last 150 years. The majority of GLOFs in the region have occurred from ice- or moraine-dammed glacial lakes (Carrivick & Tweed, 2013; M. Liu et al., 2020, Nie et al., 2017). Most GLOFs in the Karakoram are from ice-dammed glacial lakes (Emmer et al., 2022, Y. Gao et al., 2021), whereas the majority in the rest of the HKH are from moraine-dammed lakes.

The risk of GLOFs occurring in HMA is predicted to triple by the end of the century, with a significant number of potential transboundary GLOFs, primarily in the eastern Himalaya (Zheng et al., 2021). However,

a recent study stated that it is still unclear whether the increase in the number of GLOFs reported globally is associated with warming temperatures or the growing research interest in them and the access to abundant data, even though some previous GLOFs now identified were unreported or unknown earlier (Veh et al., 2022). Despite this ambiguity, a comprehensive study with detailed ground investigations should be conducted to identify potentially dangerous glacial lakes (PDGLs) and prioritise their hazard levels to prevent or reduce the risk, damage, and loss that GLOFs have repeatedly caused to downstream communities.

2.5. Snow

Snow is an essential component of the mountain ecosystem and plays a key role in glacier nourishment and water availability, but also triggers mass movements and floods. Several regions of HMA are more dependent on snowmelt than glacier melt (Kraaijenbrink et al., 2021). Snow monitoring is critical in the HKH, particularly in the spring season, as it is important for daily use by downstream communities (T. Smith et al., 2017) for agriculture, energy, drinking water supply, and industry. Despite the significance of snow (Figure 2.7), its in situ monitoring is scarce in the HKH (Bolch et al., 2019). In particular, the major proportion of the snowpack remains at high elevations and is poorly measured (Smith & Bookhagen, 2018). In contrast, remote-sensing data provide large spatio-temporal coverage and are widely used for snow monitoring on regional and global scales (Desinayak et al., 2022; Hall et al., 2010; Notarnicola, 2022).

2.5.1. Observed and projected changes in snow cover and snow line elevations

Snow cover in the northern hemisphere shows a decreasing trend since the mid-twentieth century – probably due to greenhouse gas emissions and other human influences – with an earlier onset of snowmelt contributing to seasonal changes in streamflows (IPCC, 2022a). The trends in snow cover have been clearly negative in most of the HKH since the early twenty-first century (Ackroyd et al., 2021; Bormann et al., 2018; Desinayak et al., 2022), but there are a few exceptions, including the Karakoram, where the changes have been non-significant (Bilal et al., 2019; Thapa & Muhammad, 2020). There has been a significant decrease in seasonal snow cover during the summer and winter months, as well as a decline from mid-spring through mid-fall, indicating a shift in seasonality (Naegeli et al., 2022). Snow cover days generally declined in all mountain regions globally at an average rate of 5 snow cover days per decade since the mid-twentieth century with most of the changes at lower elevations, attributed to the conversion of solid precipitation to liquid precipitation due to warmer air temperatures in most places, causing an increase in melt throughout (Hock et al., 2019). Most of the river

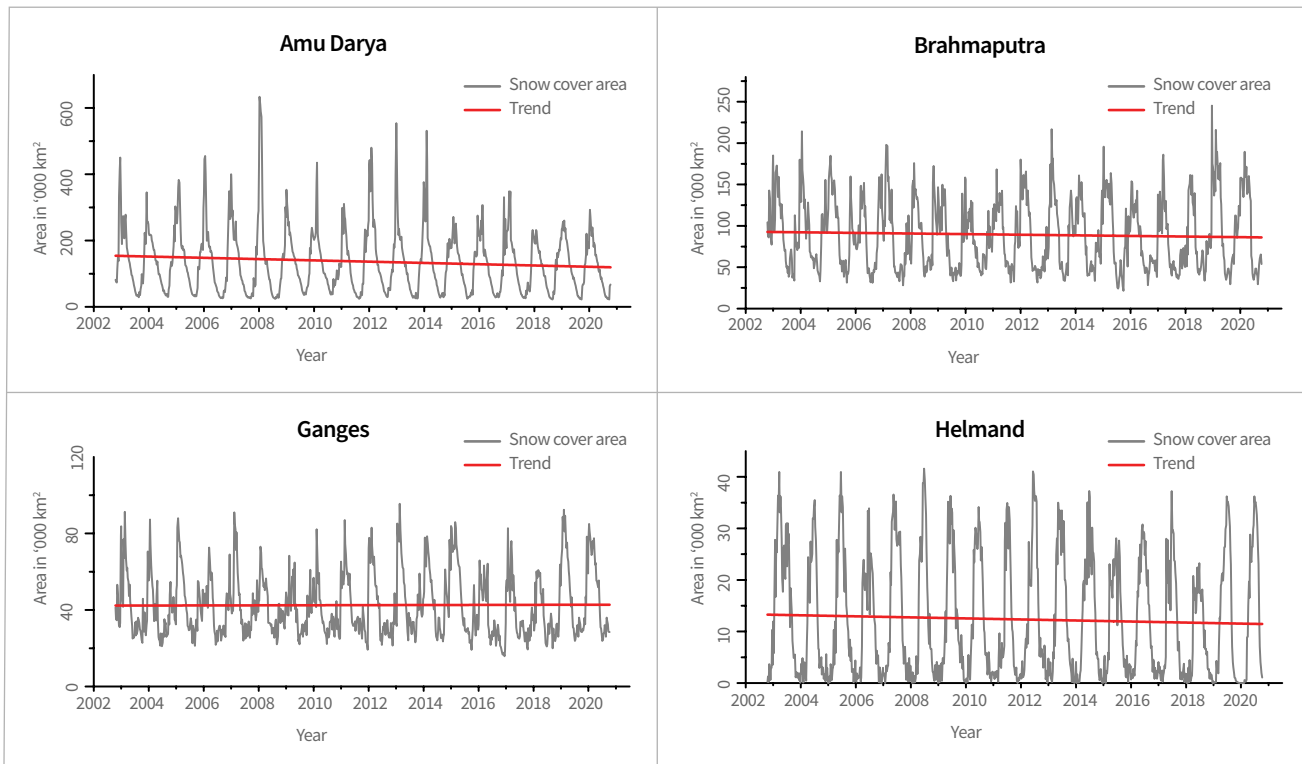
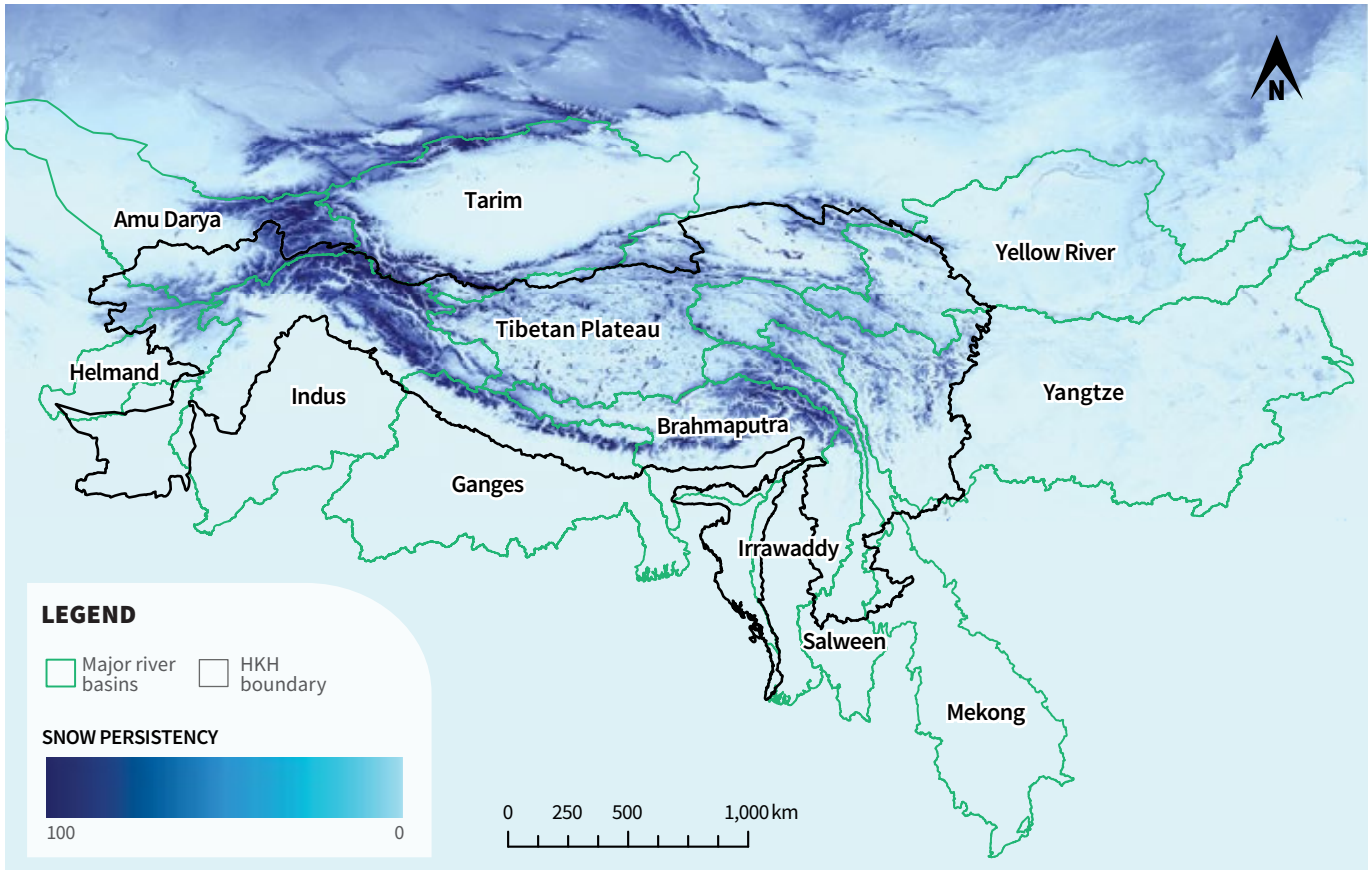
basins show a decreasing snow cover trend between 2003 to 2020 with a heterogeneous pattern on the Tibetan Plateau and the eastern Himalaya (Figure 2.7). The seasonal snow cover also shows significant fluctuations in the Mekong, Salween, Tarim, Tibetan Plateau, Yangtze, and Yellow river basins.

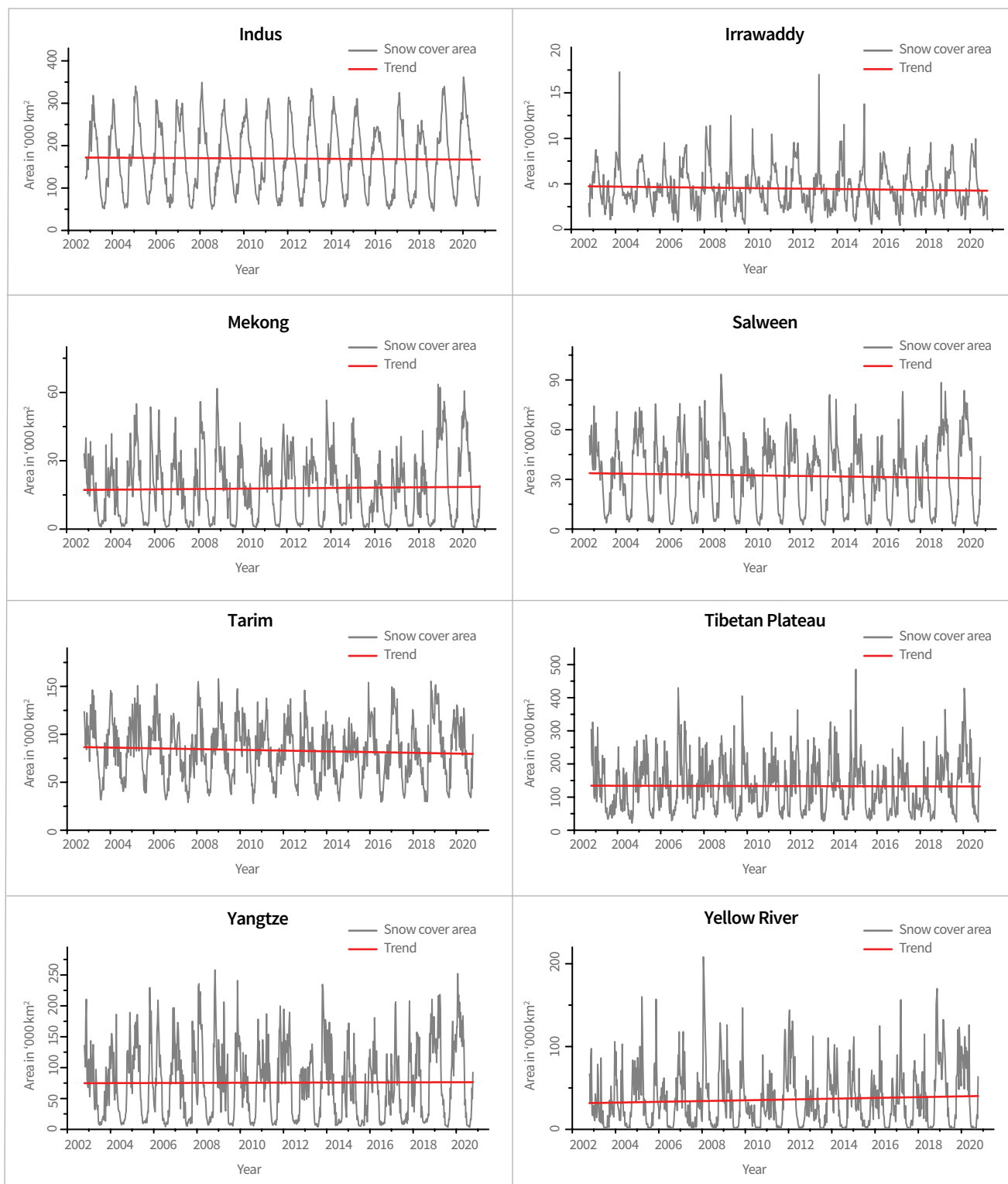
Snow line elevation at the end of the melting season showed a large spatial variability in HMA, with a statistically significant upward shift in 26.3% of its area and a statistically significant downward trend in 0.74% of its area between 2001 and 2016 (Tang et al., 2020). Tien Shan, Inner Tibet, South and East Tibet, eastern Himalaya, and Hengduan Shan experienced a significant shift upward, while there was no clear or significant trend in the Karakoram (Thapa & Muhammad, 2020), Pamir, Hindu Kush, West Kunlun, and the western Himalaya (Tang et al., 2020). The annual maximum snowline altitude, derived from Landsat, fluctuated between 4,917 m and 5,336 m in the Hunza catchment in the Karakoram Region between 2002 and 2016, whereas it fluctuated between 5,395 m and 5,565 m in Trishuli River sub-basin, central Himalaya (Racoviteanu et al., 2019). The regional snowline altitude in HMA generally decreases with an increase in latitude (Tang et al., 2020).

Few projections of future snowpack in the region are available. Snow cover is likely to experience an accelerated loss over the HKH region, including the Tibetan Plateau, under different global warming levels (Kraaijenbrink et al., 2021; Lalande et al., 2021). Nepal et al. (2021) predicted decreasing snow cover across all elevation bands in the Panjshir catchment, Afghanistan under CMIP5 (Coupled Model Intercomparison Project Phase 5) climate scenarios. Snowfall over HMA is projected to decrease by 18.9% and 32.8% under representative concentration pathway RCP4.5 and RCP8.5 climate scenarios, respectively, by the end of the century (Y. Li et al., 2020). Another study suggests that under RCP8.5, snowfall in the Indus Basin will decrease by 30%–50%, in the Ganges by 50%–60%, and in the Brahmaputra by 50%–70% in the last three decades of this century compared to the average snowfall between 1971 and 2000 (Viste & Sorteberg, 2015). With a temperature rise of 2°C, a widespread decrease in snow cover is projected for the northern hemisphere (Thackeray et

FIGURE 2.7

MEAN ANNUAL SNOW PERSISTENCY AND TREND IN SNOW-COVER AREA IN MAJOR RIVER BASINS OF THE HKH DURING 2003–2020 USING CLOUD-FREE MODIS DATA.





Source: Derived from Muhammad and Thapa (2020)

al., 2016) as early as the mid-21st century, which will adversely affect agriculture, energy production, and other sectors. The projected changes in precipitation patterns and the rise in temperatures (Krishnan et al., 2019) will reduce snow cover in the future (Nepal et al., 2021) and cause a shift in the snow line toward higher elevations (Mir et al., 2017).

Much of the current research uses optical remote sensing satellites such as MODIS, Landsat, and Sentinel-2. While the data from these sources can provide a long-term comparison of historical changes in snow cover, cloud cover and polar darkness can affect the results. The use of SAR data from space offers an alternative approach to monitoring snow

cover since it is independent of cloud cover and illumination conditions (Tsai et al., 2019). The existing estimates are also inconsistent in space and time due to variable methodologies and data sources. Furthermore, projections in precipitation are subject to high uncertainty. Future snow projections are likely to have biases when based on projected precipitation. Therefore, the assessment of future changes in snowpack is still subject to a great deal of uncertainty due to a lack of sufficient knowledge regarding underlying physical mechanisms (Q. You et al., 2020).

2.5.2. Measurements and changes in snow depth and snow water equivalent

Despite its significance, snow is one of the most poorly observed components of the cryosphere globally. Assessing snow depth (SD) and snow water equivalent (SWE) remains difficult over the HKH region because of heterogeneous snowpacks and the complex terrain. However, some effort has been made to establish field-based snow stations in the region (Kirkham et al., 2019; Matthews, Perry, Lane et al., 2020; Stigter et al., 2021). These measurements reveal spatio-temporal heterogeneity of the snowpack even in small catchments (Stigter et al., 2017). Emerging evidence suggests an important role for sublimation in the cryosphere of the HKH (for example, Azam et al. [2021]). Stigter et al. (2018) observed 1 mm of snow sublimation per day in the Langtang catchment, Nepal, during the post-monsoon season, which signifies a considerable loss of annual snowfall back to the atmosphere (~21%). Mandal et al. (2022) used a 11-year meteorological record from an AWS on a side moraine (at 4,863 m a.s.l.) of Chhota Shigri Glacier and computed the sublimation amounts to be 16%–42% of total winter precipitation. Research conducted in the Langtang catchment revealed that a significant fraction of snowmelt (>20%) is refrozen within the snowpack (Saloranta et al., 2019; Stigter et al., 2021; Veldhuijsen et al., 2022).

Wind transport and erosion are other key processes that influence the redistribution of snow and glacier mass balance in mountainous terrain. Wind plays a critical role in the sublimation of snow. Meteorological conditions such as low atmospheric pressure, high wind speed, and dry air favour sublimation in high-

elevation areas (Stigter et al., 2018). These studies so far only cover the central (Saloranta et al., 2019; Stigter et al., 2018) and western Himalaya (Mandal et al., 2022) and hence we have limited knowledge about how these processes affect larger basins and regional hydrology. So far, the influence of wind on the redistribution of snow has not been quantified in the Himalaya.

The maximum annual amount of water stored as snow over large regions in HMA decreased significantly during 1979–2019 (Kraaijenbrink et al., 2021). The average of the peak total SWE volume over HMA during 2000–2018, derived from high resolution HMA Snow Reanalysis (HMASR) data, is found to be around 163 km³. The lowest volume is observed in the water year 2001 and the highest in 2005 (Y. Liu et al., 2021). Coarser (25 km × 25 km) passive microwave data from 1987 to 2009 demonstrate the declining trend of SWE in HMA with the most negative trends from mid-elevation zones of most catchments (Smith & Bookhagen, 2018). High-resolution passive microwave data (3.125 km × 3.125 km) from 1987 to 2015 showed a similar decreasing trend but areas with a positive glacier mass balance record, such as the Pamir, Karakoram, Hindu Kush, and Kunlun mountains, experienced an increased volume of snow, particularly during the winter season (Smith & Bookhagen, 2020).

Consensus estimates of future snow depth/mass in the lower elevations of the Himalaya, European Alps, western North America, and subtropical Andes suggest they are projected to decline by 25% by 2050 regardless of GHG emission scenarios, and up to 50% under RCP4.5 and 80% under RCP8.5 by the end of this century (2081–2100) (Hock et al., 2019).

Despite these estimates, information on the spatio-temporal variability of SWE remains highly uncertain in HMA due to its complex terrain and limited field observations (Y. Liu et al., 2021). Most of the regional SD and SWE analysis is based on reanalysis data such as ERA5 and microwave remote sensing products such as AMSR-E (Advanced Microwave Scanning Radiometer-Earth Observing System), which do not provide sufficient information about SWE due to their coarser spatial resolution. High-resolution datasets generated by combining reanalysis data with optical remote sensing products such as HMASR provide a better picture of the spatio-temporal distribution of SWE in HMA but still have limitations in monsoon-dominated regions such as central and eastern

Himalaya due to persistent cloud cover (Y. Liu et al., 2021). Long-term snow mass information is derived from coarse (25-km) resolution images (Larue et al., 2017), excluding mountain areas with high SWE values or requiring bias correction under deep snow conditions (>150 mm SWE) (Pulliainen et al., 2020). The NASA-ISRO SAR (NISAR) mission is likely to reduce many of these uncertainties since it provides images detailed enough to see local changes, and yet has wide enough coverage to identify regional trends (NISAR, 2018).

2.5.3. Observed and projected changes in the snow season and extreme snow events

Snow remains on the ground for longer in the western than the eastern basins of the HKH. The average snow cover duration in five major river basins (Syr Darya, Amu Darya, Indus, Ganges, and Brahmaputra) from 2002 to 2017 was found to be 102 days. The general trends in snow cover duration across HMA indicate a decline in recent years at the rate of 0.844 days per year (Ackroyd et al., 2021). About 78% of mountainous regions globally demonstrate negative trends in snow cover duration, associated with a delayed onset of snowfall and earlier melt in 58% of the area (Notarnicola, 2020). By considering snow cover duration analysis at smaller spatial scales across HMA, the existing broad-scale assessment that uses coarser data could be refined.

Heavy snowfall has increased in recent years. Frequent snowstorms are observed over the Tibetan Plateau and the Himalaya (Fujita et al., 2017; Y. Liu et al., 2021). Anomalous snowfall has the potential to amplify avalanche hazards (Fujita et al., 2017). Such events are predicted to become more frequent and intense in future (Dong et al., 2020).

The contribution of snowmelt to streamflow is expected to diminish in future regardless of the climate scenario; however, the impacts of these changes depend largely on the magnitude of climate change (Kraaijenbrink et al., 2021). The onset of snowmelt is anticipated to occur earlier in the future (Khanal et al., 2021) but its influence

on the seasonality of river run-off in larger rivers may be dampened by increased rainfall. High-elevation catchments in the HKH region, however, are likely to be affected by the reduced snow cover duration and earlier snowmelt, as snow is their major source of water.

2.5.4. Relationship between elevation-dependent warming and snow

The distribution of snow strongly depends on latitude and elevation. The variable altitudinal distribution and melting of snow make it complex to directly compare the relationship between snow and temperature. While snow depth data are in principle suitable for understanding the relationship of snow and EDW, an altitudinal understanding of changes in snow depth is still lacking due to spatio-temporal assessment being limited (Smith & Bookhagen, 2018). The trends in elevation-dependent snow cover and snow depth remain unclear, with no consensus estimates (Q. You et al., 2020). Snow depth remains extremely sensitive to warming and has been observed to have decreased significantly at higher elevations compared to lower elevations on the Tibetan Plateau between 1980 and 2014 (Shen et al., 2021). The length of the snow-cover season is declining at all elevations, with the greatest rate of decline at 4,000–6,000 m a.s.l. in the Himalaya and the Tibetan Plateau (Desinayak et al., 2022).

The high snow cover persistence at higher elevations reduces the effects of the positive feedbacks responsible for EDW at low to middle elevations. Analysing the relationship between snow depth and EDW becomes more complex for extremely high elevations above 5,000 m due to the lack of data, or uncertainty in the models and gridded data in accurately capturing EDW (Y. Gao et al., 2018). Mountainous regions worldwide indicate a decrease in snow-covered area at high elevations and thus the data support a positive relationship between EDW and snow (Notarnicola, 2020), whereas no decline has been observed at similar elevations in the HKH (Desinayak et al., 2022). The relationship between EDW and snow is still not well established in the HKH and requires further investigation.

2.6. Permafrost

Research on mountain permafrost is currently more critical than ever due to climate change leading to a thawing permafrost, with unprecedented consequences (Oliva & Fritz, 2018). A comprehensive review of high mountain permafrost in the HKH region showed that the distribution of permafrost surpasses that of glaciers in almost all of the HKH (Gruber et al., 2017) (Figure 2.1). Estimates of permafrost area for the HKH vary, from 2.25×10^6 km² (Obu et al., 2019) and 2.09×10^6 km² (Gruber, 2012) to 1.19×10^6 km² (Ran et al., 2022). Despite varying estimates from multiple simulations, the wide-ranging presence of permafrost in the HKH is evident. A few existing field-based measurements suggest the existence of considerable areas of permafrost in the cold-arid Himalaya (Wani et al., 2020). As limited field-based evidence exists, rock glaciers are often considered as visual indicators of, and ground-truth data for the occurrence of permafrost in the HKH (Haq & Baral, 2019; Hassan et al., 2021; Khan et al., 2021; Pandey, 2019). This could, however, lead to overestimations of the extent of permafrost because rock glaciers generally represent more suitable premises for the existence of permafrost compared to adjoining ground (Cao et al., 2021).

The possible widespread impacts of a thawing permafrost due to climate change in this region are poorly understood. A broader understanding is necessary to recommend the appropriate adaptation actions to combat the scale and intensity of these impacts.

2.6.1. Observed changes in permafrost

There has recently been an increase in the number of permafrost-related investigations in the HKH. The number of scientific papers published after 2015 exceeds the total sum of research articles published before it. Studies before 2000 do not mention climate change and its impacts. Most of the studies published after 2000 focus on the geomorphological aspects of climate change and permafrost while only a few articles after 2015 discuss the hydrological consequences of a changing permafrost for the region.

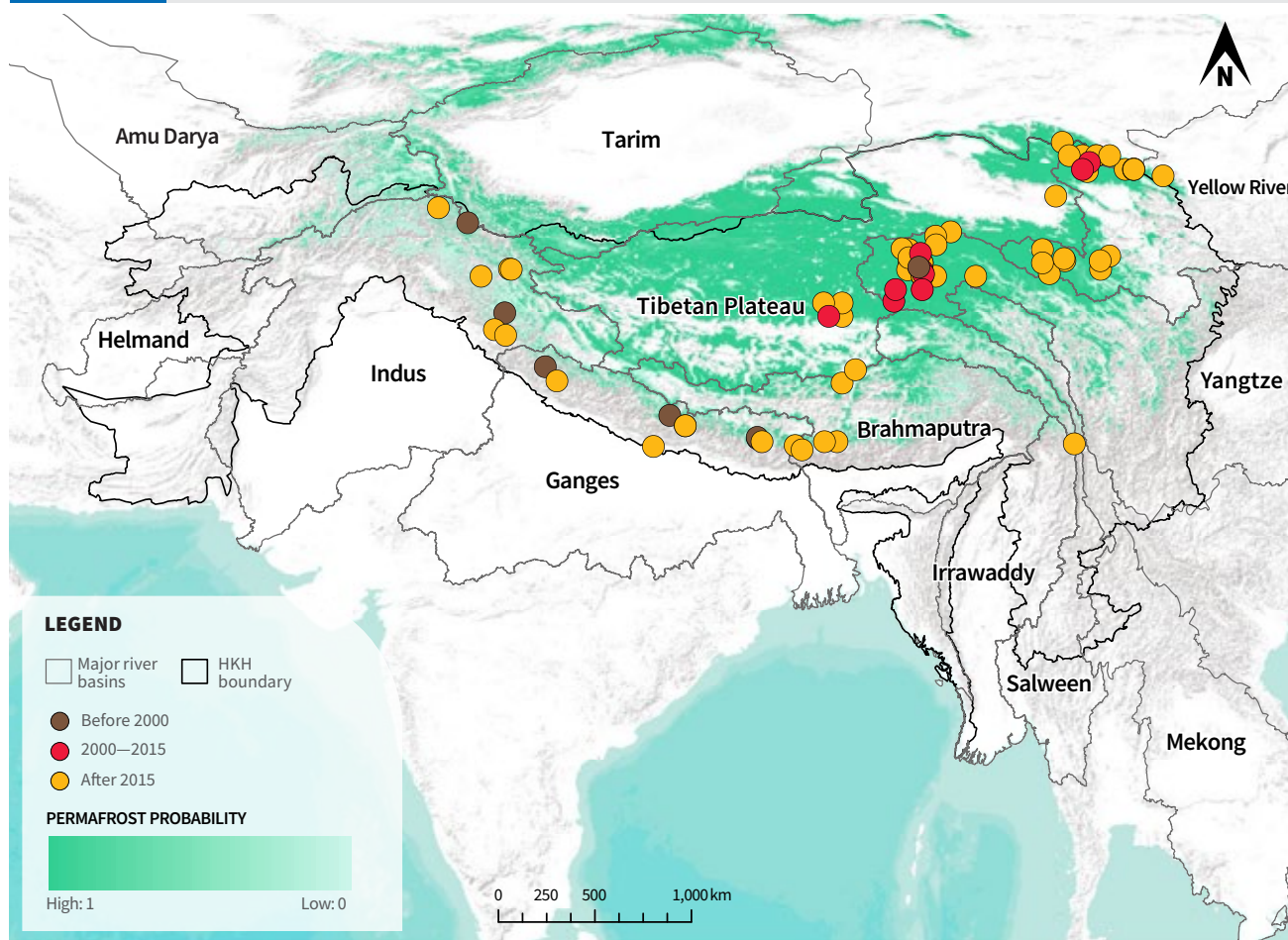
The average global permafrost temperature has increased by $0.29 \pm 0.12^\circ\text{C}$ between 2007 and 2016; the average mountain permafrost temperature increased by $0.19 \pm 0.05^\circ\text{C}$ over the same period (Biskaborn et al., 2019). Prolonged warming has led to permafrost degradation: continuous permafrost zones at lower elevations are turning wet whereas discontinuous permafrost zones at higher elevations are turning dry (H. Jin et al., 2022). Ground-based measurements from a cold and arid Himalayan region conclude that net radiation exerts the strongest influence on the ground thermal regime (Wani et al., 2021). Field observations suggest changes in Himalayan permafrost (Kalvoda & Emmer, 2021). Remote sensing estimates confirm a decrease in permafrost cover in the Indian Himalayan region. A loss of about 8,340 km² in permafrost area was calculated from modelled results for the western Himalaya between 2002–2004 and 2018–2020 (Khan et al., 2021). Another study indicated that the probable areal extent of permafrost decreased from 7,897 km² to 6,932 km² in the Uttarakhand Himalaya between 1970–2000 and 2001–2017 (Baral et al., 2020).

2.6.2. Consequences of changes in permafrost

The number of documents reporting loss and damage resulting from changes in the cryosphere due to climate change are relatively high for the HKH compared to other mountain ranges in the world (Huggel et al., 2019). Hazard assessments in the HKH generally depend on remote sensing for observing permafrost landscape dynamics (Scapozza et al., 2019). Disappearing subterranean ice, transitional permafrost landscapes, and mass wasting associated with a thawing permafrost are increasing threats to high-mountain communities and infrastructure (Haeberli et al., 2017; Huss et al., 2017). More frequent slope failure events in the high mountains can probably be linked to climate change causing subsequent changes in permafrost environments in the HKH. For instance, permafrost bedrock, exposed to thermal perturbation due to continuously amplified warming, could have triggered the Chamoli disaster in the Indian Himalaya in 2021 (Shugar et al., 2021).

FIGURE 2.8

OVERVIEW OF PERMAFROST AREA AND RESEARCH IN THE HKH



Notes: Articles representing permafrost research in the region were selected based on a systematic review. Dots indicate where investigations have been carried out, with different colours corresponding to the years of the study. Specific coordinates for latitude and longitude mentioned in the articles were plotted as dots. For studies where coordinates were mentioned as a range, mean values were taken.

Source: Obu et al. (2019) for permafrost area

In the HKH, permafrost hazards are reported mostly for the Karakoram, followed by the Himalaya (Ding et al., 2021). For example, changes in permafrost account for about 30% of road damage in the Qinghai-Tibetan Plateau. Mass wasting events, associated with permafrost degradation, will increase in future. It is anticipated that damage to infrastructure associated with permafrost degradation could cost several billion US dollars by 2100 globally (Hjort et al., 2022); such impacts on infrastructure are already visible in the HKH.

Seasonal ground deformation along the engineering corridor on the Qinghai-Tibetan Plateau fluctuated between -20 and +10 mm per year during 2015-2018 compared to -5 mm and +5 mm per year during 1997-1999 (Z. Zhang et al., 2019); recently developing

thaw slumps in permafrost areas can be linked to these increasing ranges in deformation. Seasonal slope deformations in permafrost sites at low elevations in the Bhutan Himalaya ranged from 5 mm to 17 mm in 2007-2011 (Dini et al., 2019), with maximum deformation occurring during the summer. The same study suggests that on gentle slopes and in high-elevation areas, the mean freeze-thaw related displacement was 10 mm, and the maximum deformation reached up to 28 mm; these deformations could be linked to changes in the groundwater table.

In the HKH, a thawing permafrost is responsible for changes in hydrology, increased sediment flux, and subsequent changes in the carbon cycle (H. Gao et al., 2021; D. Li et al., 2021). On the Tibetan Plateau,

changes in permafrost govern the hydrological equilibrium of thermokarst lakes, with significant spatial as well as temporal differences in hydrological regimes of thermokarst lake systems anticipated under continued warming and thawing of permafrost (Y. Yang et al., 2021).

Changes in permafrost impact the plant community through variations in soil moisture content, the groundwater table, biogeochemical cycles, and microbial species, eventually causing shifts in the composition and distribution of vegetation (X. Jin et al., 2021). On the Tibetan Plateau, climate change has led to an increase in above-ground net primary production (ANPP) in wet permafrost areas and a decrease in ANPP in dry non-permafrost areas (Yang et al., 2018). Climate change will almost equally affect the production and release of greenhouse gases from the active layer as well as greater depths of permafrost on the Tibetan Plateau (Mu et al., 2018).

This indicates that water availability – in a warming climate and changing permafrost conditions – will be crucial for biodiversity and ecosystem functioning on the Tibetan Plateau. Further, projections regarding the distribution of native plant species through to 2050 (J. You et al., 2018) indicated that the species could shift to higher elevations in search of appropriate habitats. However, many plant species could also adapt to different habitat conditions under changing permafrost conditions.

The management of freshwater stored in rock glaciers in permafrost regions of the HKH could be important under future climate change contexts as rock glacier meltwater streams could significantly contribute to downstream regions (Jones et al., 2019). For example, the Himalayan region of Nepal has more than 6,000 rock glaciers, covering an area of about 1,371 km² potentially storing 16.72–25.08 billion m³ of water (Jones et al., 2018). However, little is known about the consequences of thawing rock glaciers on downstream water quality in the HKH (Colombo et al., 2018).

In addition to overuse, continuously rising temperatures and a thawing permafrost are considered responsible for the gradual decline in the growth of the Himalayan caterpillar fungus, a valuable biological resource (Hopping et al., 2018).

2.6.3. Projections for permafrost

Although regional variations exist, there has been a consistent rise in the average temperature of high mountain permafrost worldwide since the 1980s (S. Smith et al., 2022); for several permafrost regions, the highest annual temperatures were observed in 2018–2019. Projections indicate that this warming and thawing will persist, but their degree and duration may differ for different regions. When projections of permafrost degradation for multiple RCPs (RCP2.6, RCP4.5, and RCP8.5) are compared, results indicate the largest areal degradation in 2010–2140, 2040–2070, and 2070–2100 for RCP8.5 (S. Zhao et al., 2022). Permafrost areas highly likely to degrade are distributed in East Asia and West Asia.

A recent study suggests that alpine permafrost (permafrost at high mountain elevations or on mountain plateaux) is more vulnerable to rising temperatures than circumpolar permafrost (Cheng et al., 2022). If the global average temperature was 2°C–3°C higher than the present, nearly 60% of alpine permafrost would be subjected to thawing. About 37.3% of the 0.80–1.28 × 10⁶ km² area of the Qinghai–Tibetan Plateau underlain by permafrost is endangered (Ni et al., 2021). Projections under RCP8.5 predict a reduction of approximately 42% in permafrost area by 2061–2080.

A recent permafrost map of the Tibetan Plateau shows that permafrost distribution could range between 105.47 × 10⁴ and 129.59 × 10⁴ km², with transitional and unstable permafrost areas covering about 42.29 × 10⁴ and 23.80 × 10⁴ km², respectively (Ran et al., 2021). Projections of permafrost distribution on the Tibetan Plateau through the end of the twenty-first century indicate the lowest degradation in 2011–2040 and the highest degradation in 2071–2099 for RCP2.6, RCP4.5, RCP6.0, and RCP8.5 (Lu et al., 2017). The increase in area undergoing permafrost degradation ranges from 12.95% in 2011–2040 for RCP6.0 to 64.31% in 2071–2099 for RCP8.5. Projections of permafrost active layer thickness (ALT) through the end of the twenty-first century (Zhao & Wu, 2019) indicate a significant increase in ALT in the northwestern region of the Tibetan Plateau. Changes in the ALT range from 5 centimetres (cm) to 30 cm in 2011–2040 for RCP2.6, RCP4.5, RCP6.0, and RCP8.5. The active layer thickness is projected to further increase in 2041–2070 and exceed 30 cm in 2071–2099 for warming levels of 3.1°C or higher above the 1981–2010 baseline.

2.7. Major knowledge gaps

The chapter on the cryosphere in *The Hindu Kush Himalaya assessment* report (Bolch et al., 2019) made several recommendations to close knowledge gaps about the cryosphere in the HKH. These are briefly summarised below (noted in *italics*), highlighting where gaps have been closed and where they remain open. Each section then moves to a single paragraph on gaps that have since been identified, and related recommendations.

2.7.1. Glaciers

Glaciers are the component of the cryosphere that receives the most attention in the region, and several of the recommendations have been followed. *Mass changes* have been successfully documented *before 2000* for the region, relying on declassified satellite imagery (Maurer et al., 2019). Similarly, a number of models have been employed to *estimate sub-debris melt* in the region (Rounce et al., 2015; Steiner et al., 2021), also addressing ice melt from features such as cliffs (Buri et al., 2021) and ponds (Miles et al., 2018). Scherler and Egholm (2020) also showed the potential of ice flow models including debris transport. Model intercomparisons have so far not been attempted for any of these approaches, likely also due to the small number of different approaches taken.

A crucial gap remaining is the *paucity of measurements of ice and debris thickness and their melt response throughout a glacier*. Ice thickness data have been collated at a global scale but such estimates for glaciers in the HKH diverge considerably (Farinotti et al., 2019; Millan et al., 2022), with implications for future projections of loss of mass and dynamic behaviour. However, field validation is still lacking. Debris thickness has also been identified as the crucial variable in estimating sub-debris melt and has been computed on a global scale (Rounce et al., 2021). However, measurements from the HKH are scarce (McCarthy et al., 2017; Rounce & McKinney, 2014), with few observations outside the central Himalayan region (Muhammad et al., 2020). The rapid development of satellite technology has made new progress possible, including the observation of seasonal melt from space by relying on repeated radar data from different configurations (Jakob et al., 2021; Scher et al., 2021). The efficient use

of radar data requires more investigation into the relationship between penetration depth of the wave and surface melt on glacier surfaces (G. Li et al., 2021). To understand the dynamic behaviour of ice, investigations into ice temperatures and percolation are crucial but remain rare (Gilbert et al., 2020). Such measurements will be crucial for our understanding of the recently highlighted importance of glacier detachments (Kääb et al., 2021) and break-offs of hanging glaciers (Shugar et al., 2021).

RECOMMENDATIONS

- Field measurements of ice thickness, debris thickness, ice temperatures, and glacier velocity should be continued to further expand field validation of regional and global datasets.
- Better integration of observations of essential glacier processes (such as ice dynamics, glacier calving, debris, and surface features) and models is needed to improve future projections.
- Glaciers should not be studied in isolation but as part of the high-elevation water cycle and more effort should be devoted to integrating advanced glacier models with hydrological models.
- Attribution of glacier change to anthropogenic forcing should be investigated in the region, to make clear where and how climate change manifests itself.

2.7.2. Glacial lakes

Glacial lake risk assessments, including projected changes in lake extent and volume, have been conducted on a regional scale (Furian et al., 2022; Zheng et al., 2021) as well as for more localised cases (N. Khadka et al., 2021; Muhammad et al., 2021; Sattar, Goswami et al., 2021; Sattar, Haritashya et al., 2021). Projections generally refer to an increase in lake volume; however, future sediment fluxes are ignored, and could also lead to aggradation (Furian et al., 2022; Steffen et al., 2022). A standardised approach for hazard and risk assessments is still lacking. Uncertainties in permafrost estimates also hamper hazard projections. While new lake inventories have been compiled and increasingly easy access to satellite imagery makes this possible repeatedly (Chen et al., 2021; X. Wang et al., 2020), estimates of

total lake area and number vary considerably due to different approaches taken and image resolutions used. Manually delineated inventories (X. Wang et al., 2020) capture considerably smaller lakes but are more labour-intensive and subject to operator bias.

Lake level changes have been observed over the past few decades due to glacial melt (Song et al., 2016; Zheng et al., 2021) as an important component of the cryosphere in the southeastern Tibetan Plateau. Secondary effects on ecosystems around, and downstream of these lakes have, however, not been investigated so far.

RECOMMENDATIONS

- UAV surveys of glacial lake dams have been performed but some results are not yet easily available. Studies should investigate dam stability and ice content through in situ (for example, ground-penetrating radar/GPR) surveys.
- Multi-sensor as well as machine-learning approaches should be used to explore the ability to capture all lakes, including small ones and those with varying areas. This would help reconcile previous estimates that diverge widely.
- Lake formation due to glacier calving and the associated positive feedback mechanisms are poorly understood. Observation-based studies linked with modelling are recommended to unravel these mechanisms.
- Field surveys should investigate the secondary effects of changes in lake area on the surrounding geomorphology, ecosystems, and hydrology.

2.7.3. Snow

Estimates of *changes in regional snow line elevations* using optical imagery have received some attention (Girona-Mata et al., 2019; Racoviteanu et al., 2019; Tang et al., 2020). Conversely, studies on the *rain-snow transition* remain rare (Y. Li et al., 2020). However, there have been studies on the *influence of pollution transport on the snow energy balance*. While these would previously often focus on the Tibetan Plateau, work has also been forthcoming on the southern slopes of the HKH (Santra et al., 2019; Skiles et al., 2018). The *monitoring of snow water equivalent using microwave data* has also seen some initial work but is generally still hampered by the coarse resolution of the products and the lack

of ground validation (Smith & Bookhagen, 2018). Similarly, the lack of validation from field sites hampers understanding of the *spatial variability of snowpack changes*. Lievens et al. (2019) showed the potential of Sentinel-1 data for snow depth retrieval from space, which was also validated for sites in the HKH. However, seasonal snow depth changes remain poorly covered in field-based models for a lack of knowledge about specific properties like albedo (Stigter et al., 2021), which makes accuracy in time and space a challenge.

Continuous snow monitoring has been successful in a few locations, showing the potential of multiple sensors on the ground (Bair et al., 2019; Kirkham et al., 2019). However, process understanding of snowpack development remains poor. Initial work has been conducted on sublimation (Gascoin, 2021; S. Guo et al., 2021; S. Guo et al., 2022; Mandal et al., 2022; Stigter et al., 2018) and refreezing (Stigter et al., 2021; Veldhuijsen et al., 2021) but local changes in albedo and wind-driven erosion (Mott et al., 2018) have gained no further attention and should be prioritised. These processes are not only crucial for simulating snowpack evolution and melt but also for a better understanding of avalanche hazards (Reuter et al., 2022; Vionnet et al., 2018). Additionally, the increasing patchiness of snow cover needs further attention, as it has influences on the local surface boundary layer above (Mott et al., 2017), as well as permafrost and the resulting storage capacity of soil below (T. Zhang, 2005).

RECOMMENDATIONS

- More studies need to be conducted on field processes, including wind-blown snow, interception, and the effect of light-absorbing particles on snow.
- Investments in benchmark snow observatories where SWE, snow depth, snowfall, turbulence, and the energy balance are monitored are required to understand key snow processes such as sublimation, refreezing, and the energy balance of the snowpack.
- Studies investigating the effects of a changing snowpack and snow cover on ecosystems should be conducted in different climatic environments.
- High-intensity snowfall events as well as rain-on-snow events in a hazard context need further attention.

2.7.4. Permafrost

The number of permafrost monitoring sites has increased in the HKH, and efforts towards transnational cooperation have increased. Future work should build on these catchment-scale studies and ensure the exchange of data and experience.

As a number of recent hazard events have been associated with a thawing permafrost, systematic documentation of observed changes that may have, or could result in hazards should be carried out in the HKH (Byers et al., 2020; Coe, 2020). Studies that link a changing permafrost to ecosystems, livelihoods, and infrastructure development are lacking in the HKH. Field measurements have been limited to surface and borehole temperature measurements on the Tibetan Plateau (Sun et al., 2020; L. Zhao et al., 2021). Outside of the Tibetan Plateau, surface temperature measurements have been carried out at a few locations whereas borehole measurements have not been attempted.

RECOMMENDATIONS

- Permafrost should be elevated in national discourses on the cryosphere both among the public as well as at multiple government levels to create awareness about its associated challenges.
- In close collaboration with global networks of permafrost researchers, a regional platform should be established that enables collaboration and the exchange of knowledge.

- Dedicated observation sites should be established in the HKH region with a plan for sustainable monitoring.
- Research into the relation between changes in snow and permafrost should be prioritised, as well as how changes in permafrost affect ecosystems, infrastructure, and livelihoods.

2.7.5. Conclusions

Important progress has been made in research on all components of the cryosphere in the HKH in recent years. Monitoring, process understanding, and remote sensing capacities have increased, resulting in an improved understanding of changes in ice, snow, and permafrost as well as associated water resources. Future focus in research should be on making a link between crucial fields within the cryosphere (for example, the effect of a changing snowpack on permafrost) and beyond (for example, the effects of changing glacier melt on livelihoods in the HKH or of changing glacial lakes on ecosystems). While field monitoring should still be promoted and expanded, care should be taken to enable the long-term sustainability of well-instrumented catchments. The rapidly developing remote sensing capabilities need to be closely monitored to make data readily available for research purposes as well as policy support. There is increasing attention to hazards associated with the cryosphere. An assessment of vulnerable livelihoods, infrastructure, and ecosystems should be attempted to enable focused studies on relevant cryospheric processes.

References

- Ackroyd, C., Skiles, S. M., Rittger, K., & Meyer, J. (2021). Trends in snow cover duration across river basins in High Mountain Asia from daily gap-filled MODIS fractional snow covered area. *Frontiers in Earth Science*, 9, Article 713145. <https://doi.org/10.3389/feart.2021.713145>
- Ahmed, R., Wani, G. F., Ahmad, S. T., Sahana, M., Singh, H., & Ahmed, P. (2021). A review of glacial lake expansion and associated glacial lake outburst floods in the Himalayan region. *Earth Systems and Environment*, 5, 695–708. <https://doi.org/10.1007/s41748-021-00230-9>
- Angchuk, T., Ramanathan, A., Bahuguna, I. M., Mandal, A., Soheb, M., Singh, V. B., Mishra, S., & Vatsal, S. (2021). Annual and seasonal glaciological mass balance of Patsio Glacier, western Himalaya (India) from 2010 to 2017. *Journal of Glaciology*, 67(266), 1137–1146. <https://doi.org/10.1017/jog.2021.60>
- Arias, P. A., Bellouin, N., Coppola, E., Jones, R. G., Krinner, G., Marotzke, J., Naik, V., Palmer, M. D., Plattner, G.-K., Rogelj, J., Rojas, M., Sillmann, J., Storelvmo, T., Thorne, P. W., Trevin, B., AchutRao, K., Adhikary, B., Allan, R. P., Armour, K., ... Zickfeld, K. (2021). Technical summary. In V. Masson-Delmotte, P. Zhai, S. L. Pirani, S. L. Connors, C. Pean, S. Berger, N. Caud, Y. Chen, L. Goldfarb, M. I. Gomis, M. Huang, K. Leitzell, E. Lonnoy, J. B. R. Mathews, T. K. Maycock, T. waterfield, O. Yelekçi, R. Yu & B. Zhou (Eds.), *Climate change 2021: The physical science basis. Contribution of working group I to the sixth assessment report of the Intergovernmental Panel on Climate Change* (pp. 33–144). Cambridge University Press. <https://doi.org/10.1017/9781009157896.002>
- Azam, M. F., Kargel, J. S., Shea, J. M., Nepal, S., Haritashya, U. K., Srivastava, S., Maussion, F., Qazi, N., Chevallier, P., Dimri, A. P., Kulkarni, A. V., Cogley, J. G., & Bahuguna, I. (2021). Glaciohydrology of the Himalaya-Karakoram. *Science*, 373(6557), Article eabf3668. <https://doi.org/10.1126/science.abf3668>
- Azam, M. F., Ramnathan, A. L., Wagnon, P., Vincent, C., Linda, A., Berthier, E., Sharma, P., Mandal, A., Angchuk, T., Singh, V. B., & Pottakkal, J. G. (2016). Meteorological conditions, seasonal and annual mass balances of Chhota Shigri Glacier, western Himalaya, India. *Annals of Glaciology*, 57(71), 328–338. <https://doi.org/10.3189/2016AoG71A570>
- Azam, M. F., Wagnon, P., Berthier, E., Vincent, C., Fujita, K., & Kargel, J. S. (2018). Review of the status and mass changes of Himalayan-Karakoram glaciers. *Journal of Glaciology*, 64(243), 1–14. <https://doi.org/10.1017/jog.2017.86>
- Bair, E. H., Rittger, K., Skiles, S. M., & Dozier, J. (2019). An examination of snow albedo estimates from MODIS and their impact on snow water equivalent reconstruction. *Water Resources Research*, 55(9), 7826–7842. <https://doi.org/10.1029/2019WR024810>
- Bamber, J. L., & Rivera, A. (2007). A review of remote sensing methods for glacier mass balance determination. *Global and Planetary Change*, 59(1–4), 138–148. <http://dx.doi.org/10.1016/j.gloplacha.2006.11.031>
- Banerjee, A.: Brief communication: Thinning of debris-covered and debris-free glaciers in a warming climate, *The Cryosphere*, 11, 133–138, <https://doi.org/10.5194/tc-11-133-2017>
- Baral, P., Haq, M. A., & Yaragal, S. (2020). Assessment of rock glaciers and permafrost distribution in Uttarakhand, India. *Permafrost and Periglacial Processes*, 31(1), 31–56. <https://doi.org/10.1002/ppp.2008>
- Benestad, R. (2016). Downscaling climate information. *Oxford Research Encyclopedia of Climate Science*. Retrieved January 2, 2023, from <https://doi.org/10.1093/acrefore/9780190228620.013.27>
- Benestad, R. E., Lussana C., Lutz J., Dobler A., Landgren O. A., Haugen, J. E. Mezghani A., Casati, B., & Parding, K. M. (2022). Global hydro-climatological indicators and changes in the global hydrological cycle and rainfall patterns, *PLOS Climate*, PCLM-D-21-00079R1. <https://doi.org/10.1371/journal.pclm.0000029>
- Benestad, R. E., Parding, K. M., Erlandsen, H. B., & Mezghani, A. (2019). A simple equation to study changes in rainfall statistics. *Environment Research Letters*, 14(8), Article 084017. <https://doi.org/10.1088/1748-9326/ab2bb2>
- Beniston, M., Farinotti, D., Stoffel, M., Andreassen, L. M., Coppola, E., Eckert, N., Fantini, A., Giacomoni, F., Hauck, C., Huss, M., Huwald, H., Lehning, M., López-Moreno, J.-I., Magnusson, J., Marty, C., Morán-Tejeda, E., Morin, S., Naaïm, M., Provenzale, A., ... Vincent, C. (2018). The European mountain cryosphere: A review of its current state, trends, and future challenges. *The Cryosphere*, 12, 759–794. <https://doi.org/10.5194/tc-12-759-2018>
- Bhattacharya, A., Bolch, T., Mukherjee, K., King, O., Menounos, B., Kapitsa, V., Neckel, N., Yang, W., & Yao, T. (2021). High Mountain Asian glacier response to climate revealed by multi-temporal satellite observations since the 1960s. *Nature Communications*, 12, Article 4133. <https://doi.org/10.1038/s41467-021-24180-y>
- Bilal, H., Chamhuri, S., Mokhtar, M. B., & Kanniah, K. D. (2019). Recent snow cover variation in the Upper Indus Basin of Gilgit Baltistan, Hindukush Karakoram Himalaya. *Journal of Mountain Science*, 16(2), 296–308. <https://doi.org/10.1007/s11629-018-5201-3>

- Biskaborn, B. K., Smith, S. L., Noetzi, J., Matthes, H., Vieira, G., Streletskiy, D. A., Schoeneich, P., Romanovsky, V. E., Lewkowicz, A. G., Abramov, A., Allard, M., Boike, J., Cable, W. L., Christiansen, H. H., Delaloye, R., Diekmann, B., Drozdov, D., Etzelmüller, B., Grosse, G., ... Lantuit, H. (2019). Permafrost is warming at a global scale. *Nature Communications*, *10*(1), 1–11. <https://doi.org/10.1038/s41467-018-08240-4>
- Bolch, T., Pieczonka, T., & Benn, D. I. (2011). Multi-decadal mass loss of glaciers in the Everest area (Nepal Himalaya) derived from stereo imagery. *The Cryosphere*, *5*, 349–358. <https://doi.org/10.5194/tc-5-349-2011>
- Bolch, T., Pieczonka, T., Mukherjee, K., & Shea, J. (2017). Brief communication: Glaciers in the Hunza catchment (Karakoram) have been nearly in balance since the 1970s. *The Cryosphere*, *11*(1), 531–539. <https://doi.org/10.5194/tc-11-531-2017>
- Bolch, T., Shea, J. M., Liu, S., Azam, F. M., Gao, Y., Gruber, S., Immerzeel, W. W., Kulkarni, A., Li, H., Tahir, A. A., Zhang, G., & Zhang, Y. (2019). Status and change of the cryosphere in the extended Hindu Kush Himalaya region. In P. Wester, A. Mishra, A. Mukherji, & A. B. Shrestha (Eds.), *The Hindu Kush Himalaya assessment: Mountains, climate change, sustainability and people* (pp. 209–255). Springer Nature Switzerland AG. Retrieved December 5, 2019, from https://doi.org/10.1007/978-3-319-92288-1_7
- Bookhagen, B., & Burbank, D. W. (2006). Topography, relief, and TRMM-derived rainfall variations along the Himalaya. *Geophysical Research Letters*, *33*(8). <https://doi.org/10.1029/2006GL026037>
- Bormann, K. J., Brown, R. D., Derksen, C., & Painter, T. H. (2018). Estimating snow-cover trends from space. *Nature Climate Change*, *8*(11), 924–928. <https://doi.org/10.1038/s41558-018-0318-3>
- Bove, C. B., Mudge, L., & Bruno, J. F. (2022). A century of warming on Caribbean reefs. *PLOS Climate*, *1*(3), Article e0000002. <https://doi.org/10.1371/journal.pclm.0000002>
- Brombierstäudl, D., Schmidt, S., & Nüsser, M. (2021). Distribution and relevance of aufeis (icing) in the Upper Indus Basin. *Science of the Total Environment*, *780*, Article 146604. <https://doi.org/10.1016/j.scitotenv.2021.146604>
- Brun, F., Berthier, E., Wagnon, P., Kääb, A., & Treichler, D. (2017). A spatially resolved estimate of High Mountain Asia glacier mass balances from 2000 to 2016. *Nature Geoscience*, *10*, 668–673. <https://doi.org/10.1038/ngeo2999>
- Brun, F., Treichler, D., Shean, D. & Immerzeel, W. W. (2020). Limited contribution of glacier mass loss to the recent increase in Tibetan Plateau lake volume. *Frontiers in Earth Science*, *8*, Article 582060. <https://doi.org/10.3389/feart.2020.582060>
- Brun, F., Wagnon, P., Berthier, E., Jomelli, V., Maharjan, S. B., Shrestha, F., & Kraaijenbrink, P. D. A. (2019). Heterogeneous influence of glacier morphology on the mass balance variability in High Mountain Asia. *JGR Earth Surface*, *124*(6), 1331–1345. <https://doi.org/10.1029/2018JF004838>
- Buri, P., Miles, E. S., Steiner, J. S., Ragettli, S., & Pellicciotti, F. (2021). Supraglacial ice cliffs can substantially increase the mass loss of debris-covered glaciers. *Geophysical Research Letters*, *48*(6), Article e2020GL092150. <https://doi.org/10.1029/2020GL092150>
- Byers, A. C., Chand, M. B., Lala, J., Shrestha, M., Byers, E. A., & Watanabe, T. (2020). Reconstructing the history of glacial lake outburst floods (GLOF) in the Kanchenjunga Conservation Area, East Nepal: An interdisciplinary approach. *Sustainability*, *12*(13), Article 5407. <https://doi.org/10.3390/su12135407>
- Cao, B., Li, X., Feng, M., & Zheng, D. (2021). Quantifying overestimated permafrost extent driven by rock glacier inventory. *Geophysical Research Letters*, *48*(8), Article e2021GL092476. <https://doi.org/10.1029/2021GL092476>
- Carrivick, J. L., & Tweed, F. S. (2013). Proglacial lakes: Character, behaviour and geological importance. *Quaternary Science Reviews*, *78*, 34–52. <https://doi.org/10.1016/j.quascirev.2013.07.028>
- Chen, F., Zhang, M., Guo, H., Allan, S., Kargel, J. S., Haritashya, U. K., & Watson, C. S. (2021). Annual 30 m dataset for glacial lakes in High Mountain Asia from 2008 to 2017. *Earth System Science Data*, *13*(2), 741–766. <https://doi.org/10.5194/essd-13-741-2021>
- Cheng, F., Garzzone, C., Li, X., Salzmann, U., Schwarz, F., Haywood, A. M., Tindall, J., Nie, J., Li, L., Wang, L., Abbott, B. W., Elliott, B., Liu, W., Upadhyay, D., Arnold, A., & Tripathi, A. (2022). Alpine permafrost could account for a quarter of thawed carbon based on Plio-Pleistocene paleoclimate analogue. *Nature Communications*, *13*, Article 1329. <https://doi.org/10.1038/s41467-022-29011-2>
- Chettri, N., Shrestha, A. B., & Sharma, E. (2020). Climate change trends and ecosystem resilience in the Hindu Kush Himalayas. In A. P. Dimri, B. Bookhagen, M. Stoffel, & T. Yasunari (Eds.), *Himalayan Weather and Climate and their Impact on the Environment* (pp. 525–552). Springer International Publishing. https://doi.org/10.1007/978-3-030-29684-1_25
- Coe, J. A. (2020). Bellwether sites for evaluating changes in landslide frequency and magnitude in cryospheric mountainous terrain: A call for systematic, long-term observations to decipher the impact of climate change. *Landslides*, *17*(11), 2483–2501. <https://doi.org/10.1007/s10346-020-01462-y>

- Colombo, N., Salerno, F., Gruber, S., Freppaz, M., Williams, M., Fratianni, S., & Giardino, M. (2018). Review: Impacts of permafrost degradation on inorganic chemistry of surface fresh water. *Global and Planetary Change*, *162*, 69–83. <https://doi.org/10.1016/j.gloplacha.2017.11.017>
- Compagno, L., Huss, M., Miles, E. S., McCarthy, M. J., Zekollari, H., Dehecq, A., Pellicciotti, F., & Farinotti, D. (2022). Modelling supraglacial debris-cover evolution from the single-glacier to the regional scale: An application to High Mountain Asia. *The Cryosphere*, *16*, 1697–1718. <https://doi.org/10.5194/tc-16-1697-2022>
- Cook, S. J., & Quincey, D. J. (2015). Estimating the volume of alpine glacial lakes. *Earth Surface Dynamics*, *3*, 559–575. <https://doi.org/10.5194/esurf-3-559-2015>
- Cui, P., & Jia, J. (2015). Mountain hazards in the Tibetan Plateau: Research status and prospects. *National Science Review*, *2*(4), 397–402. <https://doi.org/10.1093/nsr/nwv061>
- Dehecq, A., Gardner, A. S., Alexandrov, O., McMichael, S., Hugonnet, R., Shean, D., & Marty, M. (2020). Automated processing of declassified KH-9 Hexagon satellite images for global elevation change analysis since the 1970s. *Frontiers in Earth Science*, *8*. <https://doi.org/10.3389/feart.2020.566802>
- Dehecq, A., Gourmelen, N., Gardner, A. S., Brun, F., Goldberg, D., Nienow, P. W., Berthier, E., Vincent, C., Wagnon, P., & Trouvé, E. (2019). Twenty-first century glacier slowdown driven by mass loss in High Mountain Asia. *Nature Geoscience*, *12*, 22–27. <https://doi.org/10.1038/s41561-018-0271-9>
- de Kok, R. J., Kraaijenbrink, P. D. A., Tuinenburg, O. A., Bonekamp, P. N. J., & Immerzeel, W. W. (2020). Towards understanding the pattern of glacier mass balances in High Mountain Asia using regional climatic modelling. *The Cryosphere*, *14*(9), 3215–3234. <https://doi.org/10.5194/tc-14-3215-2020>
- Deser, C., Knutti, R., Solomon, S., & Phillips, A. S. (2012). Communication of the role of natural variability in future North American climate. *Nature Climate Change*, *2*(11), 775–779. <https://doi.org/10.1038/nclimate1562>
- Desinayak, N., Prasad, A. K., El-Askary, H., Kafatos, M., & Asrar, G. R. (2022). Snow cover variability and trend over the Hindu Kush Himalayan region using MODIS and SRTM data. *Annales Geophysicae*, *40*(1), 67–82. <https://doi.org/10.5194/angeo-40-67-2022>
- Ding, Y., Mu, C., Wu, T., Hu, G., Zou, D., Wang, D., Li, W., & Wu, X. (2021). Increasing cryospheric hazards in a warming climate. *Earth-Science Reviews*, *213*. <https://doi.org/10.1016/j.earscirev.2020.103500>
- Dini, B., Daout, S., Manconi, A., & Loew, S. (2019). Classification of slope processes based on multitemporal DInSAR analyses in the Himalaya of NW Bhutan. *Remote Sensing of Environment*, *233*, Article 11408. <https://doi.org/10.1016/j.rse.2019.111408>
- Dobhal, D. P., Gergan, J. T. & Thayyen, R. J. (2008). Mass balance studies of the Dokriani Glacier from 1992 to 2000, Garhwal Himalaya. *Indian Bulletin of Glaciological Research*, *25*, 9–17.
- Dobhal, D. P., Mehta, M., & Srivastava, D. (2013). Influence of debris cover on terminus retreat and mass changes of Chorabari Glacier, Garhwal region, central Himalaya, India. *Journal of Glaciology*, *59*(217), 961–971. <https://doi.org/10.3189/2013JoG12J180>
- Dobhal, D. P., Pratap, B., Bhambri, R., & Mehta, M. (2021). Mass balance and morphological changes of Dokriani Glacier (1992–2013), Garhwal Himalaya, India. *Quaternary Science Advances*, *4*, Article 100033. <https://doi.org/10.1016/j.qsa.2021.100033>
- Dong, H., Li, Q., Zhu, X., Zhang, X., Zhang, Z., Shi, J., & He, Y. (2020). Analysis of the variability and future evolution of snowfall trends in the Huaihe River Basin under climate change. *Frontiers in Earth Science*, *8*, Article 594704. <https://doi.org/10.3389/feart.2020.594704>
- Edwards, T. L., Nowicki, S., Marzeion, B., Hock, R., Goelzer, H., Seroussi, H., Jourdain, N. C., Slater, D. A., Turner, F. E., Smith, C. J., McKenna, C. M., Simon, E., Abe-Ouchi, A., Gregory, J. M., Larour, E., Lipscomb, W. H., Payne, A. J., Shepherd, A., Agosta, C., ... Zwinger, T. (2021). Projected land ice contributions to twenty-first-century sea level rise. *Nature*, *593*(7857), 74–82. <https://doi.org/10.1038/s41586-021-03302-y>
- Emmer, A., Allen, S. K., Carey, M., Frey, H., Huggel, C., Korup, O., Mergili, M., Sattar, A., Veh, G., Chen, T. Y., Cook, S. J., Correas-Gonzalez, M., Das, S., Diaz Moreno, A., Drenkhan, F., Fischer, M., Immerzeel, W. W., Izagirre, E., Joshi, R. C., ... Yde, J. C. (2022). Progress and challenges in glacial lake outburst flood research (2017–2021): A research community perspective. *Natural Hazards and Earth System Sciences*, *22*(9), 3041–3061. <https://doi.org/10.5194/nhess-22-3041-2022>
- Farinotti, D., Huss, M., Furst, J. J., Landmann, J., Machguth, H., Maussion, F., & Pandit, A. (2019). A consensus estimate for the ice thickness distribution of all glaciers on Earth. *Nature Geoscience*, *12*(3), 168–173. <https://doi.org/10.1038/s41561-019-0300-3>
- Farinotti, D., Immerzeel, W. W., de Kok, R. J., Quincey, D. J., & Dehecq, A. (2020). Manifestations and mechanisms of the Karakoram glacier anomaly. *Nature Geoscience*, *13*, 8–16. <https://doi.org/10.1038/s41561-019-0513-5>
- Forsythe, N., Fowler, H. J., Li, X.-F., Blenkinsop, S., & Pritchard, D. (2017). Karakoram temperature and glacial melt driven by regional atmospheric circulation variability. *Nature Climate Change*, *7*, 664–670. <https://doi.org/10.1038/nclimate3361>

- Fowler, H. J., Lenderink, G., Prein, A. F., Westra, S., Allan, R. P., Ban, N., Barbero, R., Berg, P., Blenkinsop, S., Do, H. X., Guerrero, S., Haertler, J. O., Kendon, E. J., Lewis, E., Schaer, C., Sharma, A., Villarini, G., Wasko, C., & Zhang, X. (2021). Anthropogenic intensification of short-duration rainfall extremes. *Nature Reviews Earth and Environment*, 2, 107–122. <https://doi.org/10.1038/s43017-020-00128-6>
- Frey, H., Machguth, H., Huss, M., Huggel, C., Bajracharya, S., Bolch, T., Kulkarni, A., Linsbauer, A., Salzmann, N., & Stoffel, M. (2014). Estimating the volume of glaciers in the Himalayan-Karakoram region using different methods. *The Cryosphere*, 8, 2313–2333. <https://doi.org/10.5194/tc-8-2313-2014>
- Friedl, P., Seehaus, T., & Braun, M. (2021). Global time series and temporal mosaics of glacier surface velocities derived from Sentinel-1 data. *Earth System Science Data*, 13(10), 4653–4675. <https://doi.org/10.5194/essd-13-4653-2021>
- Fugger, S., Fyffe, C. L., Fatichi, S., Miles, E., McCarthy, M., Shaw, T. E., Ding, B., Yang, W., Wagnon, P., Immerzeel, W., Liu, Q., & Pellicciotti, F. (2022). Understanding monsoon controls on the energy and mass balance of glaciers in the central and eastern Himalaya. *The Cryosphere*, 16, 1631–1652. <https://doi.org/10.5194/tc-16-1631-2022>
- Fujita, K., Inoue, H., Izumi, T., Yamaguchi, S., Sadakane, A., Sunako, S., Nishimura, K., Immerzeel, W. W., Shea, J. M., Kayastha, R. B., Sawagaki, T., Breashears, D. F., Yagi, H., & Sakai, A. (2017). Anomalous winter-snow-amplified earthquake-induced disaster of the 2015 Langtang avalanche in Nepal. *Natural Hazards and Earth System Sciences*, 17(5), 749–764. <https://doi.org/10.5194/nhess-17-749-2017>
- Fujita, K., Kadota, T., Rana, B., Kayastha, R. B., & Ageta, Y. (2001). Shrinkage of glacier AX010 in Shorong Region, Nepal in 1990s. *Bulletin of Geological Research*, 18, 51–54.
- Furian, W., Loibl, D., & Schneider, C. (2021). Future glacial lakes in High Mountain Asia: An inventory and assessment of hazard potential from surrounding slopes. *Journal of Glaciology*, 67(264), 653–670. <https://doi.org/10.1017/jog.2021.18>
- Furian, W., Maussion, F., & Schneider, C. (2022). Projected 21st-century glacial lake evolution in High Mountain Asia. *Frontiers in Earth Science*, 10(March), 1–21. <https://doi.org/10.3389/feart.2022.821798>
- Gao, H., Wang, J., Yang, Y., Pan, X., Ding, Y., & Duan, Z. (2021). Permafrost hydrology of the Qinghai-Tibet Plateau: A review of processes and modeling. *Frontiers in Earth Science*, 8. <https://doi.org/10.3389/feart.2020.576838>
- Gao, Y., Chen, F., Lettenmaier, D. P., Xu, J., Xiao, L., & Li, X. (2018). Does elevation-dependent warming hold true above 5000 m elevation? Lessons from the Tibetan Plateau. *Npj Climate and Atmospheric Science*, 1(1), Article 19. <https://doi.org/10.1038/s41612-018-0030-z>
- Gao, Y., Liu, S., Qi, M., Xie, F., Wu, K., & Zhu, Y. (2021). Glacier-related hazards along the international Karakoram highway: Status and future perspectives. *Frontiers in Earth Science*, 9, Article 611501. <https://doi.org/10.3389/feart.2021.611501>
- Gardelle, J., Berthier, E., & Arnaud, Y. (2012). Slight mass gain of Karakoram glaciers in the early twenty-first century. *Nature Geoscience*, 5(5), 322–325. <https://doi.org/10.1038/ngeo1450>
- Gardelle, J., Berthier, E., Arnaud, Y., & Kääh, A. (2013). Region-wide glacier mass balances over the Pamir-Karakoram-Himalaya during 1999–2011. *The Cryosphere*, 7(4), 1263–1286. <https://doi.org/10.5194/tc-7-1263-2013>
- Gardner, A. S., Fahnestock, M. A., & Scambos, T. A. (2022). MEaSURES ITS_LIVE regional glacier and ice sheet surface velocities, Version 1 [Data Set]. Boulder, Colorado USA. NASA National Snow and Ice Data Center Distributed Active Archive Center. <https://doi.org/10.5067/6II6VW8LLWJ7>
- Gascoin, S. (2021). Snowmelt and snow sublimation in the Indus Basin. *Water*, 13(19), Article 2621. <https://doi.org/10.3390/w13192621>
- Gautam, C. K., & Mukherjee, B. P. (1992). Synthesis of glaciological studies on Tipra Bank Glacier Bhyundar Ganga Basin, district Chamoli. Uttar Pradesh (FS 1980–1988) Geological Survey of India, Northern Region, Lucknow.
- Geological Survey of India. (1991). *Annual general report, Part 8. Volume 124*. Ministry of Mines, Government of India.
- Geological Survey of India. (1992). *Annual general report. Part 8. Volume 125*. Ministry of Mines, Government of India.
- Geological Survey of India. (2001). *Glaciology of Indian Himalaya*. Special Publication no 63. Ministry of Mines, Government of India.
- Geological Survey of India. (2011). *Annual general report, Part 8. Volume 144*. Ministry of Mines, Government of India.
- Giese, A., Arcone, S., Hawley, R., Lewis, G., & Wagnon, P. (2021). Detecting supraglacial debris thickness with GPR under suboptimal conditions. *Journal of Glaciology*, 67, 1108–1120. <https://doi.org/10.1017/jog.2021.59>
- Gilbert, A., Sinisalo, A., Gurung, T. R., Fujita, K., Maharjan, S. B., Sherpa, T. C., & Fukuda, T. (2020). The influence of water percolation through crevasses on the thermal regime of a Himalayan mountain glacier. *The Cryosphere*, 14, 1273–1288. <https://doi.org/10.5194/tc-14-1273-2020>
- Girona-Mata, M., Miles, E. S., Ragettli, S., & Pellicciotti, F. (2019). High-resolution snowline delineation from Landsat imagery to infer snow cover controls in a Himalayan catchment. *Water Resources Research*, 55(8), 6754–6772. <https://doi.org/10.1029/2019WR024935>

- GLIMS & NSIDC (2005/2018). Global land ice measurements from space glacier database. International GLIMS community and the National Snow and Ice Data Center. Boulder, USA. <https://doi.org/10.7265/N5V98602>
- Gruber, S. (2012). Derivation and analysis of a high-resolution estimate of global permafrost zonation. *The Cryosphere*, 6, 221–233. <https://doi.org/10.5194/tc-6-221-2012>
- Gruber, S., Fleiner, R., Guegan, E., Panday, P., Schmid, M. O., Stumm, D., Wester, P., Zhang, Y., & Zhao, L. (2017). Review article: Inferring permafrost and permafrost thaw in the mountains of the Hindu Kush Himalaya region. *The Cryosphere*, 11(1), 81–99. <https://doi.org/10.5194/tc-11-81-2017>
- Guillet, G., King, O., Lv, M., Ghuffar, S., Benn, D., Quincey, D., & Bolch, T. (2022). A regionally resolved inventory of High Mountain Asia surge-type glaciers, derived from a multi-factor remote sensing approach. *The Cryosphere*, 16(2), 603–623. <https://doi.org/10.5194/tc-16-603-2022>
- Guo, C. K. (2017). *The change of glacial lakes and its influence in Everest region* [Unpublished master's thesis]. Hunan University of Science and Technology, China.
- Guo, S., Chen, R., Han, C., Liu, J., Wang, X., & Liu, G. (2021). Five-year analysis of evaporesublimation characteristics and its role on surface energy balance SEB on a midlatitude continental glacier. *Earth and Space Science*, 8(12), Article e2021EA001901. <https://doi.org/10.1029/2021EA001901>
- Guo, S., Chen, R., & Li, H. (2022). Surface sublimation/evaporation and condensation/deposition and their links to westerlies during 2020 on the August-One Glacier, the semi-arid Qilian Mountains of Northeast Tibetan Plateau. *Journal of Geophysical Research: Atmospheres*, 127(11), Article e2022JD036494. <https://doi.org/10.1029/2022JD036494>
- Haerberli, W., Schaub, Y., & Huggel, C. (2017). Increasing risks related to landslides from degrading permafrost into new lakes in de-glaciating mountain ranges. *Geomorphology*, 293(B), 405–417. <https://doi.org/10.1016/j.geomorph.2016.02.009>
- Hall, D. K., Riggs, G. A., Foster, J. L., and Kumar, S. V.: Development and evaluation of a cloud-gap-filled MODIS daily snow-cover product, *Remote Sens. Environ.*, 114, 496–503, <https://doi.org/10.1016/j.rse.2009.10.007>, 2010
- Haq, M. A., & Baral, P. (2019). Study of permafrost distribution in Sikkim Himalayas using Sentinel-2 satellite images and logistic regression modelling. *Geomorphology*, 333, 123–136. <https://doi.org/10.1016/j.geomorph.2019.02.024>
- Hassan, J., Chen, X., Muhammad, S., & Bazai, N. A. (2021). Rock glacier inventory, permafrost probability distribution modeling and associated hazards in the Hunza River Basin, Western Karakoram, Pakistan. *Science of the Total Environment*, 782, Article 146833. <https://doi.org/10.1016/j.scitotenv.2021.146833>
- Herreid, S., & Pellicciotti, F. (2020). The state of rock debris covering Earth's glaciers. *Nature Geoscience*, 13, 621–627. <https://doi.org/10.1038/s41561-020-0615-0>
- Hersbach, H., Bell, B., Berrisford, P., Hirahara, S., Horányi, A., Muñoz Sabater, J., Nicolas, J., Peubey, C., Radu, R., Schepers, D., Simmons, A., Soci, C., Abdalla, S., Abellan, X., Balsamo, G., Bechtold, P., Biavati, G., Bidlot, J., Bonavita, M., ...Thépaut, J.-N. (2020). The ERA5 global reanalysis. *Quarterly Journal of the Royal Meteorological Society*, 146, 1999–2049. <https://doi.org/10.1002/qj.3803>
- Hjort, J., Streletskiy, D., Doré, G., Wu, Q., Bjella, K., & Luoto, M. (2022). Impacts of permafrost degradation on infrastructure. *Nature Reviews Earth and Environment*, 3(1), 24–38. <https://doi.org/10.1038/s43017-021-00247-8>
- Hock, R., Rasul, G., Adler, C., Cáceres, B., Gruber, S., Hirabayashi, Y., Jackson, M., Kääh, A., Kang, S., Kutuzov, S., Milner, A., Molau, U., Morin, S., Orlove, B., & Steltzer, H. (2019). High mountain areas. In H.-O. Pörtner, D. C. Roberts, V. Masson-Delmotte, P. Zhai, M. Tignor, E. S. Poloczanska, K. Mintenbeck, A. Alegría, M. Nicolai, A. Okem, J. Petzold, B. Rama, & N. M. Weyer (Eds.), *IPCC special report on the ocean and cryosphere in a changing climate* (1st ed., pp. 131–202). Cambridge University Press. <https://doi.org/10.1017/9781009157964>
- Hopping, K. A., Chignell, S. M., & Lambin, E. F. (2018). The demise of caterpillar fungus in the Himalayan region due to climate change and overharvesting. *Proceedings of the National Academy of Sciences*, 115(45), 11489–11494. <https://doi.org/10.1073/pnas.1811591115>
- Huggel, C., Muccione, V., Carey, M., James, R., Jurt, C., & Mechler, R. (2019). *Loss and damage in the mountain cryosphere. Regional Environmental Change*, 19, 1387–1399. <https://doi.org/10.1007/s10113-018-1385-8>
- Hugonnet, R., McNabb, R., Berthier, E., Menounos, B., Nuth, C., Girod, L., Farinotti, D., Huss, M., Dussailant, I., Brun, F., & Kääh, A. (2021). Accelerated global glacier mass loss in the early twenty-first century. *Nature*, 592(7856), 726–731. <https://doi.org/10.1038/s41586-021-03436-z>
- Huss, M., Bookhagen, B., Huggel, C., Jacobsen, D., Bradley, R. S., Clague, J. J., Vuille, M., Buytaert, W., Cayan, D. R., Greenwood, G., Mark, B. G., Milner, A. M., Weingartner, R., & Winder, M. (2017). Toward mountains without permanent snow and ice. *Earth's Future*, 5(5), 418–435. <https://doi.org/10.1002/2016EF000514>
- IPCC. (2021). *Climate change 2021: The physical science basis. Contribution of working group I to the sixth assessment report of the Intergovernmental Panel on Climate Change* (V. Masson-Delmotte, P. Zhai, A. Pirani, S. L. Connors, C. Péan, S. Berger, N. Caud, Y. Chen, L. Goldfarb, M. I. Gomis, M. Huang, K. Leitzell, E. Lonnoy, J. B. R. Matthews, T. K. Maycock, T. Waterfield, O. Yelekçi, R. Yu and B. Zhou [Eds.]). Cambridge University Press. In press. doi:10.1017/9781009157896

- IPCC. (2022a). *Climate change 2022: Impacts, adaptation, and vulnerability. Contribution of working group II to the sixth assessment report of the Intergovernmental Panel on Climate Change* (H.-O. Pörtner, D. C. Roberts, M. Tignor, E. S. Poloczanska, K. Mintenbeck, A. Alegría, M. Craig, S. Langsdorf, S. Lösschke, V. Möller, A. Okem, & B. Rama [Eds.]). Cambridge University Press. doi:10.1017/9781009325844
- IPCC. (2022b). Annex II: Glossary (V. Möller, R. van Diemen, J. B. R. Matthews, C. Méndez, S. Semenov, J. S. Fuglested, & A. Reisinger [Eds.]). In H.-O. Pörtner, D. C. Roberts, M. Tignor, E. S. Poloczanska, K. Mintenbeck, A. Alegría, M. Craig, S. Langsdorf, S. Lösschke, V. Möller, A. Okem, & B. Rama (Eds.), *Climate change 2022: Impacts, adaptation, and vulnerability. Contribution of working group II to the sixth assessment report of the Intergovernmental Panel on Climate Change* (pp. 2897–2930). Cambridge University Press. doi:10.1017/9781009325844.029
- Jakob, L., Gourmelen, N., Ewart, M., & Plummer, S. (2021). Spatially and temporally resolved ice loss in High Mountain Asia and the Gulf of Alaska observed by CryoSat-2 swath altimetry between 2010 and 2019. *The Cryosphere*, 15(4), 1845–1862. <https://doi.org/10.5194/tc-15-1845-2021>
- Jia, G., Shevliakova, E., Artaxo, P., De Noblet-Ducoudré, N., Houghton, R., House, J., Kitajima, K., Lennard, C., Popp, A., Sirin, A., Sukumar, R., & Verchot, L. (2019). Land–climate interactions. In P. R. Shukla, J. Skea, E. Calvo Buendía, V. Masson-Delmotte, H.-O. Pörtner, D. C. Roberts, P. Zhai, R. Slade, S. Connors, R. van Diemen, M. Ferrat, E. Haughey, S. Luz, S. Neogi, M. Pathak, J. Petzold, J. Portugal Pereira, P. Vyas, E. Huntley, K. Kissick, M. Belkacemi, & J. Malley (Eds.), *Climate change and land: An IPCC special report on climate change, desertification, land degradation, sustainable land management, food security, and greenhouse gas fluxes in terrestrial ecosystems*. <https://doi.org/10.1017/9781009157988.004>
- Jin, H., Huang, Y., Bense, V. F., Ma, Q., Marchenko, S. S., Shepelev, V. V., Hu, Y., Liang, S., Spektor, V. V., Jin, X., Li, X., & Li, X. (2022). Permafrost degradation and its hydrogeological impacts. *Water*, 14(3). <https://doi.org/10.3390/w14030372>
- Jin, X. Y., Jin, H. J., Iwahana, G., Marchenko, S. S., Luo, D. L., Li, X. Y., & Liang, S. H. (2021). Impacts of climate-induced permafrost degradation on vegetation: A review. *Advances in Climate Change Research*, 12(1), 29–47. <https://doi.org/10.1016/j.accre.2020.07.002>
- Jones, D. B., Harrison, S., Anderson, K., Selley, H. L., Wood, J. L., & Betts, R. A. (2018). The distribution and hydrological significance of rock glaciers in the Nepalese Himalaya. *Global and Planetary Change*, 160, 123–142. <https://doi.org/10.1016/j.gloplacha.2017.11.005>
- Jones, D. B., Harrison, S., Anderson, K., & Whalley, W. B. (2019). Rock glaciers and mountain hydrology: A review. *Earth-Science Reviews*, 193, 163–190. <https://doi.org/10.1016/j.earscirev.2019.04.001>
- Kääb, A., Jacquemart, M., Gilbert, A., Leinss, S., Girod, L., Huggel, C., Falaschi, D., Ugalde, F., Petrakov, D., Chernomorets, S., Dokukin, M., Paul, F., Gascoin, S., Berthier, E., & Kargel, J. (2021). Sudden large-volume detachments of low-angle mountain glaciers: More frequent than thought. *The Cryosphere*, 15, 1751–1785. <https://doi.org/10.5194/tc-2020-243>
- Kalvoda, J., & Emmer, A. (2021). Mass wasting and erosion in different morphoclimatic zones of the Makalu Barun region, Nepal Himalaya. *Geografiska Annaler, Series A: Physical Geography*, 103(4), 368–396. <https://doi.org/10.1080/04353676.2021.2000816>
- Kaul, M. K. (1986). Mass balance of Liddar glaciers. *Transactions of the Institute of Indian Geographers*, 8, 95–112.
- Khadka, A., Wagnon, P., Brun, F., Shrestha, D., Lejeune, Y., & Arnaud, Y. (2022). Evaluation of ERA5-Land and HARv2 reanalysis data at high elevation in the Upper Dudh Koshi Basin (Everest region, Nepal). *Journal of Applied Meteorology and Climatology*, 61, 931–954. <https://doi.org/10.1175/JAMC-D-21-0091.1>
- Khadka, N., Chen, X., Nie, Y., Thakuri, S., Zheng, G., & Zhang, G. (2021). Evaluation of glacial lake outburst flood susceptibility using multi-criteria assessment framework in Mahalangur Himalaya. *Frontiers in Earth Science*, 8. <https://www.frontiersin.org/article/10.3389/feart.2020.601288>
- Khan, M. A. R., Singh, S., Pandey, P., Bhardwaj, A., Ali, S. N., Chaturvedi, V., & Ray, P. K. C. (2021). Modelling permafrost distribution in western Himalaya using remote sensing and field observations. *Remote Sensing*, 13(21). <https://doi.org/10.3390/rs13214403>
- Khanal, S., Lutz, A. F., Kraaijenbrink, P. D. A., van den Hurk, B., Yao, T., & Immerzeel, W. W. (2021). Variable 21st century climate change response for rivers in High Mountain Asia at seasonal to decadal time scales. *Water Resources Research*, 57(5), Article e2020WR029266. <https://doi.org/10.1029/2020WR029266>
- King, O., Bhattacharya, A., Bhambri, R., & Bolch, T. (2019). Glacial lakes exacerbate Himalayan glacier mass loss. *Science Reports*, 9, Article 18145. <https://doi.org/10.1038/s41598-019-53733-x>
- King, O., Bhattacharya, A., & Bolch, T. (2021). The presence and influence of glacier surging around the Geladandong ice caps, North East Tibetan Plateau. *Advances in Climate Change Research*, 12(3), 299–312. <https://doi.org/10.1016/j.accre.2021.05.001>

- Kirkham, J. D., Koch, I., Saloranta, T. M., Litt, M., Stigter, E. E., Moen, K., Thapa, A., Melvold, K., & Immerzeel, W. W. (2019). Near real-time measurement of snow water equivalent in the Nepal Himalayas. *Frontiers in Earth Science*, 7. <https://doi.org/10.3389/feart.2019.00177>
- Kneib, M., Miles, E. S., Jola, S., Buri, P., Herreid, S., Bhattacharya, A., Watson, C. S., Bolch, T., Quincey, D., & Pellicciotti, F. (2021). Mapping ice cliffs on debris-covered glaciers using multispectral satellite images. *Remote Sensing of Environment*, 253, Article 112201. <https://doi.org/10.1016/j.rse.2020.112201>
- Koul, M. N., & Ganjoo, R. K. (2010). Impact of inter- and intra-annual variation in weather parameters on mass balance and equilibrium line altitude of Naradu Glacier (Himachal Pradesh), NW Himalaya, India. *Climatic Change*, 99, 119–139. <https://doi.org/10.1007/s10584-009-9660-9>
- Kraaijenbrink, P. D. A., Bierkens, M. F. P., Lutz, A. F., & Immerzeel, W. W. (2017). Impact of a global temperature rise of 1.5 degrees celsius on Asia's glaciers. *Nature*, 549(7671), 257–260. <https://doi.org/10.1038/nature23878>
- Kraaijenbrink, P. D. A., Stigter, E. E., Yao, T., & Immerzeel, W. W. (2021). Climate change decisive for Asia's snow meltwater supply. *Nature Climate Change*, 11(7), 591–597. <https://doi.org/10.1038/s41558-021-01074-x>
- Krishnan, R., Shrestha, A. B., Ren, G., Rajbhandari, R., Saeed, S., Sanjay, J., Syed, A., Vellore, R., Xu, Y., You, Q., & Ren, Y. (2019). Unravelling climate change in the Hindu Kush Himalaya: Rapid warming in the mountains and increasing extremes. In P. Wester, A. Mishra, A. Mukherji, & A. B. Shrestha A. (Eds.), *The Hindu Kush Himalaya assessment: Mountains, climate change, sustainability and people* (pp. 57–97). Springer Nature Switzerland AG. <https://doi.org/10.1007/978-3-319-92288-1>
- Kumar, P., Saharwardi, M. S., Banerjee, A., Azam, Md. F., Dubey, A. K., & Murtugudde, R. (2019). Snowfall variability dictates glacier mass balance variability in Himalaya-Karakoram. *Science Reports*, 9, Article 18192. <https://doi.org/10.1038/s41598-019-54553-9>
- Laha, S., Kumari, R., Singh, S., Mishra, A., Sharma, T., Banerjee, A., . . . Shankar, R. (2017). Evaluating the contribution of avalanching to the mass balance of Himalayan glaciers. *Annals of Glaciology*, 58(75pt2), 110–118. <https://doi.org/10.1017/aog.2017.27>
- Lalande, M., Ménégot, M., Krinner, G., Naegeli, K., & Wunderle, S. (2021). Climate change in the High Mountain Asia in CMIP6. *Earth System Dynamics*, 12(4), 1061–1098. <https://doi.org/10.5194/esd-12-1061-2021>
- Larue, F., Royer, A., De Seve, D., Langlois, A., Roy, A., & Brucker, L. (2017). Validation of GlobSnow-2 snow water equivalent over Eastern Canada. *Remote Sensing of Environment*, 194, 264–277. <http://dx.doi.org/10.1016/j.rse.2017.03.027>
- Li, D., Lu, X., Overeem, I., Walling, D. E., Syvitski, J., Kettner, A. J., Bookhagen, B., Zhou, Y., & Zhang, T. (2021). Exceptional increases in fluvial sediment fluxes in a warmer and wetter High Mountain Asia. *Science*, 374(6567), 599–603. <https://doi.org/10.1126/science.abi9649>
- Li, G., Li, Y., Lin, H., Ye, Q., & Jiang, L. (2021). Two periods of geodetic glacier mass balance at Eastern Nyainqentanglha derived from multi-platform bistatic SAR interferometry. *International Journal of Applied Earth Observation and Geoinformation*, 104, Article 102541. <https://doi.org/10.1016/j.jag.2021.102541>
- Li, W., Wang, W., Gao, X., Wang, X., & Wang, R. (2022). Inventory and spatiotemporal patterns of glacial lakes in the HKH-TMHA region from 1990 to 2020. *Remote Sensing*, 14(6), Article 1351. <https://doi.org/10.3390/rs14061351>
- Li, Y., Chen, Y., Wang, F., He, Y., & Li, Z. (2020). Evaluation and projection of snowfall changes in High Mountain Asia based on NASA's NEX-GDDP high-resolution daily downscaled dataset. *Environmental Research Letters*, 15(10), Article 104040. <https://doi.org/10.1088/1748-9326/aba926>
- Lievens, H., Demuzere, M., Marshall, H.-P., Reichle, R. H., Brucker, L., Brangers, I., de Rosnay, P., Dumont, M., Giroto, M., Immerzeel, W. W., Jonas, T., Kim, E. J., Koch, I., Marty, C., Saloranta, T., Schober, J., & de Lannoy, G. J. M. (2019). Snow depth variability in the Northern Hemisphere mountains observed from space. *Nature Communications*, 10(1), 1–12. <https://doi.org/10.1038/s41467-019-12566-y>
- Linsbauer, A., Frey, H., Haeberli, W., Machguth, H., Azam, M. F., & Allen, S. (2015). Modelling glacier-bed overdeepenings and possible future lakes for the glaciers in the Himalaya-Karakoram region. *Annals of Glaciology*, 57(71), 119–130. <https://doi.org/10.3189/2016AoG71A627>
- Litt, M., Shea, J., Wagnon, P., Steiner, J., Koch, I., Stigter, E., & Immerzeel, W. (2019). Glacier ablation and temperature indexed melt models in the Nepalese Himalaya. *Science Reports*, 9, Article 5264. <https://doi.org/10.1038/s41598-019-41657-5>
- Liu, M., Chen, N., Zhang, Y., & Deng, M. (2020). Glacial lake inventory and lake outburst flood/debris flow hazard assessment after the Gorkha earthquake in the Bhoté Koshi Basin. *Water*, 12(2), Article 464. <https://doi.org/10.3390/w12020464>
- Liu, S., Xie, Z., Song, G., Ma, L., Ageta, Y. (1996). Mass balance of Kangwure (flat-top) Glacier on the north side of Mt. Xixiabangma, China. *Bulletin of Glacier Research* 14, 37–43.

- Liu, Y., Fang, Y., & Margulis, S. A. (2021). Spatiotemporal distribution of seasonal snow water equivalent in High Mountain Asia from an 18-year Landsat–MODIS era snow reanalysis dataset. *The Cryosphere*, *15*(11), 5261–5280. <https://doi.org/10.5194/tc-15-5261-2021>
- Livingstone, S. J., Li, Y., Rutishauser, A., Sanderson, R. J., Winter, K., Mikucki, J. A., Bjornsson, H., Bowling, J. S., Chu, W., Dow, C. F., Fricker, H. A., McMillan, M., Ng, F. S. L., Ross, N., Siegert, M. J., Seigfried, M., & Sole, A. J. (2022). Subglacial lakes and their changing role in a warming climate. *Nature Reviews Earth and Environment*, *3*, 106–124. <https://doi.org/10.1038/s43017-021-00246-9>
- Lu, Q., Zhao, D., & Wu, S. (2017). Simulated responses of permafrost distribution to climate change on the Qinghai-Tibet Plateau. *Scientific Reports*, *7*, Article 3845. <https://doi.org/10.1038/s41598-017-04140-7>
- Lutz, A. F., Immerzeel, W. W., Shrestha, A. B., & Bierkens, M. F. P. (2014). Consistent increase in High Asia's runoff due to increasing glacier melt and precipitation. *Nature Climate Change*, *4*(7), 587–592. <https://doi.org/10.1038/nclimate2237>
- Lützow, Natalie, & Veh, Georg. (2022). Glacier Lake Outburst Flood Database V3.0 (3.0) [Data set]. Zenodo. <https://doi.org/10.5281/zenodo.7330345>
- Madhura, R. K., Krishnan, R., Revadekar, J. V., Mujumdar, M., & Goswami, B. N. (2015). Changes in western disturbances over the Western Himalayas in a warming environment. *Climate Dynamics*, *44*(3), 1157–1168. <https://doi.org/10.1007/s00382-014-2166-9>
- Maharjan, S. B., Mool, P. K., Lizong, W., Xiao, G., Shrestha, F., Shrestha, R. B., Khanal, N. R., Bajracharya, S. R., Joshi, S., Shai, S., & Baral, P. (2018). *The status of glacial lakes in the Hindu Kush Himalaya*. ICIMOD Research Report 2018/1. ICIMOD. <https://doi.org/10.53055/ICIMOD.742>
- Mandal, A., Angchuk, T., Azam, M. F., Ramanathan, A., Wagnon, P., Soheb, M., & Singh, C. (2022). 11-year record of wintertime snow surface energy balance and sublimation at 4863 m a.s.l. on Chhota Shigri Glacier moraine (western Himalaya, India). *The Cryosphere*, *16*, 3775–3799. <https://doi.org/10.5194/tc-16-3775-2022>
- Mandal, A., Ramanathan, A., Azam, M. F., Angchuk, T., Soheb, M., Kumar, M., Pottakkal, J. G., Vatsal, S., Mishra, S., & Singh, V. B. (2020). Understanding the interrelationships among mass balance, meteorology, discharge and surface velocity on Chhota Shigri Glacier over 2002–2019 using in situ measurements. *Journal of Glaciology*, *66*(259). <https://doi.org/10.1017/jog.2020.42>
- Marzeion, B., Hock, R., Anderson, B., Bliss, A., Champollion, N., Fujita, K., Huss, M., Immerzeel, W. W., Kraaijenbrink, P., Malles, J.-H., Maussion, F., Radic, V., Rounce, D. R., Sakai, A., Shannon, S., van de Wal, R., & Zekollari, H. (2020). Partitioning the uncertainty of ensemble projections of global glacier mass change. *Earth's Future*, *8*, Article e2019EF001470. <https://doi.org/10.1029/2019EF001470>
- Matthews, T., Perry, L. B., Koch, I., Aryal, D., Khadka, A., Shrestha, D., Abernathy, K., Elmore, A. C., Seimon, A., Tait, A., Elvin, S., Tuladhar, S., Baidya, S. K., Potocki, M., Birkel, S. D., Kang, S., Sherpa, T. C., Gajurel, A., & Mayewski, P. A. (2020). Going to extremes: Installing the world's highest weather stations on Mount Everest. *Bulletin of the American Meteorological Society*, *101*, E1870–E1890. <https://doi.org/10.1175/BAMS-D-19-0198.1>
- Matthews, T., Perry, L. B., Lane, T. P., Elmore, A. C., Khadka, A., Aryal, D., Shrestha, D., Tuladhar, S., Baidya, S. K., Gajurel, A., Potocki, M., & Mayewski, P. A. (2020). Into thick(er) air? Oxygen availability at humans' physiological frontier on Mount Everest. *IScience*, *23*(12), Article 101718. <https://doi.org/10.1016/j.isci.2020.101718>
- Maurer, J. M., Rupper, S. B., & Schaefer, J. M. (2016). Quantifying ice loss in the eastern Himalayas since 1974 using declassified spy satellite imagery. *The Cryosphere*, *10*(5), 2203–2215. <https://doi.org/10.5194/tc-10-2203-2016>
- Maurer, J. M., Schaefer, J. M., Rupper, S., & Corley, A. (2019). Acceleration of ice loss across the Himalayas over the past 40 years. *Science Advances*, *5*(6), Article eaav7266. <https://doi.org/10.1126/sciadv.aav7266>
- McCarthy, M., Miles, E., Kneib, M., Buri, P., Fugger, S., & Pellicciotti, F. (2022). Supraglacial debris thickness and supply rate in High-Mountain Asia. *Communications Earth and Environment*, *3*, 269. <https://doi.org/10.1038/s43247-022-00588-2>
- McCarthy, M., Pritchard, H. D., Willis, I., and King, E. (2017). Ground-penetrating radar measurements of debris thickness on Lirung Glacier, Nepal. *Journal of Glaciology*, *63*(239), 543–555. <https://doi.org/10.1017/jog.2017.18>
- Miles, E., McCarthy, M., Dehecq, A., Kneib, S., Fugger, S., & Pellicciotti, F. (2021). Health and sustainability of glaciers in High Mountain Asia. *Nature Communications*, *12*, Article 2868. <https://doi.org/10.1038/s41467-021-23073-4>
- Miles, E., Willis, I., Arnold, N., Steiner, J., & Pellicciotti, F. (2017). Spatial, seasonal and interannual variability of supraglacial ponds in the Langtang Valley of Nepal, 1999–2013. *Journal of Glaciology*, *63*(237), 88–105. <https://doi.org/10.1017/jog.2016.120>
- Miles, E. S., Willis, I., Buri, P., Steiner, J. F., Arnold, N. S., & Pellicciotti, F. (2018). Surface pond energy absorption across four Himalayan glaciers accounts for 1/8 of total catchment ice loss. *Geophysical Research Letters*, *45*(19), 10464–10473. <https://doi.org/10.1029/2018GL079678>

- Millan, R., Mouginot, J., Rabatel, A., & Morlighem, M. (2022). Ice velocity and thickness of the world's glaciers. *Nature Geoscience*, 15(2), 124–129. <https://doi.org/10.1038/s41561-021-00885-z>
- Mir, R. A., Jain, S. K., Jain, S. K., Thayyen, R. J., & Saraf, A. K. (2017). Assessment of recent glacier changes and its controlling factors from 1976 to 2011 in Baspa Basin, Western Himalaya. *Arctic, Antarctic, and Alpine Research*, 49(4), 621–647. <https://doi.org/10.1657/AAAR0015-070>
- Mishra, R., Kumar, A., & Singh, D. (2014). Long term monitoring of mass balance of Hamtah Glacier, Lahaul and Spiti district, Himachal Pradesh. *Geological Survey of India*, 147(8), 230–231.
- Mott, R., Schlogl, S., Dirks, L., & Lehning, M. (2017). Impact of extreme land surface heterogeneity on micrometeorology over spring snow cover. *Journal of Hydrometeorology*, 18(10), 2705–2722. <https://doi.org/10.1175/JHM-D-17-0074.1>
- Mott, R., Vionnet, V., & Grünewald, T. (2018). The seasonal snow cover dynamics: Review on wind-driven coupling processes. *Frontiers in Earth Science*, 6. <https://doi.org/10.3389/feart.2018.00197>
- Mu, C., Li, L., Wu, X., Zhang, F., Jia, L., Zhao, Q., & Zhang, T. (2018). Greenhouse gas released from the deep permafrost in the northern Qinghai-Tibetan Plateau. *Scientific Reports*, 8, Article 4205. <https://doi.org/10.1038/s41598-018-22530-3>
- Muhammad, S., Li, J., Steiner, J. F., Shrestha, F., Shah, G. M., Berthier, E., Guo, L., Wu, L., & Tian, L. (2021). A holistic view of Shisper Glacier surge and outburst floods: From physical processes to downstream impacts. *Geomatics, Natural Hazards and Risk*, 12(1), 2755–2775. <https://doi.org/10.1080/19475705.2021.1975833>
- Muhammad, S. and Thapa, A.: An improved Terra–Aqua MODIS snow cover and Randolph Glacier Inventory 6.0 combined product (MOYDGL06*) for high-mountain Asia between 2002 and 2018, *Earth Syst. Sci. Data*, 12, 345–356, <https://doi.org/10.5194/essd-12-345-2020>, 2020.
- Muhammad, S., Tian, L., Ali, S., Latif, Y., Wazir, M. A., Goheer, M. A., Saifullah, M., Hussain, I., & Shiyin, L. (2020). Thin debris layers do not enhance melting of the Karakoram glaciers. *Science of The Total Environment*, 746, Article 141119. <https://doi.org/10.1016/j.scitotenv.2020.141119>
- Muhammad, S., Tian, L., & Nüsser, M. (2019). No significant mass loss in the glaciers of Astore Basin (North-Western Himalaya), between 1999 and 2016, *Journal of Glaciology*, 65(250), 270–278. <https://doi.org/10.1017/jog.2019.5>
- Muñoz Sabater, J. (2021). ERA5-Land hourly data from 1950 to 1980. Copernicus Climate Change Service (C3S) Climate Data Store (CDS). 10.24381/cds.e2161bac (accessed November 12, 2022).
- Mölg, N., Bolch, T., Rastner, P., Strozzi, T., & Paul, F. (2018) A consistent glacier inventory for the Karakoram and Pamir regions derived from Landsat data: Distribution of debris cover and mapping challenges. *Earth System Science Data Discussions*, 1–44. <https://doi.org/10.5194/essd-2018-35>
- Naegeli, K., Franke, J., Neuhaus, C., Rietze, N., Stengel, M., Wu, X., & Wunderle, S. (2022). Revealing four decades of snow cover dynamics in the Hindu Kush Himalaya. *Scientific Reports*, 12(1), Article 13443. <https://doi.org/10.1038/s41598-022-17575-4>
- Nepal, S., Khatiwada, K. R., Pradhananga, S., Kralisch, S., Samyn, D., Bromand, M. T., Jamal, N., Dildar, M., Durrani, F., Rassouly, F., Azizi, F., Salehi, W., Malikzooi, R., Krause, P., Koirala, S., & Chevallier, P. (2021). Future snow projections in a small basin of the Western Himalaya. *Science of the Total Environment*, 795, Article 148587. <https://doi.org/10.1016/j.scitotenv.2021.148587>
- Ni, J., Wu, T., Zhu, X., Hu, G., Zou, D., Wu, X., Li, R., Xie, C., Qiao, Y., Pang, Q., Hao, J., & Yang, C. (2021). Simulation of the present and future projection of permafrost on the Qinghai-Tibet Plateau with statistical and machine learning models. *Journal of Geophysical Research: Atmospheres*, 126(2), Article e2020JD033402. <https://doi.org/10.1029/2020JD033402>
- Nicholson, L. & Benn, D. I. (2006). Calculating ice melt beneath a debris layer using meteorological data. *Journal of Glaciology*, 52(178), 463–470. <https://doi.org/10.3189/172756506781828584>
- Nicholson, L. & Mertes, J. (2017). Thickness estimation of supraglacial debris above ice cliff exposures using a high-resolution digital surface model derived from terrestrial photography. *Journal of Glaciology*, 63(242), 989–998. <https://doi.org/10.1017/jog.2017.68>
- Nie, Y., Liu, Q., & Liu, S. (2013). Glacial lake expansion in the central Himalayas by Landsat images, 1990–2010. *PLoS ONE*, 8(12), Article e83973. <https://doi.org/10.1371/journal.pone.0083973>
- Nie, Y., Sheng, Y., Liu, Q., Liu, L., Liu, S., Zhang, Y., & Song, C. (2017). A regional-scale assessment of Himalayan glacial lake changes using satellite observations from 1990 to 2015. *Remote Sensing of Environment*, 189, 1–13. <https://doi.org/10.1016/j.rse.2016.11.008>
- NISAR. (2018). *NASA-ISRO SAR (NISAR) mission science users' handbook*. NASA Jet Propulsion Laboratory.
- Norris, J., Carvalho, L. M. V., Jones, C., & Cannon, F. (2019). Deciphering the contrasting climatic trends between the central Himalaya and Karakoram with 36 years of WRF simulations. *Climate Dynamics*, 52, 159–180. <https://doi.org/10.1007/s00382-018-4133-3>

- Notarnicola, C. (2020). Hotspots of snow cover changes in global mountain regions over 2000–2018. *Remote Sensing of Environment*, 243, Article 111781. <https://doi.org/10.1016/j.rse.2020.111781>
- Notarnicola, C. (2022). Overall negative trends for snow cover extent and duration in global mountain regions over 1982–2020. *Scientific Reports*, 12(1), Article 13731. <https://doi.org/10.1038/s41598-022-16743-w>
- Nuth, C., & Kääb, A. (2011). Co-registration and bias corrections of satellite elevation data sets for quantifying glacier thickness change. *The Cryosphere*, 5, 271–290. <https://doi.org/10.5194/tc-5-271-2011>
- Obu, J., Westermann, S., Bartsch, A., Berdnikov, N., Christiansen, H. H., Dashtseren, A., Delaloye, R., Elberling, B., Etzelmuller, B., Kholodov, A., Khomutov, A., Kaab, A., Leibman, M. O., Lewkovic, A. G., Panda, S. K., Romanovsky, V., Way, R. G., Westergaard-Nielsen, A., Wu, T., ... Zou, D. (2019). Northern Hemisphere permafrost map based on TOP modelling for 2000–2016 at 1 km² scale. *Earth-Science Reviews*, 193, 299–316. <https://doi.org/10.1016/j.earscirev.2019.04.023>
- Oerlemans, J. (2001). *Glaciers and climate change* (1st ed.). Routledge.
- Oliva, M., & Fritz, M. (2018). Permafrost degradation on a warmer Earth: Challenges and perspectives. *Current Opinion in Environmental Science & Health*, 5, 14–18. <https://doi.org/10.1016/j.coesh.2018.03.007>
- Orsolini, Y., Wegmann, M., Dutra, E., Liu, B., Balsamo, G., Yang, K., de Rosnay, P., Zhu, C., Wang, W., Senan, R., & Arduini, G. (2019). Evaluation of snow depth and snow cover over the Tibetan Plateau in global reanalyses using in situ and satellite remote sensing observations. *The Cryosphere*, 13(8), 2221–2239. <https://doi.org/10.5194/tc-13-2221-2019>
- Ortiz, A., Tian, W., Sherpa, T. C., Shrestha, F., Matin, M., Dodhia, R., Ferres, J. M. L., & Sankaran, K. (2022). Mapping glacial lakes using historically guided segmentation models. *IEEE Journal of Selected Topics in Applied Earth Observations and Remote Sensing*, 15, 9226–9240. <https://doi.org/10.1109/JSTARS.2022.3215722>
- Østrem, G., & Stanley, A. (1969). *Glacier mass balance measurements: A manual for field and office work*. Canadian Department of Energy, Mines and Resources and The Norwegian Water Resources and Electricity Board.
- Palazzi, E., von Hardenberg, J., & Provenzale, A. (2013). Precipitation in the Hindu-Kush Karakoram Himalaya: Observations and future scenarios. *Journal of Geophysical Research Atmospheres*, 118(1), 85–100. <https://doi.org/10.1029/2012JD018697>
- Panday, P. K., Thibeault, J., Frey, K. E. (2015). Changing temperature and precipitation extremes in the Hindu Kush-Himalayan region: An analysis of CMIP3 and CMIP5 simulations and projections. *International Journal of Climatology*, 35(10), 3058–3077. <https://doi.org/10.1002/joc.4192>
- Pandey, P. (2019). Inventory of rock glaciers in Himachal Himalaya, India using high-resolution Google Earth imagery. *Geomorphology*, 340, 103–115. <https://doi.org/10.1016/j.geomorph.2019.05.001>
- Pant, G. B., Pradeep Kumar, P., Revadekar, J. V., & Singh, N. (2018). *Climate change in the Himalayas*. Springer. <https://doi.org/10.1007/978-3-319-61654-4>
- Pritchard, H. D. (2019). Asia's shrinking glaciers protect large populations from drought stress. *Nature*, 569(7758), 649–654. <https://doi.org/10.1038/s41586-019-1240-1>
- Pritchard, H. D., King, E. C., Goodger, D. J., McCarthy, M., Mayer, C., & Kayastha, R. (2020). Towards Bedmap Himalayas: Development of an airborne ice-sounding radar for glacier thickness surveys in High-Mountain Asia. *Annals of Glaciology*, 61(81), 35–45. <https://doi.org/10.1017/aog.2020.29>
- Pronk, J. B., Bolch, T., King, O., Wouters, B., & Benn, D. I. (2021). Contrasting surface velocities between lake- and land-terminating glaciers in the Himalayan region. *The Cryosphere*, 15(12), 5577–5599. <https://doi.org/10.5194/tc-15-5577-2021>
- Pulliainen, J., Luojus, K., Derksen, C., Mudryk, L., Lemmetyinen, J., Salminen, M., Ikonen, J., Takala, M., Cohen, J., Smolander, T., & Norberg, J. (2020). Patterns and trends of Northern Hemisphere snow mass from 1980 to 2018. *Nature*, 581(7808), 294–298. <https://doi.org/10.1038/s41586-020-2258-0>
- Racoviteanu, A. E., Arnaud, Y., Williams, M. W., & Manley, W. F. (2015). Spatial patterns in glacier characteristics and area changes from 1962 to 2006 in the Kanchenjunga–Sikkim area, eastern Himalaya. *The Cryosphere*, 9(2), 505–523. <https://doi.org/10.5194/tc-9-505-2015>
- Racoviteanu, A. E., Rittger, K., & Armstrong, R. (2019). An automated approach for estimating snowline altitudes in the Karakoram and eastern Himalaya from remote sensing. *Frontiers in Earth Science*, 7. <https://www.frontiersin.org/articles/10.3389/feart.2019.00220>
- Ragetti, S., Bolch, T., & Pellicciotti, F. (2016). Heterogeneous glacier thinning patterns over the last 40 years in Langtang Himal, Nepal. *The Cryosphere*, 10(5), 2075–2097. <https://doi.org/10.5194/tc-10-2075-2016>
- Raina, V. K., Kaul, M. K., & Singh, S. (1977). Mass-balance studies of Gara glacier. *Journal of Glaciology*, 18(80), 415–423. <https://doi.org/10.3189/S0022143000021092>

- Ran, Y., Li, X., Cheng, G., Che, J., Aalto, J., Karjalainen, O., Hjort, J., Luoto, M., Jin, H., Obu, J., Hori, M., Yu, Q., & Chang, X. (2022). New high-resolution estimates of the permafrost thermal state and hydrothermal conditions over the northern Hemisphere. *Earth System Science Data*, *14*, 885–884. <https://doi.org/10.5194/essd-14-865-2022>
- Ran, Y., Li, X., Cheng, G., Nan, Z., Che, J., Sheng, Y., Wu, Q., Jin, H., Luo, D., Tang, Z., & Wu, X. (2021). Mapping the permafrost stability on the Tibetan Plateau for 2005–2015. *Science China Earth Sciences*, *64*, 62–79. <https://doi.org/10.1007/s11430-020-9685-3>
- Ren, Y.-Y., Ren, G.-Y., Sun, X.-B., Shrestha, A. B., You, Q.-L., Zhan, Y.-J., Rajbhandari, R., Zhang, P.-F., & Wen, K.-M. (2017). Observed changes in surface air temperature and precipitation in the Hindu Kush Himalayan region over the last 100-plus years. *Advances in Climate Change Research*, *8*(3), 148–156. <https://doi.org/10.1016/j.accre.2017.08.001>
- Reuter, B., Viallon-Galinier, L., Horton, S., van Herwijnen, A., Mayer, S., Hagenmuller, P., & Morin, S. (2022). Characterizing snow instability with avalanche problem types derived from snow cover simulations. *Cold Regions Science and Technology*, *194*, Article 103462. <https://doi.org/10.1016/j.coldregions.2021.103462>
- Rounce, D. R., Hock, R., McNabb, R. W., Millan, R., Sommer, C., Braun, M. H., Malz, P., Maussion, F., Mougnot, J., Seehaus, T. C., & Shean, D. E. (2021). Distributed global debris thickness estimates reveal debris significantly impacts glacier mass balance. *Geophysical Research Letters*, *48*(8), Article e2020GL091311. <https://doi.org/10.1029/2020GL091311>
- Rounce, D. R., Hock, R., & Shean, D. E. (2020). Glacier mass change in High Mountain Asia through 2100 using the open-source python glacier evolution model (PyGEM). *Frontiers in Earth Science*, *7*, Article 331. <https://doi.org/10.3389/feart.2019.00331>
- Rounce, D. R., & McKinney, D. C. (2014). Debris-thickness of glaciers in the Everest area (Nepal Himalaya) derived from satellite imagery using a nonlinear energy balance model. *The Cryosphere*, *8*, 1317–1329. <https://doi.org/10.5194/tc-8-1317-2014>
- Rounce, D. R., Quincey, D. J., & McKinney, D. C. (2015). Debris-covered glacier energy balance model for Imja–Lhotse Shar Glacier in the Everest region of Nepal. *The Cryosphere*, *9*(6), 2295–2310. <https://doi.org/10.5194/tc-9-2295-2015>
- Rowan, A. V., Egholm, D. L., Quincey, D. J., & Glasser, N. F. (2015). Modelling the feedbacks between mass balance, ice flow and debris transport to predict the response to climate change of debris-covered glaciers in the Himalaya. *Earth and Planetary Science Letters*, *430*, 427–438. <https://doi.org/10.1016/j.epsl.2015.09.004>
- Sabin, T. P., Krishnan, R., Vellore, R., Priya, P., Borgaonkar, H. P., Singh, B. B., & Sagar, A. (2020). Climate change over the Himalayas. In R. Krishnan, J. Sanjay, C. Gnanaseelan, M. Mujumdar, A. Kulkarni, & S. Chakraborty (Eds.), *Assessment of climate change over the Indian region: A report of the Ministry of Earth Sciences (MoES), Government of India*. Springer Open. https://doi.org/10.1007/978-981-15-4327-2_11
- Sakai, A. (2019). Brief communication: Updated GAMDAM glacier inventory over high-mountain Asia. *The Cryosphere*, *13*(7), 2043–2049. <https://doi.org/10.5194/tc-13-2043-2019>
- Sakai, A. & Fujita, K. (2017). Contrasting glacier responses to recent climate change in high-mountain Asia. *Science Reports*, *7*, Article 13717. <https://doi.org/10.1038/s41598-017-14256-5>
- Saloranta, T., Thapa, A., Kirkham, J. D., Koch, I., Melvold, K., Stigter, E., Litt, M., & Møen, K. (2019). A model setup for mapping snow conditions in High-Mountain Himalaya. *Frontiers in Earth Science*, *7*. <https://doi.org/10.3389/feart.2019.00129>
- Sangewar, C. V., & Siddiqui, M. A. (2007). *Thematic compilation of mass balance data on glaciers of Satluj Catchment in Himachal Himalaya (Field Season: 2006-07)*. Geological Survey of India, Northern Region.
- Sanjay, J., Krishnan, R., Shrestha, A. B., Rajbhandari, R., & Ren, G.-Y. (2017). Downscaled climate change projections for the Hindu Kush Himalayan region using CORDEX South Asia regional climate models. *Advances in Climate Change Research*, *8*(3), 185–198. <https://doi.org/10.1016/j.accre.2017.08.003>
- Santra, S., Verma, S., Fujita, K., Chakraborty, I., Boucher, O., Takemura, T., Burkhart, J. F., Matt, F., & Sharma, M. (2019). Simulations of black carbon (BC) aerosol impact over Hindu Kush Himalayan sites: Validation, sources, and implications on glacier runoff. *Atmospheric Chemistry and Physics*, *19*(4), 2441–2460. <https://doi.org/10.5194/acp-19-2441-2019>
- Sattar, A., Goswami, A., Kulkarni, A. V., Emmer, A., Haritashya, U. K., Allen, S., Frey, H., & Huggel, C. (2021). Future glacial lake outburst flood (GLOF) hazard of the South Lhonak Lake, Sikkim Himalaya. *Geomorphology*, *388*, Article 107783. <https://doi.org/10.1016/j.geomorph.2021.107783>
- Sattar, A., Haritashya, U. K., Kargel, J. S., Leonard, G. J., Shugar, D. H., & Chase, D. V. (2021). Modeling lake outburst and downstream hazard assessment of the Lower Barun Glacial Lake, Nepal Himalaya. *Journal of Hydrology*, *598*, Article 126208. <https://doi.org/10.1016/j.jhydrol.2021.126208>
- Scapozza, C., Ambrosi, C., Cannata, M., & Strozzi, T. (2019). Glacial lake outburst flood hazard assessment by satellite Earth observation in the Himalayas (Chomolhari area, Bhutan). *Geographica Helvetica*, *74*, 125–139. <https://doi.org/10.5194/gh-74-125-2019>

- Scher, C., Steiner, N. C., & McDonald, K. C. (2021). Mapping seasonal glacier melt across the Hindu Kush Himalaya with time series synthetic aperture radar (SAR). *The Cryosphere*, 15(9), 4465–4482. <https://doi.org/10.5194/tc-15-4465-2021>
- Scherler, D., Wulf, H., & Gorelick, N. (2018). Global assessment of supraglacial debris-cover extents. *Geophysical Research Letters*, 45(21), 11798–11805. <https://doi.org/10.1029/2018GL080158>
- Scherler, D., & Egholm, D. L. (2020). Production and transport of supraglacial debris: Insights from cosmogenic ¹⁰Be and numerical modeling, Chhota Shigri Glacier, Indian Himalaya. *Journal of Geophysical Research: Earth Surface*, 125(10). <https://doi.org/10.1029/2020JF005586>
- Sevestre, H. & Benn, D. I. (2015). Climatic and geometric controls on the global distribution of surge-type glaciers: Implications for a unifying model of surging. *Journal of Glaciology*, 61(228), 646–662. <https://doi.org/10.3189/2015JoG14J136>
- Shea, J. M., Immerzeel, W. W., Wagnon, P., Vincent, C., & Bajracharya, S. (2015). Modelling glacier change in the Everest region, Nepal Himalaya. *The Cryosphere*, 9(3), 1105–1128. <https://doi.org/10.5194/tc-9-1105-2015>
- Shean, D. E., Bhushan, S., Montesano, P., Rounce, D. R., Arendt, A., & Osmanoglu, B. (2020). A systematic, regional assessment of High Mountain Asia glacier mass balance. *Frontiers in Earth Sciences*, 7, 363. <https://doi.org/10.3389/feart.2019.00363>
- Shen, L., Zhang, Y., Ullah, S., Pepin, N., & Ma, Q. (2021). Changes in snow depth under elevation-dependent warming over the Tibetan Plateau. *Atmospheric Science Letters*, 22(9), Article e1041. <https://doi.org/10.1002/asl.1041>
- Sherpa, S. F., Wagnon, P., Brun, F., Berthier, E., Vincent, C., Lejeune, Y., Arnaud, Y., Kayastha, R. B., & Sinisalo, A. (2017). Contrasted surface mass balances of debris-free glaciers observed between the southern and the inner parts of the Everest region (2007–15). *Journal of Glaciology*, 63(240), 637–651. <https://doi.org/10.1017/jog.2017.30>
- Shugar, D. H., Burr, A., Haritashya, U. K., Kargel, J. S., Watson, C. S., Kennedy, M. C., Bevington, A. R., Betts, R. A., Harrison, S., & Strattman, K. (2020). Rapid worldwide growth of glacial lakes since 1990. *Nature Climate Change*, 10(10), 939–945. <https://doi.org/10.1038/s41558-020-0855-4>
- Shugar, D. H., Jacquemart, M., Shean, D., Bhushan, S., Upadhyay, K., Sattar, A., Schwanghart, W., McBride, S., de Vries, M. V. W., Mergili, M., Emmer, A., Deschamps-Berger, C., McDonnell, M., Bhambri, R., Allen, S., Berthier, E., Carrivick, J. L., Clague, J. J., Dokukin, M., ... Westoby, M. J. (2021). A massive rock and ice avalanche caused the 2021 disaster at Chamoli, Indian Himalaya. *Science*. <https://doi.org/10.1126/science.abh4455>
- Skiles, S. M., Flanner, M., Cook, J. M., Dumont, M., & Painter, T. H. (2018). Radiative forcing by light-absorbing particles in snow. *Nature Climate Change*, 8(11), 964–971. <https://doi.org/10.1038/s41558-018-0296-5>
- Smith, S. L., O'Neill, H. B., Isaksen, K., Noetzli, J., & Romanovsky, V. E. (2022). The changing thermal state of permafrost. *Nature Reviews Earth & Environment*, 3(1), 10–23. <https://doi.org/10.1038/s43017-021-00240-1>
- Smith, T., & Bookhagen, B. (2018). Changes in seasonal snow water equivalent distribution in High Mountain Asia (1987 to 2009). *Science Advances*, 4(1), Article e1701550. <https://doi.org/10.1126/sciadv.1701550>
- Smith, T., & Bookhagen, B. (2020). Assessing multi-temporal snow-volume trends in high mountain Asia from 1987 to 2016 using high-resolution passive microwave data. *Frontiers in Earth Science*, 8, Article 559175. <https://doi.org/10.3389/feart.2020.559175>
- Smith, T., Bookhagen, B., & Rheinwalt, A. (2017). Spatiotemporal patterns of High Mountain Asia's snowmelt season identified with an automated snowmelt detection algorithm, 1987–2016. *The Cryosphere*, 11(5), 2329–2343. <https://doi.org/10.5194/tc-11-2329-2017>
- Soheb, M., Ramanathan, A., Angchuk, T., Mandal, A., Kumar, N., & Lotus, S. (2020). Mass-balance observation, reconstruction and sensitivity of Stok glacier, Ladakh region, India, between 1978 and 2019. *Journal of Glaciology*, 66(258), 627–642. <https://doi.org/10.1017/jog.2020.34>
- Song, C., Sheng, Y., Ke, L., Nie, Y., & Wang, J. (2016). Glacial lake evolution in the southeastern Tibetan Plateau and the cause of rapid expansion of proglacial lakes linked to glacial-hydrogeomorphic processes. *Journal of Hydrology*, 540, 504–514. <https://doi.org/10.1016/j.jhydrol.2016.06.054>
- Srivastava, D. (Ed.). (2001). *Glaciology of Indian Himalaya: A bilingual contribution in 150 years of Geological Survey of India*. Special Publication No. 63. Vedam Books.
- Steffen, T., Huss, M., Estermann, R., Hodel, E., & Farinotti, D. (2022). Volume, evolution, and sedimentation of future glacier lakes in Switzerland over the 21st century. *Earth Surface Dynamics*, 10(4), 723–741. <https://doi.org/10.5194/esurf-10-723-2022>
- Steiner, J. F., Kraaijenbrink, P. D. A., & Immerzeel, W. W. (2021). Distributed melt on a debris-covered glacier: Field observations and melt modeling on the Lirung Glacier in the Himalaya. *Frontiers in Earth Science* [preprint]. <https://doi.org/10.3389/feart.2021.678375>

- Steiner, J. F., Litt, M., Stigter, E. E., Shea, J., Bierkens, M. F. P., & Immerzeel, W. W. (2018). The importance of turbulent fluxes in the surface energy balance of a debris-covered glacier in the Himalayas. *Frontiers in Earth Science*, 6. <https://doi.org/10.3389/feart.2018.00144>
- Stigter, E. E., Litt, M., Steiner, J. F., Bonekamp, P. N. J., Shea, J. M., Bierkens, M. F. P., & Immerzeel, W. W. (2018). The importance of snow sublimation on a Himalayan glacier. *Frontiers in Earth Science*, 6. <https://doi.org/10.3389/feart.2018.00108>
- Stigter, E. E., Steiner, J. F., Koch, I., Saloranta, T. M., Kirkham, J. D., & Immerzeel, W. W. (2021). Energy and mass balance dynamics of the seasonal snowpack at two high-altitude sites in the Himalaya. *Cold Regions Science and Technology*, 183, Article 103233. <https://doi.org/10.1016/j.coldregions.2021.103233>
- Stigter, E. E., Wanders, N., Saloranta, T. M., Shea, J. M., Bierkens, M. F. P., & Immerzeel, W. W. (2017). Assimilation of snow cover and snow depth into a snow model to estimate snow water equivalent and snowmelt runoff in a Himalayan catchment. *The Cryosphere*, 11(4), 1647–1664. <https://doi.org/10.5194/tc-11-1647-2017>
- Stumm D., Joshi S.P., Gurung T.R. and Silwal G. (2021). Mass balances of Yala and Rikha Samba glaciers, Nepal, from 2000 to 2017. *Earth System Science Data* 13(8), 3791–3818. <https://doi.org/10.5194/essd-13-3791-2021>
- Sun, Z., Zhao, L., Hu, G., Qiao, Y., Du, E., Zou, D., & Xie, C. (2020). Modeling permafrost changes on the Qinghai–Tibetan plateau from 1966 to 2100: A case study from two boreholes along the Qinghai–Tibet engineering corridor. *Permafrost and Periglacial Processes*, 31(1), 156–171. <https://doi.org/10.1002/ppp.2022>
- Sunako, S., Fujita, K., Sakai, A., & Kayastha, R. (2019). Mass balance of Trambau Glacier, Rolwaling region, Nepal Himalaya: In-situ observations, long-term reconstruction and mass-balance sensitivity. *Journal of Glaciology*, 65(252), 605–616. <https://doi.org/10.1017/jog.2019.37>
- Tang, Z., Wang, X., Deng, G., Wang, X., & Jiang, Z. (2020). Spatiotemporal variation of snowline altitude at the end of melting season across High Mountain Asia, using MODIS snow cover product. *Advances in Space Research*, 66(11), 2629–2645. <https://doi.org/10.1016/j.asr.2020.09.035>
- Terzi, S., Torresan, S., Schneiderbauer, S., Critto, A., Zebisch, M., & Marcomini, A. (2019). Multi-risk assessment in mountain regions: A review of modelling approaches for climate change adaptation. *Journal of Environmental Management*, 232, 759–771. <https://doi.org/10.1016/j.jenvman.2018.11.100>
- Thackeray, C. W., Fletcher, C. G., Mudryk, L. R., & Derksen, C. (2016). Quantifying the uncertainty in historical and future simulations of northern hemisphere spring snow cover. *Journal of Climate*, 29(23), 8647–8663. <https://doi.org/10.1175/JCLI-D-16-0341.1>
- Thapa, A., & Muhammad, S. (2020). Contemporary snow changes in the Karakoram region attributed to improved MODIS data between 2003 and 2018. *Water*, 12(10), Article 2681. <https://doi.org/10.3390/w12102681>
- Thompson, S. S., Benn, D. I., Dennis, K., & Luckman, A. (2012). A rapidly growing moraine-dammed glacial lake on Ngozumpa Glacier, Nepal. *Geomorphology*, 145–146, 1–11. <https://doi.org/10.1016/j.geomorph.2011.08.015>
- Tsai, Y.-L. S., Dietz, A., Oppelt, N., & Kuenzer, C. (2019). Remote sensing of snow cover using spaceborne SAR: A review. *Remote Sensing*, 11(12), Article 1456. <https://doi.org/10.3390/rs11121456>
- Tshering, P., & Fujita, K. (2016). First in situ record of decadal glacier mass balance (2003–2014) from the Bhutan Himalaya. *Annals of Glaciology*, 57(71), 289–294. <https://doi.org/10.3189/2016AoG71A036>
- Tsutaki, S., Fujita, K., Nuimura, T., Sakai, A., Sugiyama, S., Komori, J., & Tshering, P. (2019). Contrasting thinning patterns between lake- and land-terminating glaciers in the Bhutanese Himalaya. *The Cryosphere*, 13, 2733–2750. <https://doi.org/10.5194/tc-13-2733-2019>
- Vaidya, R. A., Shrestha, M. S., Nasab, N., Gurung, D. R., Kozo, N., Pradhan, N. S., Wasson, R. J., Shrestha, A. B., Gurung, C. G., & Bajracharya, A. (2019). Disaster risk reduction and building resilience in the Hindu Kush Himalaya. In P. Wester, A. Mishra, A. Mukherji, & A. B. Shrestha (Eds.), *The Hindu Kush Himalaya assessment: Mountains, climate change, sustainability and people* (pp. 389–419). Springer Nature Switzerland AG. https://doi.org/10.1007/978-3-319-92288-1_11
- Veh, G., Lützow, N., Kharlamova, V., Petrakov, D., Hugonnet, R., & Korup, O. (2022). Trends, breaks, and biases in the frequency of reported glacier lake outburst floods. *Earth's Future*, 10, Article e2021EF002426. <https://doi.org/10.1029/2021EF002426>
- Veldhuijsen, S. B. M., de Kok, R., Stigter, E. E., & Steiner, J. F. (2021). Spatial and temporal patterns of snowmelt refreezing in a Himalayan catchment. *Journal of Glaciology*, 68(268), 1–21. <https://doi.org/10.1017/jog.2021.101>
- Vionnet, V., Guyomarc'h, G., Lafaysse, M., Naaimbouvet, F., Giraud, G., & Deliot, Y. (2018). Operational implementation and evaluation of a blowing snow scheme for avalanche hazard forecasting. *Cold Regions Science and Technology*, 147, 1–10. <https://doi.org/10.1016/j.coldregions.2017.12.006>

- Vishwakarma, B. D., Ramsankaran, R., Azam, M. F., Bolch, T., Mandal, A., Srivastava, S., Kumar, P., Sahu, R., Navinkumar, P. J., Tanniru, S. R., Javed, A., Soheb, M., Dimri, A. P., Yadav, M., Devaraju, B., Chinnasamy, P., Reddy, M. J., Murugesan, G. P., Arora, M., ... Bamber, J. (2022). Challenges in understanding the variability of the cryosphere in the Himalaya and its impact on regional water resources. *Frontiers in Water*, 4, Article 909246. <https://doi.org/10.3389/frwa.2022.909246>
- Viste, E., & Sorteberg, A. (2015). Snowfall in the Himalayas: An uncertain future from a little-known past. *The Cryosphere*, 9(3), 1147–1167. <https://doi.org/10.5194/tc-9-1147-2015>
- Wagon, P., Brun, F. Khadka, A., Berthier, E., Shrestha, D., Vincent, C., Arnaud, Y., Six, D., Dehecq, A., Menegoz, M., & Jomelli, V. (2020). Reanalysing the 2007–19 glaciological mass-balance series of Mera Glacier, Nepal, Central Himalaya, using geodetic mass balance. *Journal of Glaciology*, 67(261), 117–125. <https://doi.org/10.1017/jog.2020.88>
- Wagon, P., Vincent, C., Arnaud, Y., Berthier, E., Vuillermoz, E., Gruber, S., Menegoz, M., Gilbert, A., Dumont, M., Shea, J. M., Stumm, D., & Pokhrel, B. K. (2013). Seasonal and annual mass balances of Mera and Pokalde glaciers (Nepal Himalaya) since 2007. *The Cryosphere*, 7, 1769–1786. <https://doi.org/10.5194/tc-7-1769-2013>
- Wang, R., Liu, S., Shangguan, D., Radić, V., & Zhang, Y. (2019). Spatial heterogeneity in glacier mass-balance sensitivity across High Mountain Asia. *Water*, 11(4), Article 776. <https://doi.org/10.3390/w11040776>
- Wang, X., Guo, X., Yang, C., Liu, Q., Wei, J., Zhang, Y., Liu, S., Zhang, Y., Jiang, Z., & Tang, Z. (2020). Glacial lake inventory of high-mountain Asia in 1990 and 2018 derived from Landsat images. *Earth System Science Data*, 12(3), 2169–2182. <https://doi.org/10.5194/essd-12-2169-2020>
- Wangchuk, S., & Bolch, T. (2020). Mapping of glacial lakes using Sentinel-1 and Sentinel-2 data and a random forest classifier: Strengths and challenges. *Science of Remote Sensing*, 2, Article 100008. <https://doi.org/10.1016/j.srs.2020.100008>
- Wangchuk, S., Bolch, T., & Robson, B. A. (2022). Monitoring glacial lake outburst flood susceptibility using Sentinel-1 SAR data, Google Earth Engine, and persistent scatterer interferometry. *Remote Sensing of Environment*, 271, Article 112910. <https://doi.org/10.1016/j.rse.2022.112910>
- Wani, J. M., Thayyen, R. J., Gruber, S., Ojha, C. S. P., & Stumm, D. (2020). Single-year thermal regime and inferred permafrost occurrence in the upper Ganglax catchment of the cold-arid Himalaya, Ladakh, India. *Science of The Total Environment*, 703, Article 134631. <https://doi.org/10.1016/j.scitotenv.2019.134631>
- Welty, E., Zemp, M., Navarro, F., Huss, M., Fürst, J. J., Gärtner-Roer, I., Landmann, J., Machguth, H., Naegeli, K., Andreassen, L. M., Farinotti, D., Li, H., & GliThaDa contributors (2020). Worldwide version-controlled database of glacier thickness observations. *Earth System Science Data*, 12(4), 3039–3055. <https://doi.org/10.5194/essd-12-3039-2020>
- Wester, P., Mishra, A., Mukherji, A., & Shrestha, A. B. (Eds.). (2019). *The Hindu Kush Himalaya assessment: Mountains, climate change, sustainability and people*. Springer Nature Switzerland AG. <https://doi.org/10.1007/978-3-319-92288-1>
- Wirbel, A., Jarosch, A. H., & Nicholson, L. (2018). Modelling debris transport within glaciers by advection in a full-Stokes ice flow model. *The Cryosphere*, 12(1), 189–204. <https://doi.org/10.5194/tc-12-189-2018>
- Yang, Y., Hopping, K. A., Wang, G., Chen, J., Peng, A., & Klein, J. A. (2018). Permafrost and drought regulate vulnerability of Tibetan Plateau grasslands to warming. *Ecosphere*, 9(5), Article e02233. <https://doi.org/10.1002/ecs2.2233>
- Yang, Y., Wu, Q., Liu, F., & Jin, H. (2021). Spatial-temporal trends of hydrological transitions in thermokarst lakes on Northeast Qinghai-Tibet Plateau based on stable isotopes. *Journal of Hydrology*, 597, Article 126314. <https://doi.org/10.1016/j.jhydrol.2021.126314>
- Yao, T., Bolch, T., Chen, D., Gao, J., Immerzeel, W., Piao, S., Su, F., Thompson, L., Wada, Y., Wang, L., Wang, T., Wu, G., Xu, B., Yang, W., Zhang, G., & Zhao, P. (2022). The imbalance of the Asian water tower. *Nature Reviews Earth & Environment*, 3, 618–632. <https://doi.org/10.1038/s43017-022-00299-4>
- Yao, T., Thompson, L., Yang, W., Yu, W., Gao, Y., Guo, X., Yang, X., Duan, K., Zhao, H., Xu, B., Pu, J., Lu, A., Xiang, Y., Kattel, D. B., & Joswiak, D. (2012). Different glacier status with atmospheric circulations in Tibetan Plateau and surroundings. *Nature Climate Change*, 2, 663–667. <https://doi.org/10.1038/nclimate1580>
- You, J., Qin, X., Ranjitkar, S., Loughheed, S. C., Wang, M., Zhou, W., Ouyang, D., Zhou, Y., Xu, J., Zhang, W., Wang, Y., Yang, J., & Song, Z. (2018). Response to climate change of montane herbaceous plants in the genus *Rhodiola* predicted by ecological niche modelling. *Scientific Reports*, 8, Article 5879. <https://doi.org/10.1038/s41598-018-24360-9>
- You, Q., Wu, F., Wang, H., Jiang, Z., Pepin, N., & Kang, S. (2020). Projected changes in snow water equivalent over the Tibetan Plateau under global warming of 1.5° and 2°C. *Journal of Climate*, 33(12), 5141–5154. <https://doi.org/10.1175/JCLI-D-19-0719.1>

- You, Q.-L., Ren, G.-Y., Zhang, Y.-Q., Ren, Y.-Y., Sun, X.-B., Zhan, Y.-J., Shrestha, A. B., & Krishnan, R. (2017). An overview of studies of observed climate change in the Hindu Kush Himalayan (HKH) region. *Advances in Climate Change Research*, 8(3), 141–147. <https://doi.org/https://doi.org/10.1016/j.accres.2017.04.001>
- Zemp, M., Frey, H., Gärtner-Roer, I., Nussbaumer, S. U., Hoelzle, M., Paul, F., Haeberli, W., Denzinger, F., Ahlstrøm, A. P., Anderson, B., Bajracharya, S., Baroni, C., Braun, L. N., Cáceres, B. E., Casassa, G., Cobos, G., Dávila, L. R., Delgado Granados, H., Demuth, M. N., ... Vincent, C. (2015). Historically unprecedented global glacier decline in the early 21st century. *Journal of Glaciology*, 61(228), 745–762. <https://doi.org/10.3189/2015JoG15J017>
- Zemp, M., Huss, M., Thibert, E., Eckert, N., McNabb, R., Huber, J., Barandun, M., Machguth, H., Nussbaumer, S. U., Gärtner-Roer, I., Thomson, L., Paul, F., Maussion, F., Kutuzov, S., & Cogley, J. G. (2019). Global glacier mass changes and their contributions to sea-level rise from 1961 to 2016. *Nature*, 568, 382–386. <https://doi.org/10.1038/s41586-019-1071-0>
- Zhang, G., Yao, T., Xie, H., Wang, W., & Yang, W. (2015). An inventory of glacial lakes in the Third Pole region and their changes in response to global warming. *Global and Planetary Change*, 131, 148–157. <https://doi.org/10.1016/j.gloplacha.2015.05.013>
- Zhang, M., Chen, F., Zhao, H., Wang, J., & Wang, N. (2021). Recent changes of glacial lakes in the High Mountain Asia and its potential controlling factors analysis. *Remote Sensing*, 13(18), Article 3757. <https://doi.org/10.3390/rs13183757>
- Zhang, T. (2005). Influence of the seasonal snow cover on the ground thermal regime: An overview. *Reviews of Geophysics*, 43(4). <https://doi.org/10.1029/2004RG000157>
- Zhang, Z., Wang, M., Wu, Z., & Liu, X. (2019). Permafrost deformation monitoring along the Qinghai-Tibet Plateau engineering corridor using InSAR observations with multi-sensor SAR datasets from 1997–2018. *Sensors*, 19(23), Article 5306. <https://doi.org/10.3390/s19235306>
- Zhao, D., & Wu, S. (2019). Projected changes in permafrost active layer thickness over the Qinghai-Tibet Plateau under climate change. *Water Resources Research*, 55(9), 7860–7875. <https://doi.org/10.1029/2019WR024969>
- Zhao, L., Zou, D., Hu, G., Wu, T., Du, E., Liu, G., Xiao, Y., Li, R., Pang, Q., Qiao, Y., Wu, X., Sun, Z., Xing, Z., Sheng, Y., Zhao, Y., Shi, J., Xie, C., Wang, L., Wang, C., & Cheng, G. (2021). A synthesis dataset of permafrost thermal state for the Qinghai-Tibet (Xizang) Plateau, China. *Earth System Science Data*, 13(8), 4207–4218. <https://doi.org/10.5194/essd-13-4207-2021>
- Zhao, S., Cheng, W., Yuan, Y., Fan, Z., Zhang, J., & Zhou, C. (2022). Global permafrost simulation and prediction from 2010 to 2100 under different climate scenarios. *Environmental Modelling and Software*, 149, Article 105307. <https://doi.org/10.1016/j.envsoft.2022.105307>
- Zheng, G., Allen, S. K., Bao, A., Ballesteros-Canovas, J. A., Huss, M., Zhang, G., Li, J., Yuan, Y., Jiang, L., Yu, T., Chen, W., & Stoffel, M. (2021). Increasing risk of glacial lake outburst floods from future Third Pole deglaciation. *Nature Climate Change*, 11(5), 411–417. <https://doi.org/10.1038/s41558-021-01028-3>
- Zhou, Y., Li, Z., & Li, J. (2017). Slight glacier mass loss in the Karakoram region during the 1970s to 2000 revealed by KH-9 images and SRTM DEM. *Journal of Glaciology*, 63(238), 331–342. <https://doi.org/10.1017/jog.2016.142>
- Zhou, Y., Li, Z., Li, J., Zhao, R., & Ding, X. (2018). Glacier mass balance in the Qinghai-Tibet Plateau and its surroundings from the mid-1970s to 2000 based on Hexagon KH-9 and SRTM DEMs. *Remote Sensing of Environment*, 210, 96–112. <https://doi.org/10.1016/j.rse.2018.03.020>

Appendix

Source data used to compile region-wide mean glacier mass balances for 1975–1999

| Region ID | Study | Area covered (km ²) | Starting year | Ending year | Specific mass balance (m w.e. per year) | Specific mass balance uncertainty (m w.e. per year) |
|-----------|----------------------------|---------------------------------|---------------|-------------|---|---|
| 14-01 | Zhou et al. (2018) | 841 | 1975 | 2000 | -0.11 | 0.13 |
| 15-01 | Bhattacharya et al. (2021) | 490 | 1974 | 2004 | -0.3 | 0.1 |
| 15-01 | King et al. (2019) | 1,095 | 1974 | 2000 | -0.21 | 0.08 |
| 15-01 | King et al. (2019) | 540 | 1974 | 2000 | -0.26 | 0.08 |
| 15-01 | King et al. (2019) | 744 | 1974 | 2000 | -0.24 | 0.11 |
| 15-01 | King et al. (2019) | 840 | 1974 | 2000 | -0.27 | 0.1 |
| 15-01 | Zhou et al. (2018) | 578 | 1975 | 2000 | -0.28 | 0.11 |
| 15-01 | Zhou et al. (2018) | 228 | 1975 | 2000 | -0.23 | 0.18 |
| 15-01 | Ragetli et al. (2016) | 100 | 1974 | 2006 | -0.24 | 0.08 |
| 15-01 | Maurer et al. (2019) | 197 | 1975 | 2000 | -0.25 | 0.07 |
| 14-02 | Bolch et al. (2017) | 2,868 | 1974 | 1999 | -0.01 | 0.09 |
| 14-02 | Zhou et al. (2017) | 7,826 | 1973 | 2000 | -0.09 | 0.03 |
| 15-02 | King et al. (2019) | 746 | 1974 | 2000 | -0.29 | 0.1 |
| 15-02 | King et al. (2019) | 869 | 1974 | 2000 | -0.2 | 0.08 |
| 15-02 | Zhou et al. (2018) | 689 | 1975 | 2000 | -0.3 | 0.12 |
| 15-02 | Maurer et al. (2016) | 365 | 1974 | 2006 | -0.17 | 0.05 |
| 15-02 | Maurer et al. (2019) | 2,460 | 1975 | 2000 | -0.26 | 0.06 |
| 14-03 | Zhou et al. (2018) | 776 | 1975 | 2000 | -0.04 | 0.1 |
| 14-03 | Maurer et al. (2019) | 1,379 | 1975 | 2000 | -0.16 | 0.08 |
| 15-03 | Zhou et al. (2018) | 615 | 1975 | 2000 | -0.19 | 0.14 |
| 13-05 | Zhou et al. (2018) | 1,147 | 1975 | 2000 | -0.02 | 0.14 |
| 13-05 | Zhou et al. (2018) | 1,209 | 1975 | 2000 | 0.05 | 0.14 |
| 13-06 | Zhou et al. (2018) | 642 | 1975 | 2000 | -0.06 | 0.12 |
| 13-08 | Bhattacharya et al. (2021) | 344 | 1975 | 2000 | -0.22 | 0.07 |
| 13-08 | Bhattacharya et al. (2021) | 168 | 1976 | 2001 | -0.24 | 0.13 |
| 13-08 | Zhou et al. (2018) | 317 | 1975 | 2000 | -0.25 | 0.15 |
| 13-08 | Zhou et al. (2018) | 720 | 1975 | 2000 | -0.22 | 0.12 |
| 13-08 | Maurer et al. (2019) | 398 | 1975 | 2000 | -0.23 | 0.06 |
| 13-09 | Zhou et al. (2018) | 1,055 | 1975 | 2000 | -0.11 | 0.14 |
| 14-01 | Zhou et al. (2018) | 841 | 1975 | 2000 | -0.11 | 0.13 |
| 15-01 | Bhattacharya et al. (2021) | 490 | 1974 | 2004 | -0.3 | 0.1 |
| 15-01 | King et al. (2019) | 1,095 | 1974 | 2000 | -0.21 | 0.08 |
| 15-01 | King et al. (2019) | 540 | 1974 | 2000 | -0.26 | 0.08 |
| 15-01 | King et al. (2019) | 744 | 1974 | 2000 | -0.24 | 0.11 |